CONTRIBUTION OF PICOPLANKTON TO PHYTOPLANKTON DYNAMICS AND BIO-OPTICS OF THE EASTERN CARIBBEAN SEA.

by

Jesús Lee-Borges

A thesis submitted in partial fulfillment
of the requirements for the degree of

DOCTOR OF PHILOSOPHY
in
Biological Oceanography

UNIVERSITY OF PUERTO RICO
MAYAGÜEZ CAMPUS
2003

Approved by:

[redacted]
Fernando Gilbes, Ph. D.
Member, Graduate Committee — July 7, 2003 Date

[redacted]
José López, Ph. D.
Member, Graduate Committee — 7 julio 2003 Date

[redacted]
José Planas, Ph. D.
Member, Graduate Committee — July 07, 2003 Date

[redacted]
Roy A. Armstrong, Ph. D.
President, Graduate Committee — July 2, 2003 Date

[redacted]
Nilda E. Aponte, Ph. D.
Chairperson, Department of Marine Sciences — July 7, 2003 Date

[redacted]
Rafael Montalvo, Ph. D.
Representative of Graduate Studies — 7/julio/2003 Date

[redacted]
José A. Mari-Mutt, Ph. D.
Director of Graduate Studies — 14 julio 2003 Date

Abstract

The picoplankton contribution to the total biomass has not been considered when it is estimated using remote sensors. In this work, *In situ* chlorophyll-a values were compared to values obtained from; a) Sea-viewing Wide Field-of-view Sensor (SeaWiFS) imagery, and b) different algorithms (calculated with data from a spectroradiometer) for the Caribbean Time Series Station (CaTS) from October 1997 to August 2002. Regression analysis suggests that the Moderate-resolution Imaging Spectroradiometer (MODIS) algorithm provided the best estimate of the *in situ* chlorophyll-a value (r^2=0.67089). The SeaWiFS OC-4_{v4} algorithm overestimated chlorophyll-a values when the *in situ* value was <0.2 μg/L and underestimate it when the *in situ* value was >0.2 μg/L. This is due to sampling error resulting from the use of 0.7 μm GF/F filters. Picoplankton loss through 0.7 μm filters (Whatman GF/F) compared to 0.2 μm membrane filters (Millipore TCMF) was quantified for oceanic stations of the North Eastern Caribbean Basin and Mayagüez Bay. On average, a 20% loss of picoplankton in oceanic stations, and a 9% loss for coastal stations were observed Size fractionated phytoplankton analysis revealed that picoplankton was the dominant size class in oceanic stations (accounting for 60-85% of the total phytoplankton biomass and 61-77% of the absorption of light by particulates), while larger phytoplankton (>2.0 μm) dominate coastal stations. Temporal and spatial variability was observed in the size distribution of the phytoplankton community in all the stations. Electrophoretic patterns of Restriction Fragment Length Polymorphism (RFLP) corroborated the variability. These results emphasize the importance of picoplankton variability when temporal and spatial scales are considered, and suggests that this group of photoautotrophs, rather than

simply representing a “background noise”, constitutes an active and changing component of the microbial community in the open ocean and even in productive waters. To improve satellite estimates of phytoplankton biomass, future algorithms must take into account the contribution of the picoplankton to the phytoplankton population.

Resumen

La aportación del picoplancton a la biomasa total del fitoplancton no ha sido considerada cuando esta es estimada por sensores remotos. En este trabajo se compararon valores *in situ* de clorofila-a con valores obtenidos a través de; a) imágenes de "Sea-viewing Wide Field-of-view Sensor" ("SeaWiFS") y b) diferentes algoritmos (calculados con data obtenida de un espectroradiómetro) para la estación "Caribbean Time Series" ("CaTS") desde octubre de 1997 hasta agosto de 2002. Análisis de regresión sugieren que el algoritmo de "Moderate-resolution Imaging Spectroradiometer" ("MODIS") fue el que mejor estimó los valores *in situ* de clorofila-a (r^2=0.67089). El algoritmo de "SeaWiFS" ($OC\text{-}4_{v4}$) sobrestimo el valor de clorofila-a cuando el valor *in situ* era <2.0 μg/L y lo subestimo cuando era >2.0 μg/L. Esto es debido al error de muestreo producido al usar un filtro de 0.7 μm GF/F. Se calculó el picoplancton que se pierde con el filtro de 0.7 μm (Whatman GF/F), en comparación con un filtro de 0.2 μm (Millipore TCMF), para estaciones oceánicas de la Cuenca del Caribe Oriental y la Bahía de Mayagüez. En promedio se observó una pérdida del 20% del picoplancton para las estaciones oceánicas y un 9% para estaciones costeras. El análisis de fraccionamiento por tamaño del fitoplancton reveló que el picoplancton es el tamaño dominante en las estaciones oceánicas (contribuyendo un 60-85% de la biomasa total del fitoplancton y un 61-77% de la absorción de la luz por partículas), mientras el fitoplancton más grande (> 2.0 μm) domina en las estaciones costeras. Se observó variabilidad temporal y espacial en la distribución de tamaño en la comunidad de fitoplancton en todas las estaciones muestreadas. Patrones electroforéticos de "Restriction Fragment Length Polymorphism" ("RFLP") confirmaron la variabilidad. Los resultados enfatizan la importancia del

picoplankton y sugieren que este grupo de fotoautótrofos, en vez de ser un factor de trasfondo, constituyen un componente activo y cambiante de la comunidad microbiana en aguas oceánicas y hasta en aguas costeras. Para mejorar los estimados de biomasa de fitoplancton obtenidos de sensores remotos, los próximos algoritmos deben de tomar en consideración la aportación del picoplankton a la población de fitoplancton.

This work is dedicated to my wife Lizzy and my mother Yolanda (RIP), words can't express what your love and unconditional support have meant to me.

Acknowledgements

I would like to thank my wife, Lizzy, sons Jonathan and Joshua, father, Pou, and brothers, Javier and José, I love you all dearly. I would like to acknowledge my friends, Marcos, José and Fernando whom without their help and support, this research and manuscript would not have been possible. I would also like to thank my graduate committee, Dr. Roy Armstrong, Dr. Fernando Gilbes, Dr. José López, and Dr. José Planas, for their support and guidance through this whole process. Members of the bio-optical lab, Debby Cedeño and Dr. Yazmin Detres, were always there to provide help and support. To the Captain and crew of the R/V Chapman and R/V Sultana, their assistance and help in the field operations is genuinely appreciated. This research was supported in part by NASA grants NAG13-99029, NAG13-54, and NCC5-518.

.

TABLE OF CONTENTS

LIST OF TABLES

LIST OF FIGURES

Introduction

Interest on marine ecosystems has accelerated in recent years with growing recognition of their importance in regulating global climate. Studies of phytoplankton are essential to understand the distribution of CO_2 between the atmosphere and the deep ocean, its function as a biological pump for carbon, and the global biological carbon cycle. Phytoplankton, although comprising only 1-2% of the total global biomass of primary producers, contributes 30-60% of the global fixation of carbon annually (Sakshaug et al., 1997).

Remote sensing of ocean color provides the capability of measuring phytoplankton biomass at large scales. Images of the spatial distribution of surface chlorophyll generated from ocean color satellite sensors, like the Coastal Zone Color Scanner (CZCS), the Sea-viewing Wide Field-of-view Sensor (SeaWiFS), and the Moderate-Resolution Imaging Spectroradiometer (MODIS), along with the proposed launch of several more ocean color sensors within the next few years, has and will continue to greatly enhance our ability to understand geophysical processes at various temporal and spatial scales. The detailed spatial coverage provided by the satellite sensors has provided data for analysis and for model comparisons that would have been impossible to obtain from available *in situ* data (McClain et al., 1998). This is of particular importance in areas such as the Eastern Caribbean, which has traditionally been viewed as a nutrient poor oligotrophic sea where high phytoplankton biomass and productivity are limited to coastal upwelling regions and the immediate vicinity of river mouths (Corredor, 1979). Recent work has revealed the dynamic nature of the

northeastern Caribbean, underscoring the significant effect of periodic intrusions of waters of continental origins (Corredor and Morell, 2001).

This research was focused on the characterization and understanding of seasonal and inter-annual variability of the picoplankton and large phytoplankton in the NE Caribbean Basin and Mayagüez Bay, Puerto Rico as affected by seasonal riverine intrusions. Picoplankton loss through 0.7 μm GF/F filters was quantified through the use of 0.2 μm Millipore filters. Finally, we focused on the use of DNA fingerprinting through the use of restriction fragment length polymorphism (RFLP) as a means to distinguish seasonal and temporal variation in picoplankton populations.

The work presented here had the following objectives:

- Determine the associated optical properties of the picoplankton found in Case 1 (Caribbean Time Series station and other oceanic stations) and Case 2 (Mayagüez Bay).
- Determine the chlorophyll-a concentration of the different size classes (> 2.0 μm, 2.0-0.7 μm range, and 0.7-0.22 μm range) in Case 1 and Case 2 waters.
- Quantify the amount of picoplankton loss through 0.7 μm filters in Case 1 and Case 2 waters.
- Compare the chlorophyll-a values obtained using different algorithms, such as the algorithm for CZCS (Gordon et al., 1983), SeaWiFS, OC-2_{v4} and OC-4_{v4} (O'Reilly et al., 1998), and MODIS (Clark et al., 1997) with values obtained *in situ*, and from SeaWiFS imagery for the Caribbean Time Series Station (CaTS).
- Identify species and/or groups of picoplankton using DNA fingerprinting with RFLP.

Temporal and Spatial Contribution of the Picoplankton to the Phytoplankton Biomass of the Eastern Caribbean Sea.

Introduction

Studies of phytoplankton are essential to understand the global carbon cycle. They provide information to evaluate the role of the so-called biological pump, which tries to explain the distribution of CO_2 between the atmosphere and the deep ocean. Phytoplankton, although forming only 1-2% of the total global biomass of primary producers, contributes 30-60% of the global fixation of carbon annually (Sakshaug et al., 1997).

Phytoplankton within the 0.2 to 200 μm range are divided into three size classes (Sieburth et al., 1978): microplankton (>20 μm), nanoplankton (2.0 to 20 μm), and picoplankton (0.2 to 2.0 μm). Microplankton are mostly found in neritic waters (Robles-Rajero and Lara-Lara, 1993). Nanoplankton tends to dominate in nutrient replete regions, while picoplankton tends to be most dominant in oligotrophic marine and freshwater systems. Autotrophic picoplankton are represented by prokaryotic coccoid cyanobacteria, frequently of the genus *Synechococcus* (Johnson and Sieburth, 1979), prochlorophytes (Chisholm, 1988) and small eukaryotic cells (Johnson and Sieburth, 1982).

No topic within marine ecology and biological oceanography has changed more in the last decade than our notions about components and structure of planktonic food webs. Knowledge about marine water column food web has considerably improved and made much more complex by recent findings about the existence and role of smaller organisms. The changes in our understanding have been significant enough (Pomeroy, 1974) to amount to a new “paradigm”. The array of new facts prompted Azam et al.

(1983) to propose a new view of the planktonic food web that included a "microbial loop", in which organic matter was cycled through microbes before entering the classic food web. Still little is known about the organismal composition of picoplankton communities. For example, less than 1% of the bacterial species have been cultured, and there are roughly a million of these unknown cells per milliliter of seawater. One approach to a better understanding of phytoplankton dynamics is to fractionate phytoplankton assemblages into different size classes. Cell size influences the response of phytoplankton communities to environmental variation (Gieskes and Kraay, 1986; Joint and Pomroy, 1986; Oviatt et al., 1989; Glibert et al., 1992; Armstrong, 1994; Hein et al., 1995; Yongsik et al., 2000; Gilabert, 2001) and associated impacts on aquatic food web structures (Walsh, 1976; Lenz, 1992; Painting et al., 1993).

A widely accepted paradigm in marine phytoplankton ecology is that most of the temporal and geographical variability in total biomass and productivity is associated with changes in the large size fractions, the picoplankton being regarded as a 'background' component whose abundance and activity remain fairly constant (Raimbult et al., 1988; Chisholm, 1992; Rodríguez et al., 1998). It is now well established that cells smaller than 2 μm (picoplankton), rather than the larger micro algae, dominate the phytoplankton community in the open ocean. In particular, the eukaryotic component of the picoplankton, the so-called picoeukaryotes, have been recognized to contribute significantly to both primary production and biomass in open ocean regions (Campbell et al., 1997; Li, 1998). These organisms play a much greater role in oligotrophic waters than previously suspected (Stockner and Antia, 1986; Raimbault et al., 1988; Peña et al., 1990; Magazzú and Decembrini, 1995; Li, 1998). As much as 40-90% of the

chlorophyll-a and 50-80% of the primary productivity may be provided by picoplankton, especially in oligotrophic oceans (Li et al., 1983; Peña et al., 1990; Carrick and Schelske, 1997; Brown et al., 1999; Charpy and Blanchot, 1999; Chen, 2000; Fouilland et al., 2000; Marañon et al., 2001).

The wealth of data on picoplankton abundance and production in the sea has led to the conclusion that these organisms play a much greater role in oligotrophic waters than previously suspected (Stockner and Antia, 1986; Raimbault et al., 1988; Peña et al., 1990; Magazzú and Decembrini, 1995; Li, 1998). This dominance would be based on that their small size is associated to small diffusion boundary layers and large surface area per unit volume (Raven, 1986). This confers small phytoplankton cells an advantage in oligotrophic waters by leading to a greater capacity to acquire nutrients and the efficiency in their use for growth and maintenance (Raven, 1998). However, oligotrophic waters are often warm, so the perceived dominance of picoplankton in these waters could derive from their greater abundance (Li, 1998) and growth (Agawin et al., 1998) in warm waters. The majority of these observations, however, have been made in coastal and/or temperate environments, with relative little attention given to tropical and subtropical open-ocean environments. In the tropical Eastern Caribbean no study has dealt with the distribution of size-fractioned phytoplankton on temporal and spatial scale.

It has been suggested that picoplanktons' relative importance is greatest in warm and nutrient-poor waters (Agawin et al., 2000). These organisms could be of particular importance to areas such as the Eastern Caribbean which has traditionally been viewed as an oligotrophic sea where high phytoplankton biomass and productivity are limited to coastal upwelling regions in the immediate vicinity of river mouths (Corredor, 1979).

Recent work has revealed the dynamic nature of the northeastern Caribbean, underscoring the significant effect of periodic intrusions of waters of continental origins (Corredor and Morell, 2001). For this reason, is that this region becomes an ideal site to study temporal and spatial changes in picoplankton populations.

Because of the importance of the picoplankton to understand the dynamics of phytoplankton populations, during the last few years increasing attention has been paid to this group. Several studies have evaluated the contribution of picoplankton by using size fractionation, and collecting the smallest particles on 0.2 μm membrane or 0.7 μm glass-fiber filters (GF/F). Numerous comparative studies of the retention properties of glass fiber and membrane filters have demonstrated that glass fiber filters inadequately retain <1.0 μm diameter cells (Venrick et al., 1987; Tagushi and Laws, 1988; Dickson and Wheeler, 1993; Lee et al., 1995; Gasol and Morán, 1999). Low retention efficiencies of glass-fiber filters result when chlorophyll-a concentrations are low and when picoplankton are a dominant fraction of the phytoplankton assemblage (Phinney and Yentsh, 1985; Tagushi and Laws, 1988). An objective of this work was to compare the chlorophyll-a concentrations of picoplankton obtained on 0.7 μm filters (Whatman GF/F) with those obtained with 0.2 μm membrane filters (Millipore TCMF) for oceanic and coastal waters.

The oceanic waters of the Caribbean Sea are oligotrophic and warm throughout most of the year, so it would be expected that picoplankton is an important fraction of the total phytoplankton. However, there are no studies to establish the importance of the picoplankton in this region and their effect on the optical properties of these waters. Therefore, the following work had the following objectives:

- Determine the chlorophyll-a concentration of the different size classes (> 2.0 μm, 2.0-0.7 μm range, and 0.7-0.22 μm range) of phytoplankton in Case 1 and 2 waters of the North Eastern Caribbean Basin and Mayagüez Bay.
- Quantify the amount of picoplankton loss through 0.7 μm filters in Case 1 and 2 waters.

Materials and Methods

Field Work

Water samples from surface (~1m) and deep chlorophyll maximum (DCM), were taken at monthly intervals in the Caribbean Time Series (CaTS) station and at different times of the year at Mayagüez Bay. CaTS is located in oceanic waters at 17°36° 00.00´ N 067° 00.00´ W (Fig. 1) at a depth of approximately 2000 m. It is approximately 28 nautical miles off the southwestern coast of Puerto Rico and has been routinely sampled since 1994.

Mayagüez Bay is an open bay located in the western part of Puerto Rico and is influenced by the discharge of the Añasco, Yagüez and Guanajibo Rivers (Fig. 2). These rivers supply a considerable load of terrigenous sediments, especially during the rainy season, extending from September through November. The Añasco River is the largest river of the western coast, and although its basin was used for agriculture in the past, nowadays is much more developed. The Yagüez basin is highly developed and highly influenced by anthropogenic activities. The Guanajibo basin was traditionally dedicated to agriculture, especially to the sugarcane industry, but it is not being cultivated actively in the present. Beside these rivers, a number of smaller streams discharge to the bay. The location of tuna processing facilities close to the Yagüez River mouth is another source of nutrients and particulate matter to the bay. These industries dump wastewaters into the bay on a regular basis. Mayagüez Bay is also subjected to sewage waters input. The Puerto Rico Waters Authority discharges primary treated water from the city sewer systems through a diffuser tube located between the Añasco River mouth and the tuna factories. Both the riverine and the anthropogenic inputs to the bay supply nutrients and

suspended particles to the system. Cruises in Mayagüez Bay took place in October, 2 - 4, 2001, February, 26 - 28, 2002, and August, 23 - 25, 2002.

Three additional cruises were taken: a) Minipex (September, 18, 2001), an oceanic station located at 16°50° 00.00′ N 067° 00.00′ W (Fig. 1), b) Caratlan II, (August, 5 - 9, 2002), in which three stations; Station 1 (22° 00.00′ N 067° 00.00′ W), Station 2 (21° 19.00′ N 067° 00.00′ W), and Station 4 (19° 35.00′ N 067° 00.00′ W), were sampled (Fig. 1), and c) Mona Cruise (May, 22 24, 2002), in which an oceanic station (18º 07'N 067º 57.25'W) was sampled at 9:00 am and 3:00 pm on May, 23, 2002 (Fig. 3).

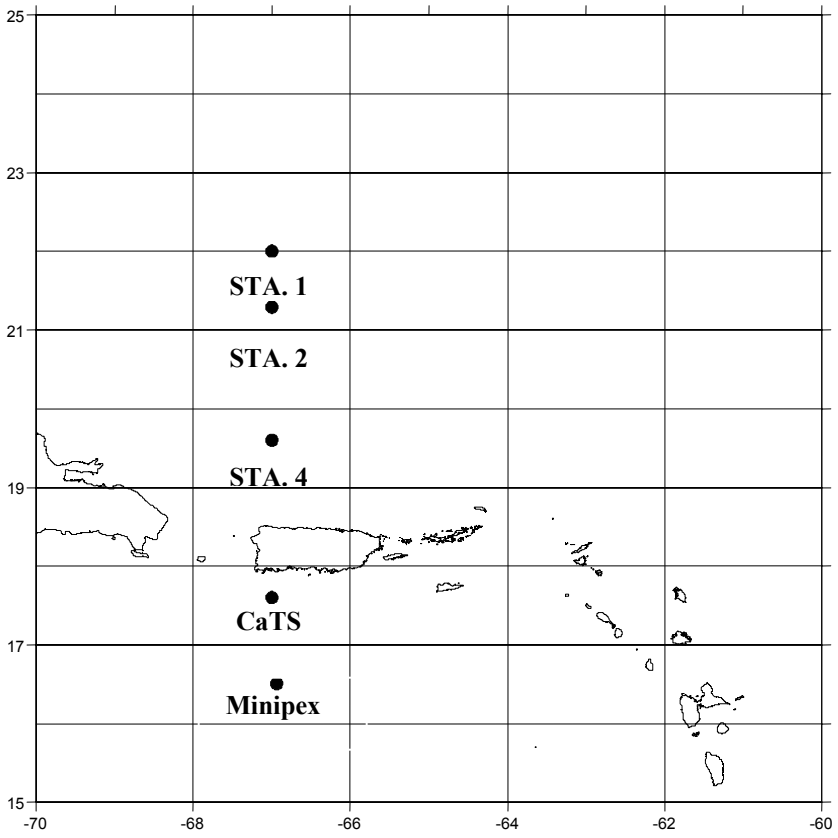

Figure 1. Map of Puerto Rico showing CaTS, Minipex, and stations 1, 2, and 4 of the Caratlan II cruise.

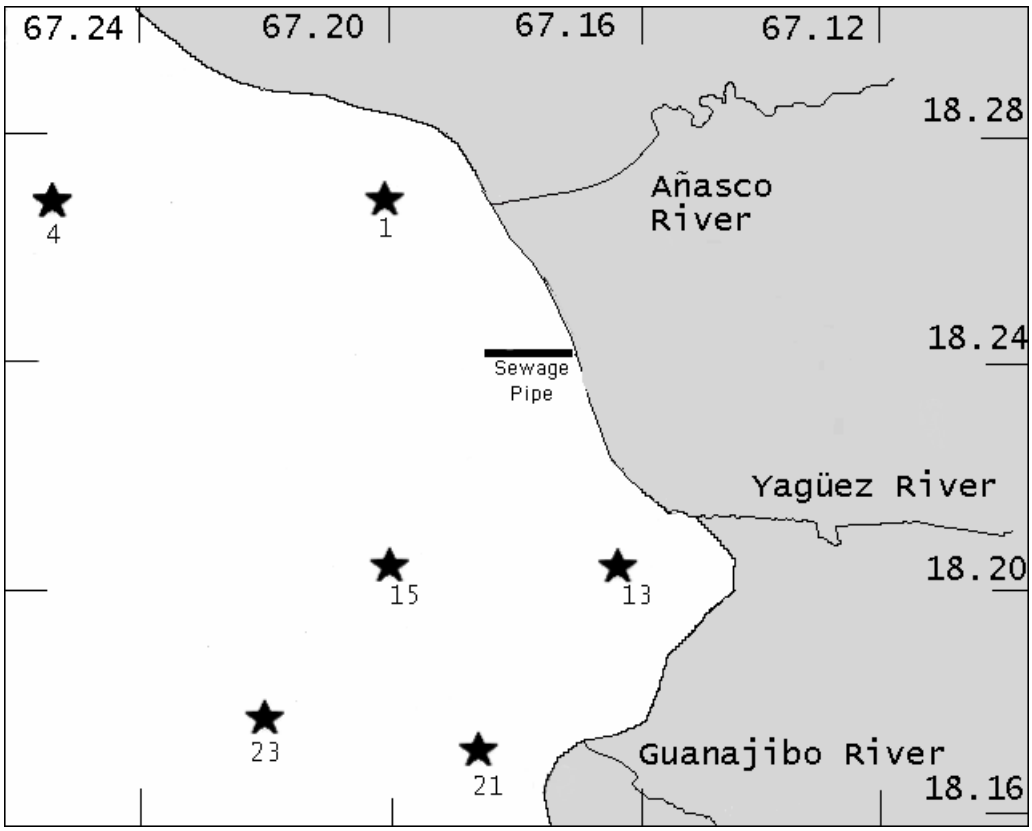

Figure 2. Map of Mayagüez Bay stations. Adapted from Rosado, 2000.

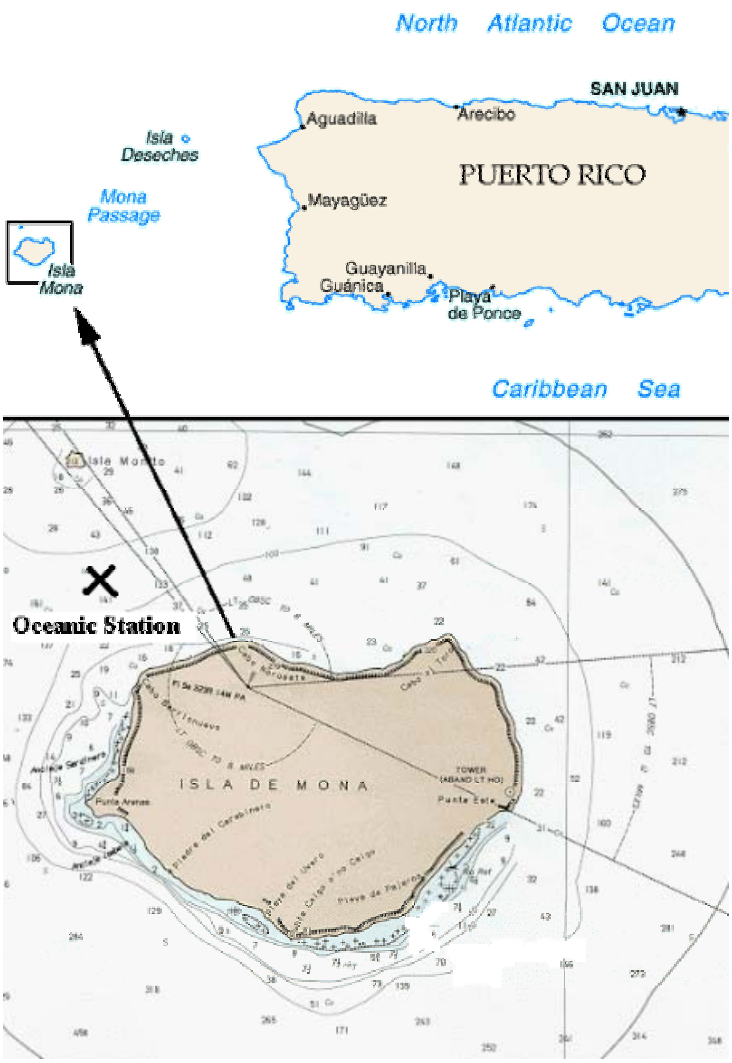

Figure 3. Map of Mona Island.

Pigment Analysis

Total chlorophyll-a was sampled by filtering the water sample (500 ml) directly on 0.7 μm glass fiber filters. To extract the pigments, the filters were immersed with 10 ml of methanol and placed in a 15 ml centrifuge tube. The samples were then kept in the dark at 4° C for approximately 16 hours. After this time the samples were centrifuged to remove the filter paper. Concentration of phytoplankton chlorophyll-a was obtained using the standard fluorometric method (Yentsch and Menzel, 1963) measured in a Turner AU-10 Fluorometer.

Size-fractionated chlorophyll-a

Seawater from the different stations were pre-filtered onto 90 mm, 2.0 μm glass microfibre filters (Whatman Multigrade GMF 150), and then through 25 mm, 0.7 μm glass fiber filters (Whatman GF/F) and 0.2 μm membrane filters (Millipore TCMF). Size fractionated chlorophyll-a was determined by filtering the samples according to Figure 4. The pigments were extracted as described above.

Phytoplankton was then grouped into three size categories, >2.0 μm, 2.0 – 0.7 μm, and 0.7- 0.2 μm. The >2.0 μm component was calculated as the difference between the chlorophyll-a concentration obtained with the 0.7 μm filter with no pre-filtration minus the chlorophyll-a value obtained with the 0.7 μm filter which had been pre-filtered (phytoplankton >2.0 μm = total phytoplankton in 0.7 μm filter – pre-filtered phytoplankton 0.7 μm filter). The 2.0 – 0.7 μm size class was obtained directly from the chlorophyll-a value obtained from the pre-filtered 0.7 μm filter. While the 0.7 – 0.2 μm category was obtained by subtracting the chlorophyll-a value obtained with the pre-

filtered 0.7 μm filter from the chlorophyll-a value obtained from the pre-filtered 0.22 μm Millipore filter. This size category also represented the amount of picoplankton that was not retained by the 0.7 μm filter.

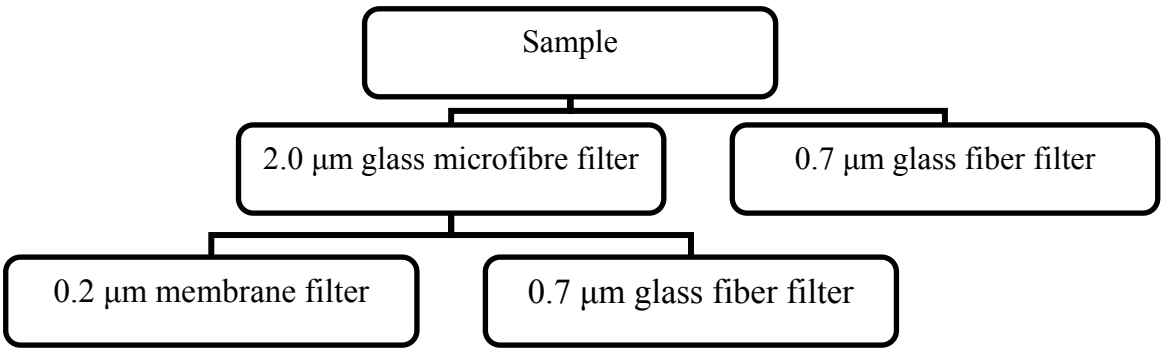

Figure 4. Flowchart of the phytoplankton size fractionation procedure.

Results and Discussion

Picoplankton lost through 0.7 μm filters

Results from CaTS show that there is a 9-68% loss of chlorophyll-a through traditional 0.7 μm filters compared to 0.2 μm membrane filters for surface samples (Fig. 5), and a 0-10% percent loss for DCM samples (Fig. 5). Temporal variation was observed in the surface samples, with September 2001 (59%) and December 2002 (68%) being the months with the highest picoplankton loss, and October 2001 (10%) and June 2002 (9%) the months with the lowest picoplankton loss. In all, the average loss of picoplankton through traditional GF/F filters in CaTS was 20% for surface samples and 9% for DCM samples. In the DCM samples the percent loss was much more uniform than in the surface. In other oceanic stations (Mona, Minipex, and Caratlan II) the results were similar; in the Minipex station there was a 20% loss in the surface and 14% loss in DCM (Fig. 6). Caratlan II cruise stations showed a 7-54% loss for surface and 13-33% loss for DCM (Fig. 6). In the Caratlan II cruise Station 1 (7% loss), Station 2 (54%), and Station 4 (23%) samples showed vastly different picoplankton loss, suggesting that even in close geographic areas there is great variability in cell size distribution. The Mona cruise, where the same station was sampled at different times, showed that at the 9:00 am sample there was a 16% loss of picoplankton while at 3:00 pm there was only a 5% loss (Fig. 6), suggesting that there is also short-time variability in cell size distribution.

These results suggest a 5-70% loss of picoplankton through traditional GF/F filters in oceanic waters and are consistent with those reported by Venrick et al. (1987), Tagushi and Laws (1988), Dickson and Wheeler (1993), Lee et al. (1995), and Gasol and

Morán (1999), who have documented the inadequate retention properties of <1 μm diameter cells in glass fiber filters.

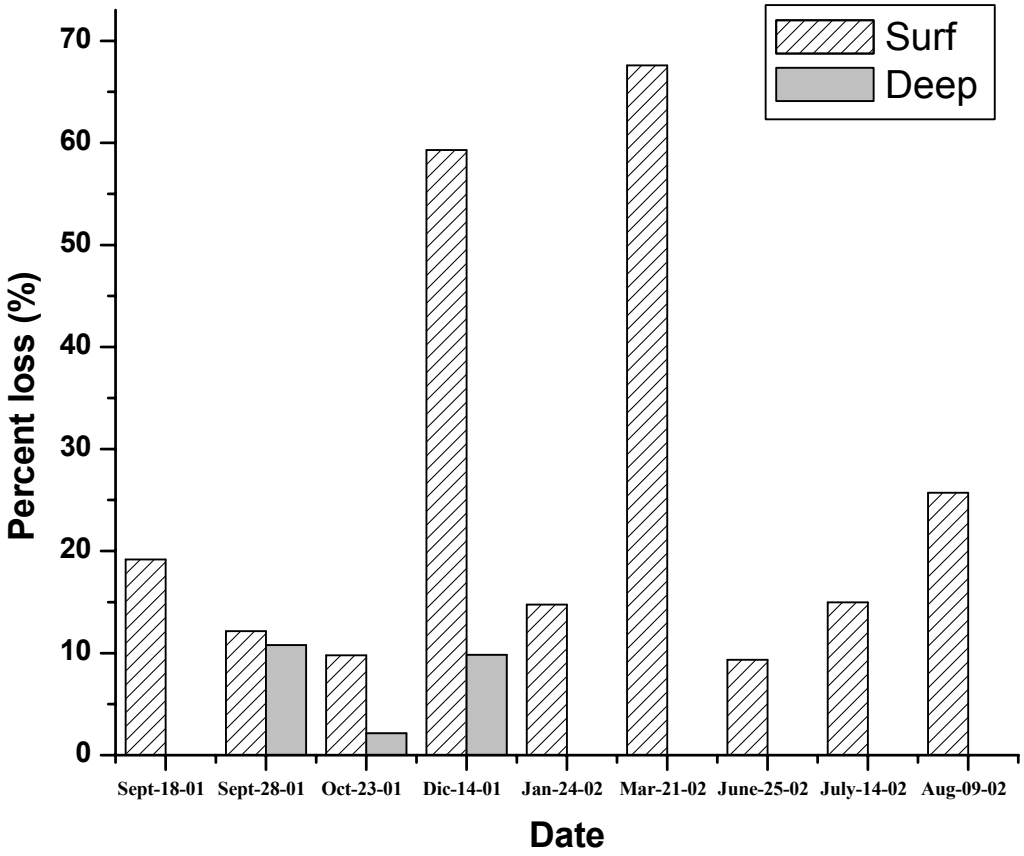

Figure 5. Percent of picoplankton loss through 0.7 μm GF/F filters in CaTS.

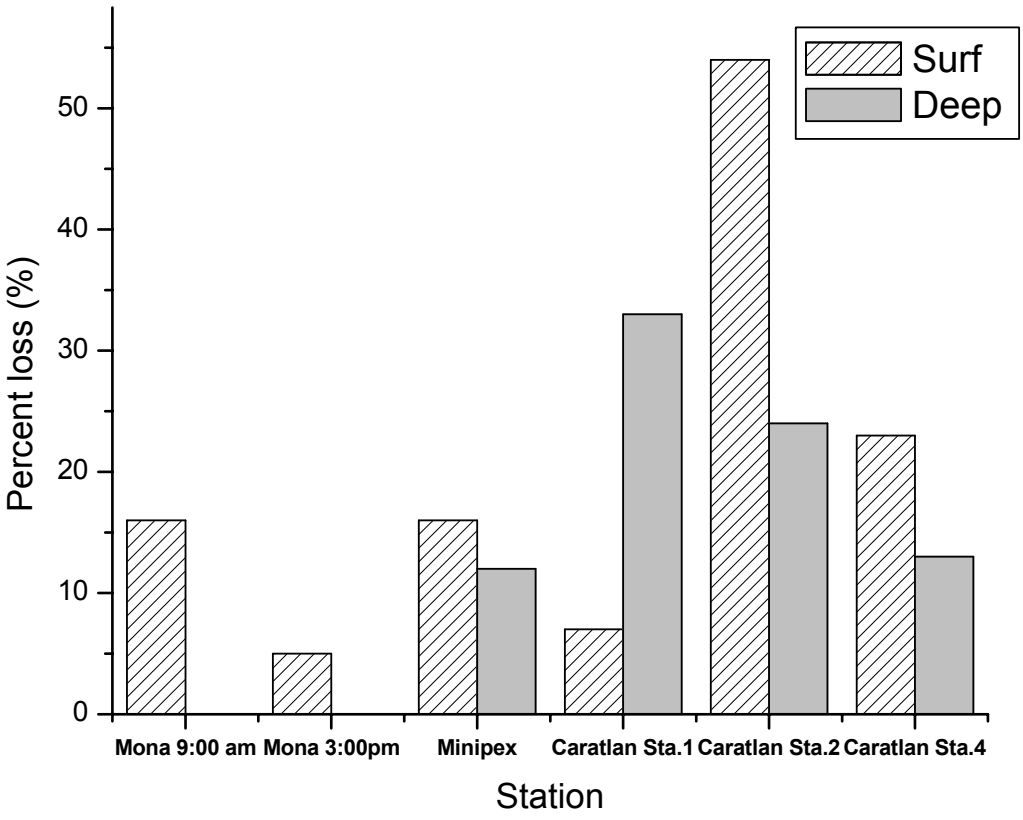

Figure 6. Percent of picoplankton loss through 0.7 μm GF/F filters in oceanic stations. No DCM samples were taken in the Mona station.

In Mayagüez Bay there is a 5-50% loss of picoplankton in station S4 surf, and 5-15% loss for the deep sample (Fig. 7). The results for this station are consistent with those for oceanic stations. The observed loss of chlorophyll-a in the more coastal stations was from 5-15% for both surf (Fig. 7) and deep samples (Fig. 8). Temporal variation in the amount of picoplankton loss in Mayagüez Bay for the coastal stations (S13, S15, S21, and S23) was observed. Surface sample of station S13 showed a 0-5% loss, S15 from 0-4%, S21 from 1-15%, and S23 from 0-10% (Fig. 7). Deep samples of stations S13 (0-2%), S15 (0-1%), S21 (1-15%), and S23 (0%) showed a similar amount of picoplankton loss (Fig. 8). Seasonal variability was evident in the surface samples, as the stations sampled on August 2002 had the highest picoplankton loss of all stations except S23 (Figs 7 and 8.) The deep samples taken on February and August 2002 had the highest percent of picoplankton loss. These results, that show temporal variability between the sampling dates, are consistent with the data obtained from United States Geological Services (USGS) on daily river discharge, which showed that the October 2001 cruise concurred with a peak of river discharge, while on February 2002 cruise took place while the river discharge was much lower.

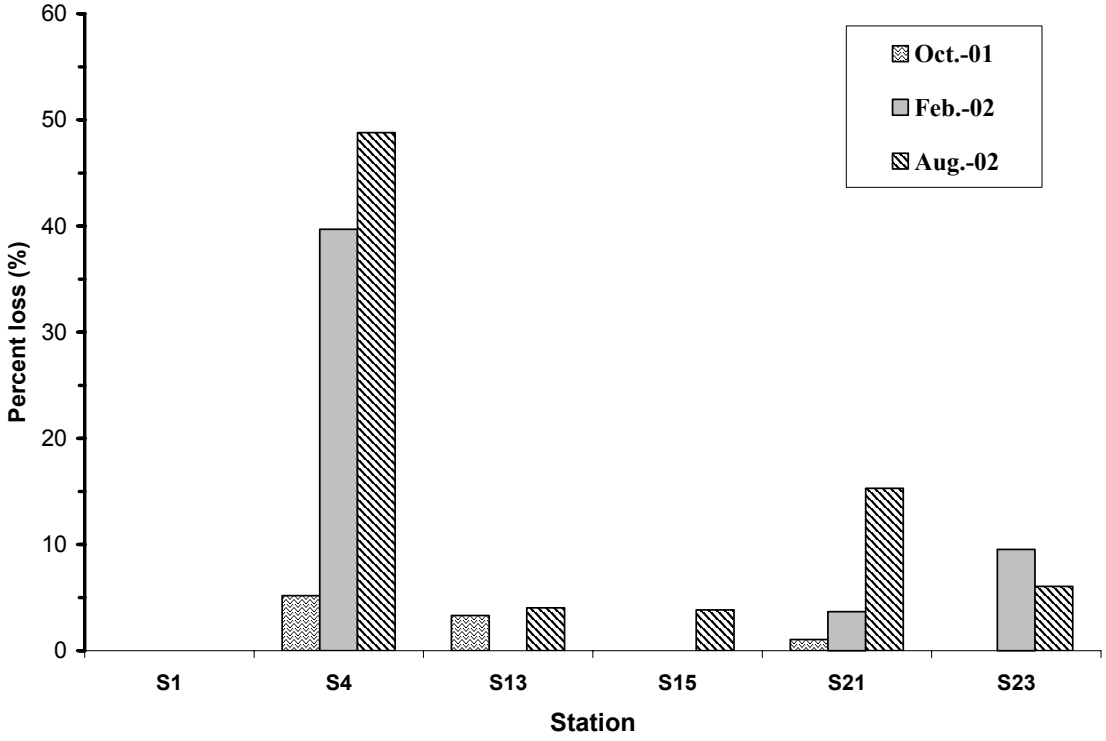

Figure 7. Percent of picoplankton loss through 0.7 μm GF/F filters on various surface samples within Mayagüez Bay.

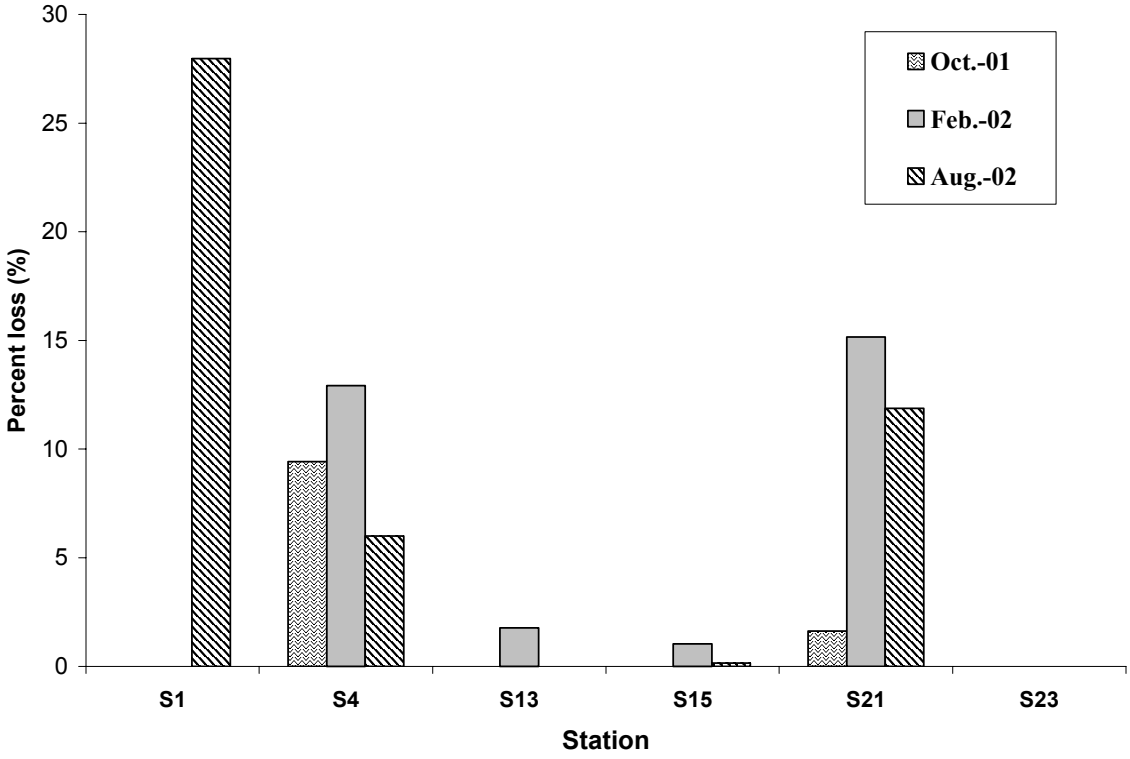

Figure 8. Percent of picoplankton loss through 0.7 µm GF/F filters on various deep samples within Mayagüez Bay.

Picoplankton is a dominant component of the phytoplankton community at CaTS, where in surface samples 48-100% (Fig. 9) and in DCM samples 62-81% (Fig. 10) of the total chlorophyll-a is accounted for by the picoplankton. These results are slightly higher than those reported by Li et al. (1983), Peña et al. (1990), Carrick and Schelske (1997), Brown et al. (1999), Charpy and Blanchot (1999), Chen (2000), Fouilland et al. (2000), Mariñon et al (2001), and Hirose et al. (2003), who have estimated that as much as 40-90% of the chlorophyll-a in oceanic waters may be provided by picoplankton. An explanation for the discrepancy between the data reported here and other reported data is that the amount of picoplankton that escaped through the traditional GF/F filters is being taken into account. If values obtained from GF/F filters were compared, then picoplankton accounts for 35-90% of the total chlorophyll-a for surface samples (Fig. 9) and 53-80% for DCM samples (Fig. 10), results very similar to those reported in the literature cited above.

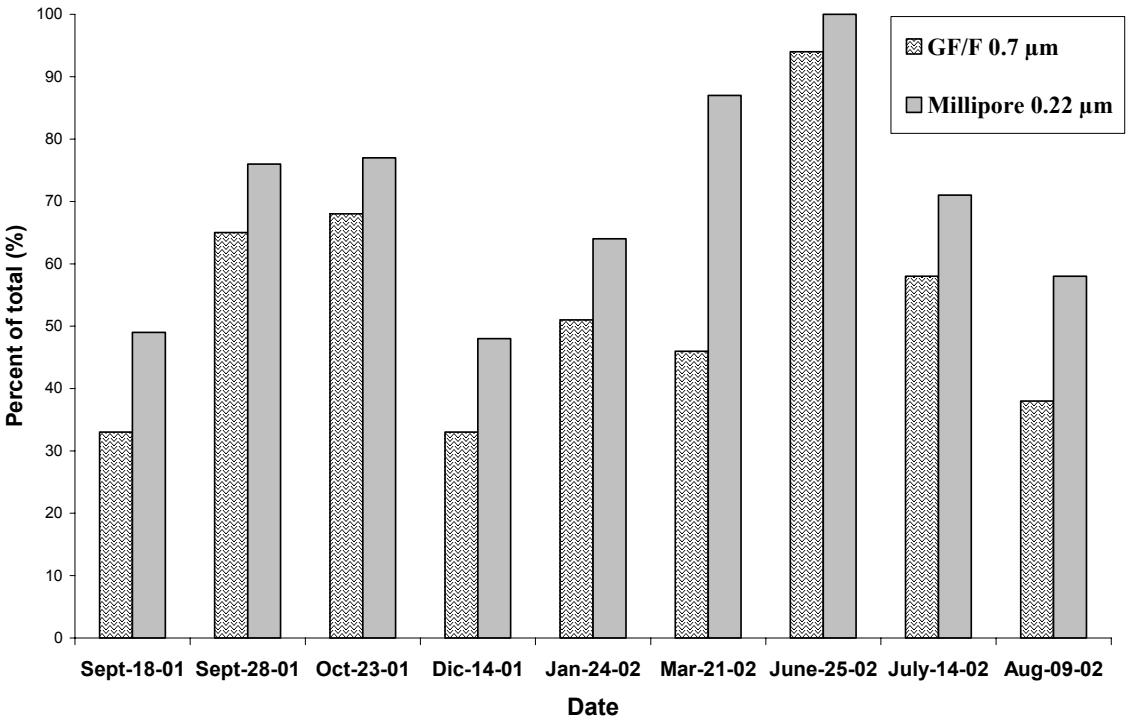

Figure 9. Percent of the total phytoplankton population retained by the different filters, after pre-filtration with a 2.0 µm filter, in CaTS surface samples.

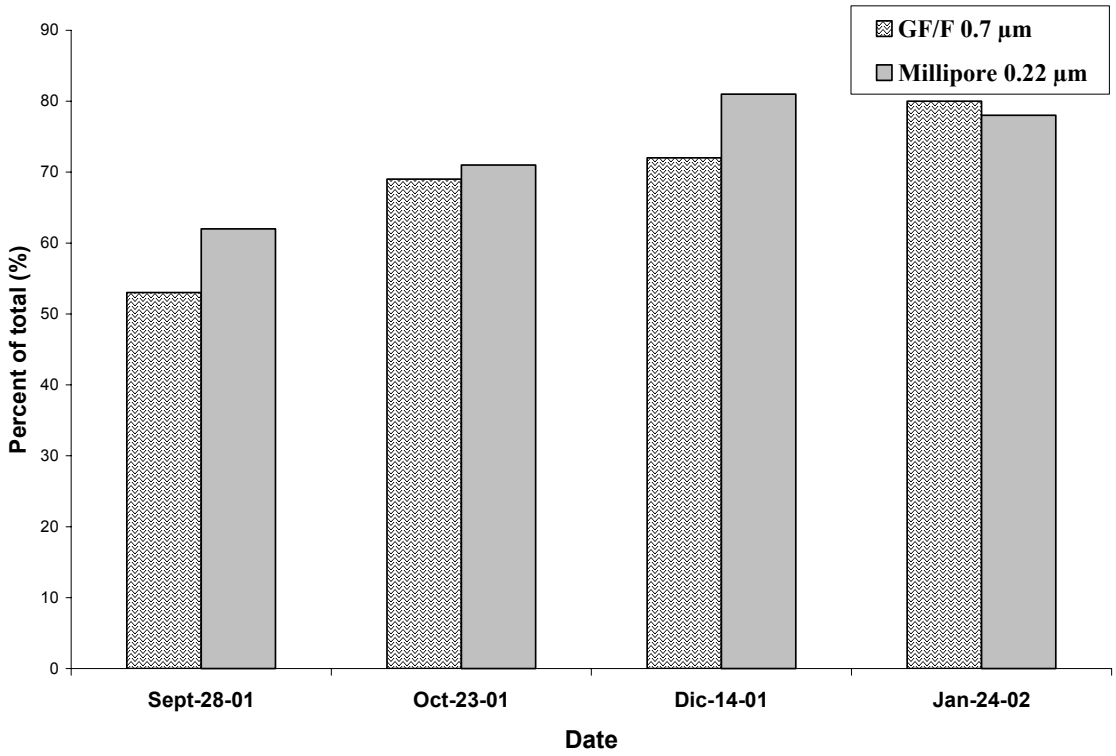

Figure 10. Percent of the total phytoplankton population retained by the different filters, after pre-filtration with a 2.0 µm filter, in CaTS DCM samples.

In other oceanic stations (Mona, Minipex, and Caratlan II) the results were similar; in the Minipex station picoplankton accounted for 55% in surf (Fig. 11) and 56% in DCM samples (Fig. 12), of the total chlorophyll-a. In the Caratlan II stations picoplankton contributed 72-96% and 60-80% for surf (Fig. 11) and DCM samples (Fig. 12) respectively. For Mona's 9:00 am sample the picoplankton contributed 78% while, the 3:00 pm sample contributed 87% of the total chlorophyll-a (Fig. 11), suggesting short-time variability in the population dynamics of phytoplankton in oceanic waters. This variability in the size structure of the phytoplankton community found in the Mona sampling could be do in part to diurnal variations in light intensity. Rapid fluctuations including the daily irradiance cycle and fluctuations that result from change in cloud cover or mixing can have significant effects on the competition between phytoplankton species, and thus on community structure (Siegel et al., 1995; Jacquet et al., 2001; Litchman and Klausmeier, 2001). Litchman and Klausmeier (2001) using simple mathematical models of light showed that the light fluctuations over a wide range of temporal scales (from hourly to seasonal) may have a significant effect on species competition and coexistence.

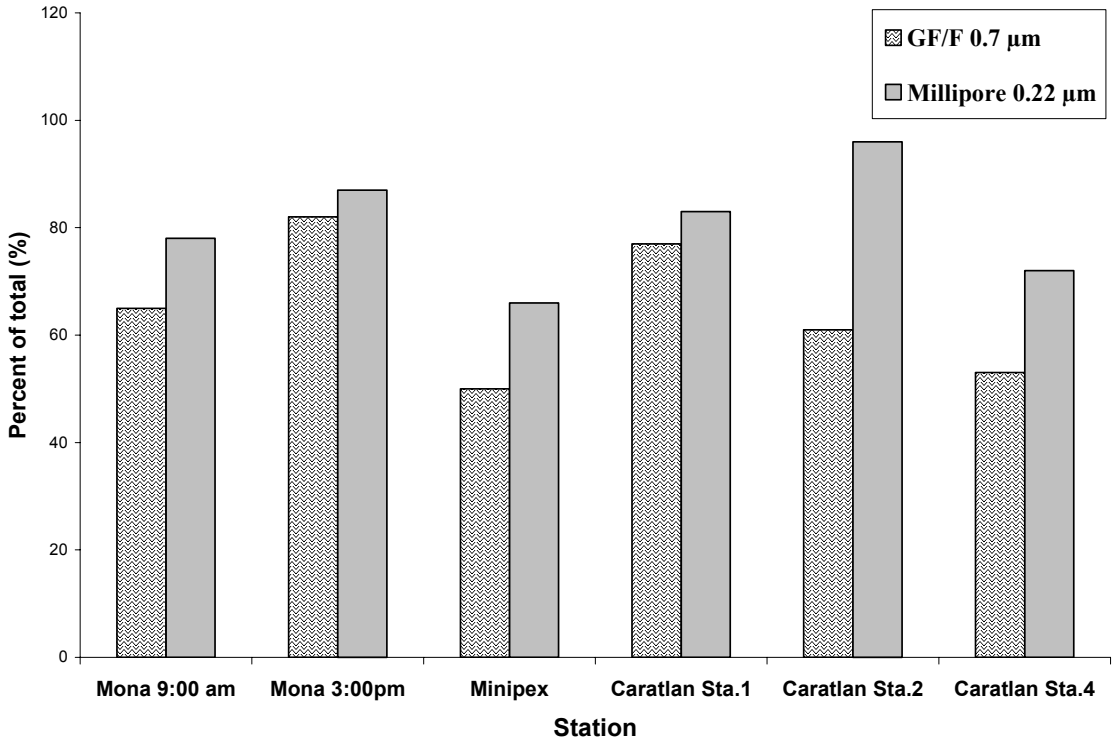

Figure 11. Percent of the total phytoplankton population retained by the different filters, after pre-filtration with a 2.0 µm filter, in oceanic surface samples.

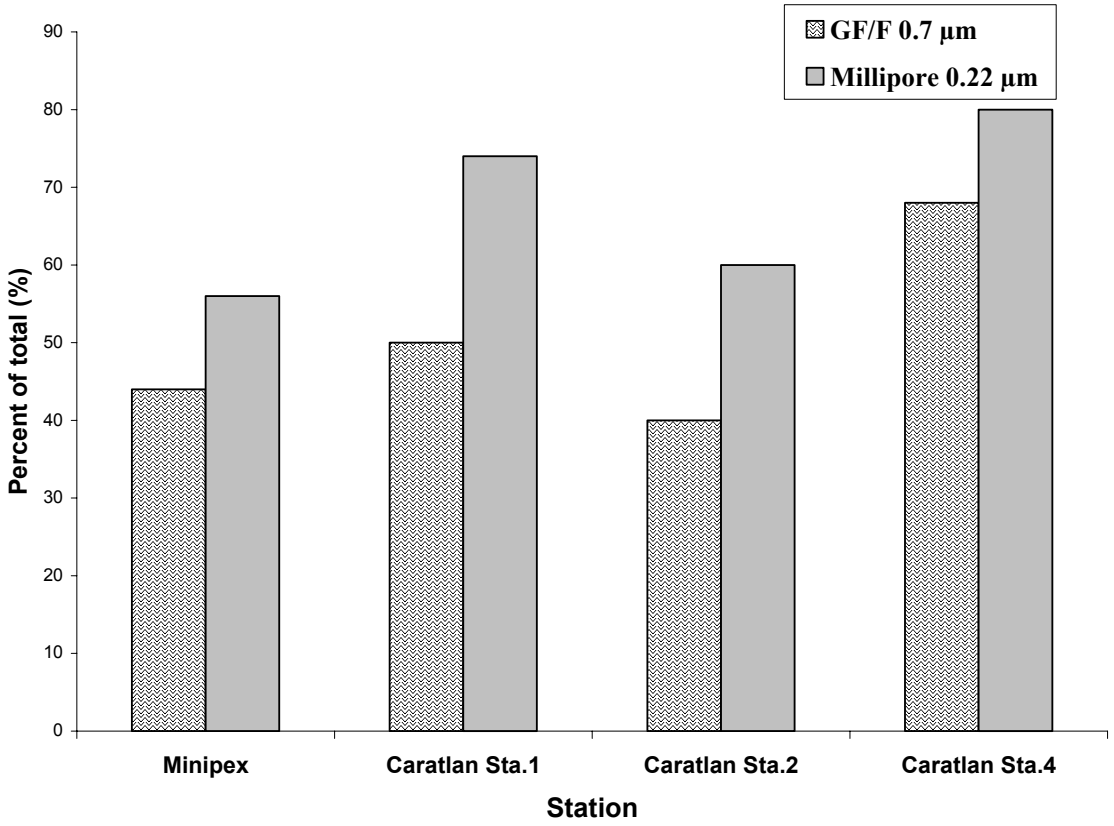

Figure 12. Percent of the total phytoplankton population retained by the different filters, after pre-filtration with a 2.0 µm filter, in oceanic DCM samples.

As in other oceanic stations, similar results where found at the oceanic station (S4) of Mayagüez Bay, where picoplankton contributed from 40-95% for surf (Fig. 13) and 5-48% for deep samples (Fig. 14), of the total chlorophyll-a. In the more coastal stations the contribution of picoplankton to total chlorophyll-a ranged from 0-74% for surface samples (Fig. 13), and from 0-25% for deep samples (Fig. 14). Temporal and spatial variability in the concentration of chlorophyll-a contributed by the picoplankton was seen among and within the different stations in Mayagüez Bay. Being the October 2001 cruise where the picoplankton contributed the least to the chlorophyll-a concentration in all the stations sampled.

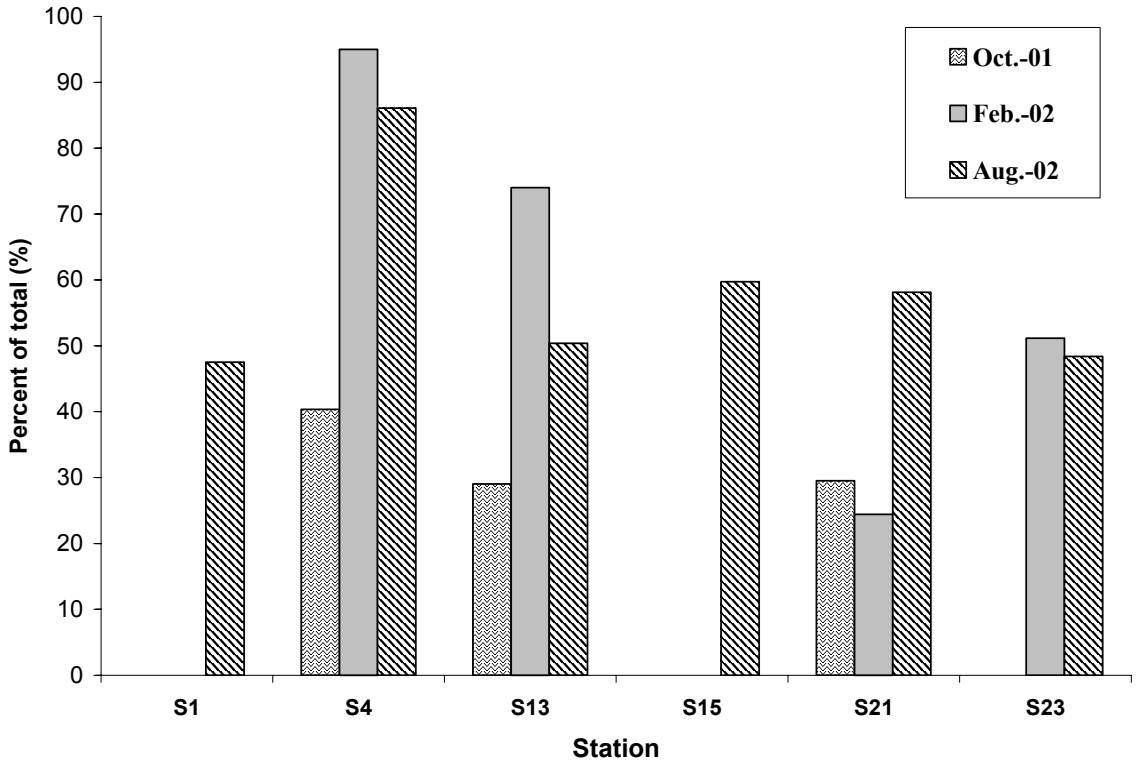

Figure 13. Percent of total chlorophyll-a concentration accounted for by picoplankton in various surface samples in Mayagüez Bay.

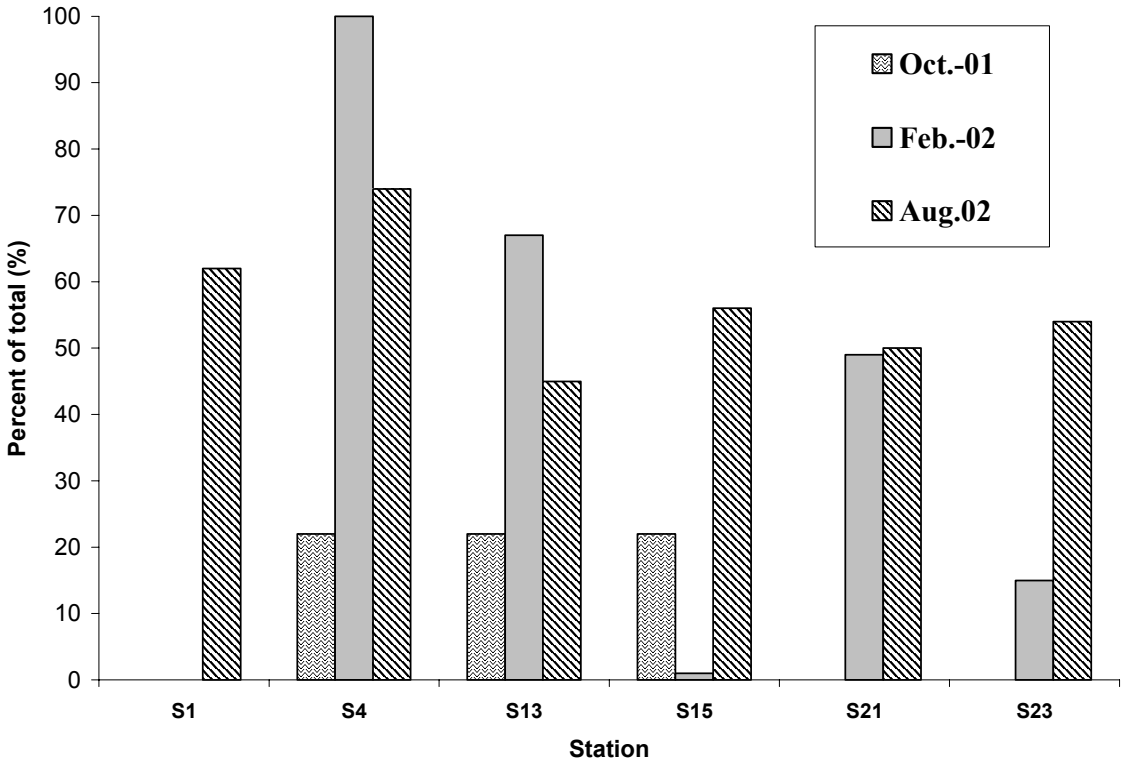

Figure 14. Percent of total chlorophyll-a concentration accounted for by picoplankton in various deep samples in Mayagüez Bay.

Size-fractionated chlorophyll-a

For surface waters at CaTS the samples taken on September 18, 2001, December 14, 2001, and August, 9, 2002, the most abundant size class was the >2.0 μm class, this can be observed in the percent of the total phytoplankton population (Fig. 15) and chlorophyll-a concentration (Fig. 16) graphs. For samples obtained during September 28, 2001, October 23, 2001, January 24, 2002, March 21, 2002, June 25, 2002, and July 14, 2002 the most abundant size class was the 2.0-0.7 μm size class, both in terms of percent of the total phytoplankton population (Fig. 15) and chlorophyll-a concentration (Fig. 16). For all the dates for the CaTS DCM dates the most abundant size class was the 2.0-0.7 μm class, while the 0.7-0.22 μm size class contributed from 0-10% both in percent of the total population (Fig. 17) and chlorophyll-a concentration (Fig.19). Temporal variability is observed for the surface samples as shifting of the size class distribution from larger phytoplankton (>2 μm) during September, December, and August, to a population dominated by picoplankton in the other months (Figs. 15 and 16).

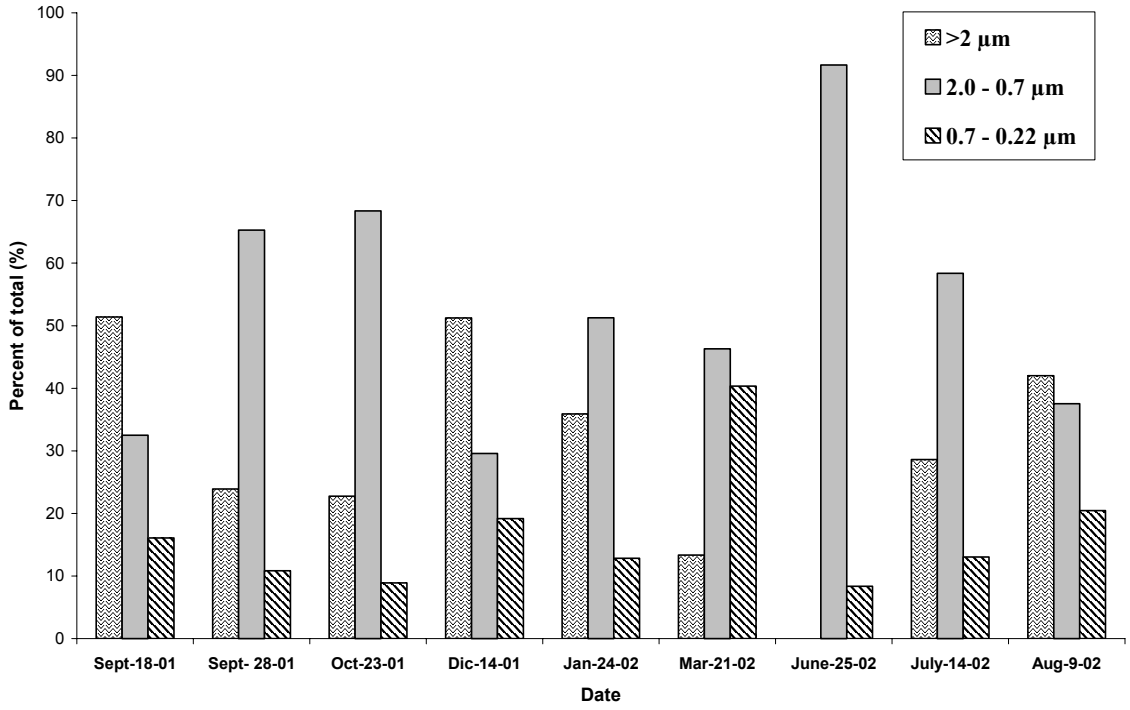

Figure 15. Percent of phytoplankton belonging to the different size classes at CaTS surface waters.

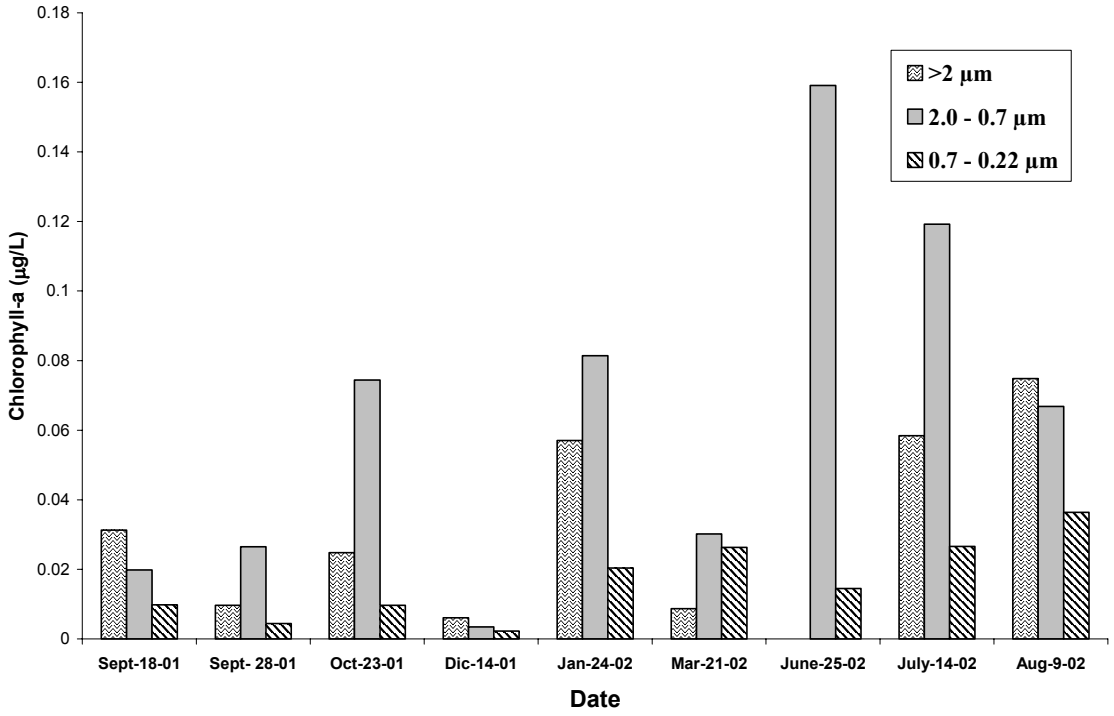

Figure 16. Chlorophyll-a concentration accounted for by the different size classes of phytoplankton at CaTS surface waters.

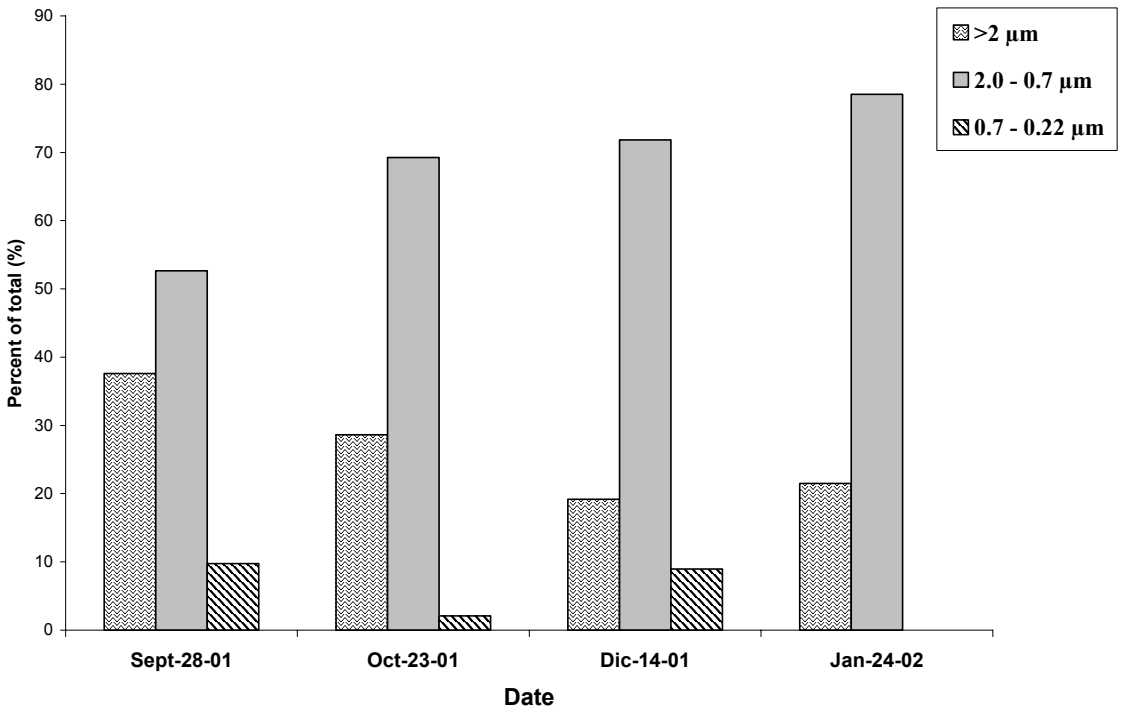

Figure 17. Percent of phytoplankton belonging to the different size classes at CaTS DCM.

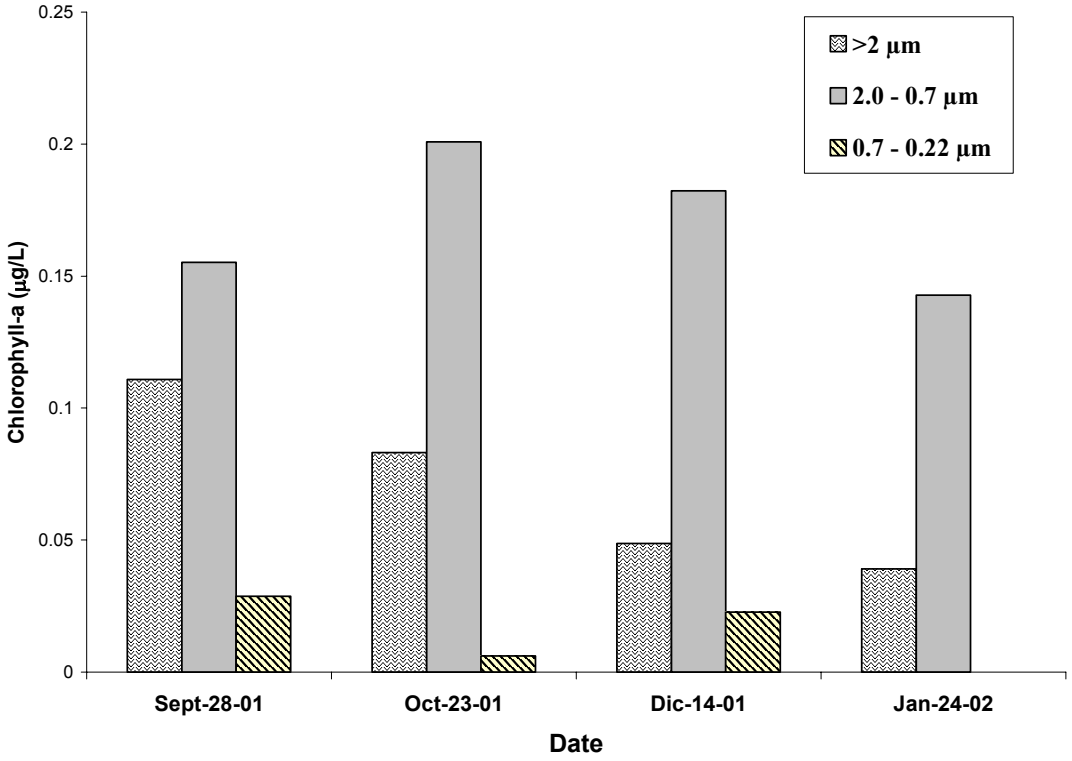

Figure 18. Chlorophyll-a concentration accounted for by the different size classes of phytoplankton at CaTS DCM.

At the other oceanic stations, Mona, Minipex, and Caratlan II, the most abundant size class at all stations was the 2.0-0.7 μm class both in percent of the total phytoplankton population (Figs. 19 and 21) and chlorophyll-a concentration (Figs. 20 and 22). The 0.7-0.22 μm size class contributed from 5-15% in the Mona and Minipex cruises, and from 5-35% in the Caratlan II cruise. In the Mona cruise, although the most abundant size class remained the same at both sampling times, there was short-time variability observed. At the 9:00 am sample the 2.0-0.7 μm size class accounted for 70% of the phytoplankton population, while at the 3:00 pm sample it accounted for 90% (Fig. 21).

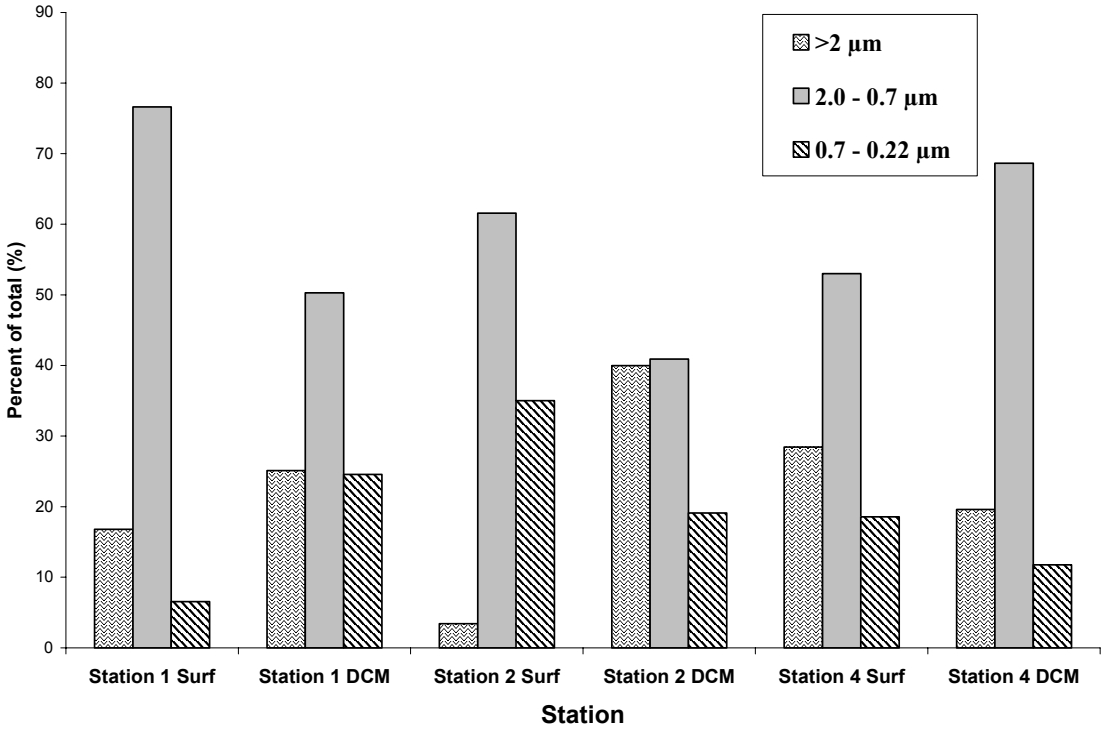

Figure 19. Percent of phytoplankton belonging to the different size classes at the Caratlan II station.

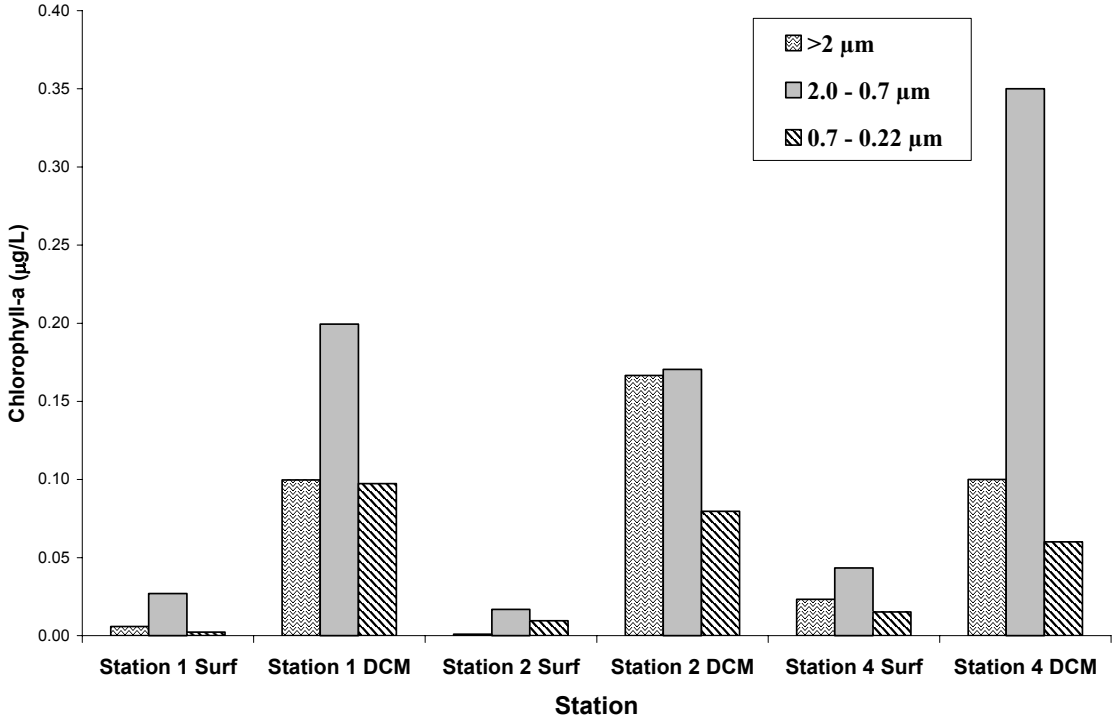

Figure 20. Chlorophyll-a concentration accounted for by the different size classes of phytoplankton at Caratlan II station.

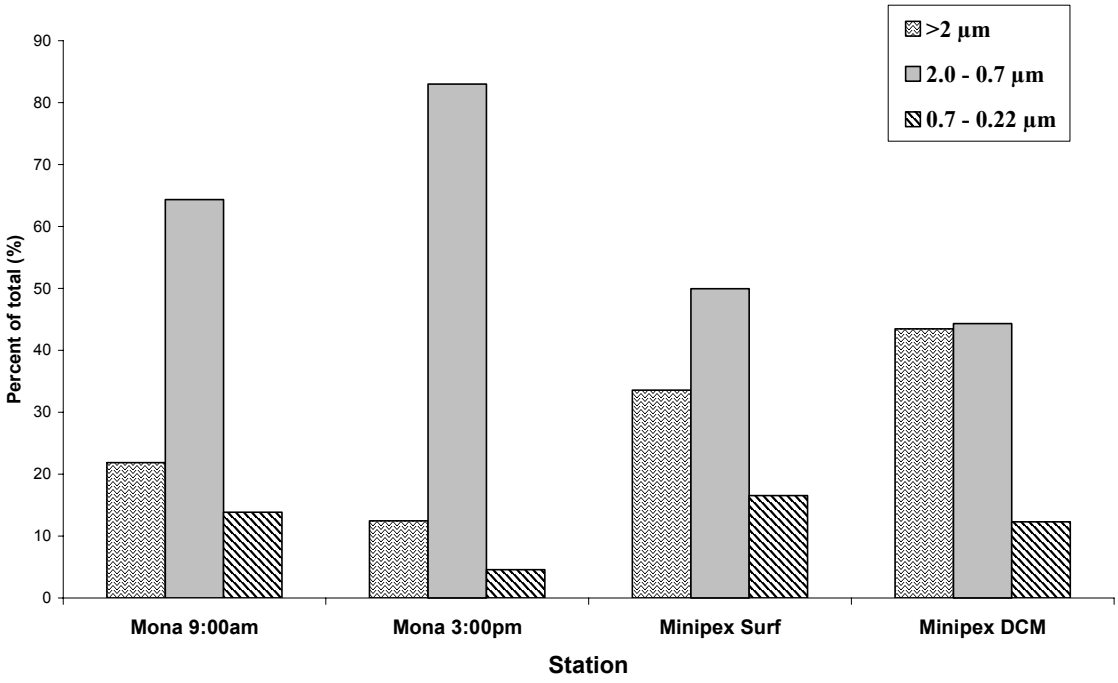

Figure 21. Percent of phytoplankton belonging to the different size classes at Mona and Minipex stations.

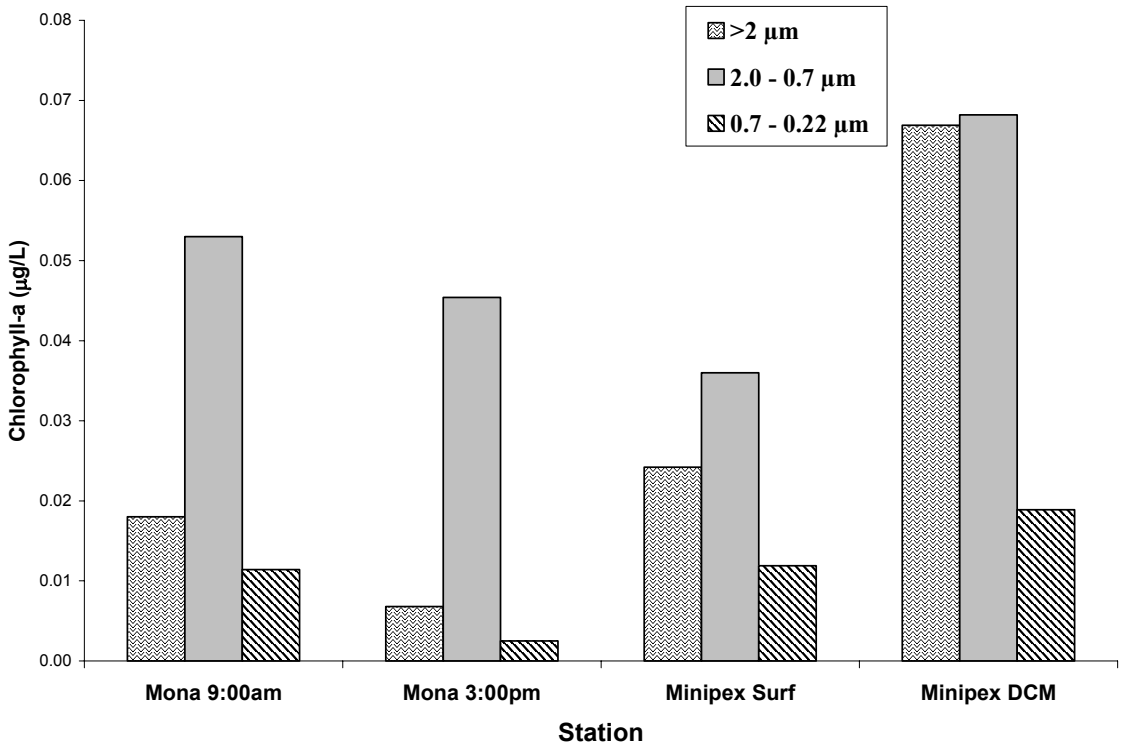

Figure 22. Chlorophyll-a concentration accounted for by the different size classes of phytoplankton at Mona and Minipex stations.

In the October 2001 Mayagüez Bay cruise we observed that for all six stations sampled, including surf and deep, the most abundant size class was that >2.0 μm both in terms of the percent of the total phytoplankton population(Fig. 23) and chlorophyll-a concentration (Fig. 24). For the February 2002 cruise the S4 Surf station was dominated by the 0.7-0.22 μm size class, while the S4 Deep and S13 Surf and Deep stations were dominated by the 2.0-0.7 μm size class, for the rest of the stations (S15 Surf and Deep, S21 Surf and Deep, and S23 Surf and Deep) the most abundant size class was the >2.0 μm class both for percent of total phytoplankton population (Fig. 25) and chlorophyll-a concentration (Fig. 26). For the August 2002 cruise stations; S1 Surf, S1 Deep, S4 Surf, S13 Surf, S13 Deep, S21 Surf, S21 Surf, S21 Deep, and S23 Surf, were dominated by the >2.0 μm size class, while for the rest of the stations, S4 Deep, S15 Surf, S15 Deep, and S23 Deep, the 0.7-.22 μm class was the most abundant both for percent of total population (Fig. 26) and chlorophyll-a concentration (Fig. 28). Of the three cruises, the August 2002 showed the least variability among the different size classes, both in terms of percent of the total phytoplankton population (Fig. 27) and chlorophyll-a concentration (Fig. 28).

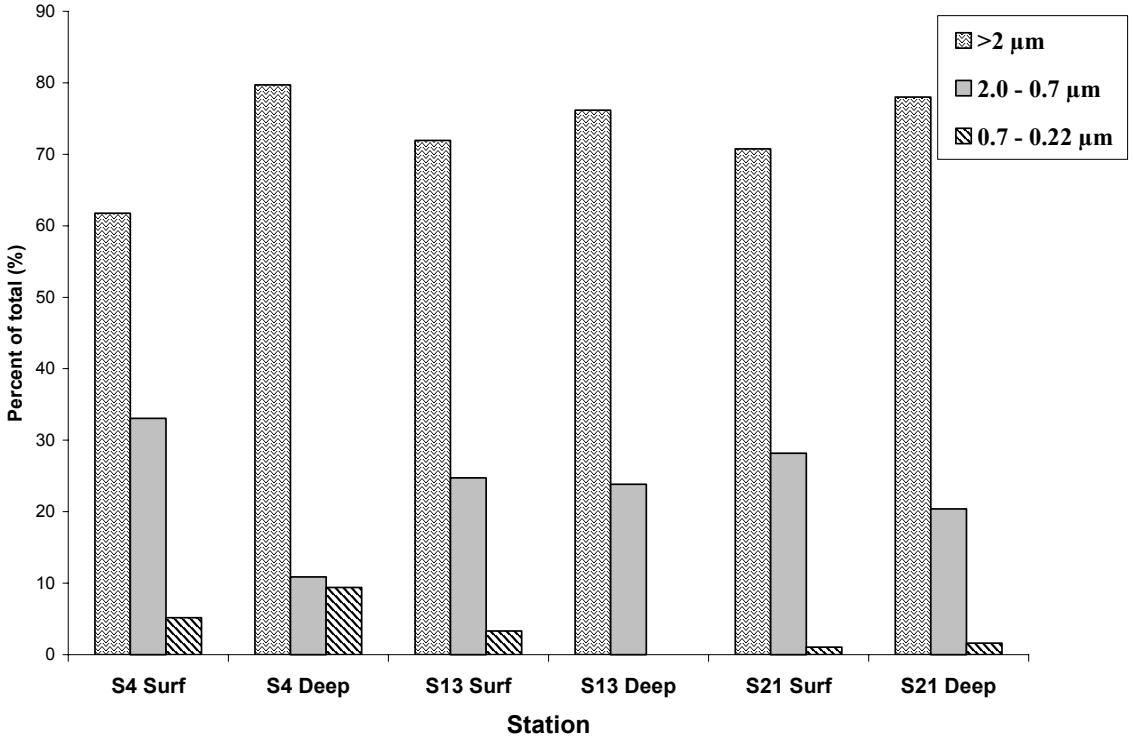

Figure 23. Percent of phytoplankton belonging to the different size classes at the Mayagüez Bay stations during the October 2001 cruise.

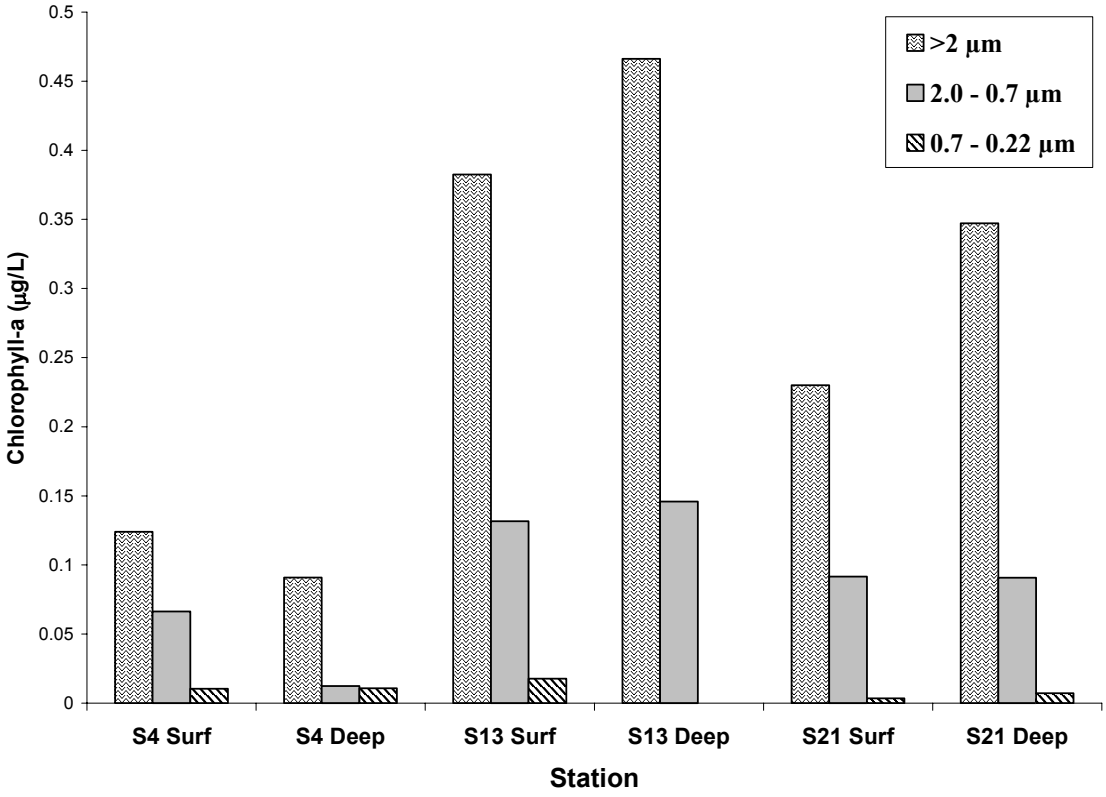

Figure 24. Chlorophyll-a concentration accounted for by the different size classes of phytoplankton at the Mayagüez Bay stations during the October 2001 cruise

.

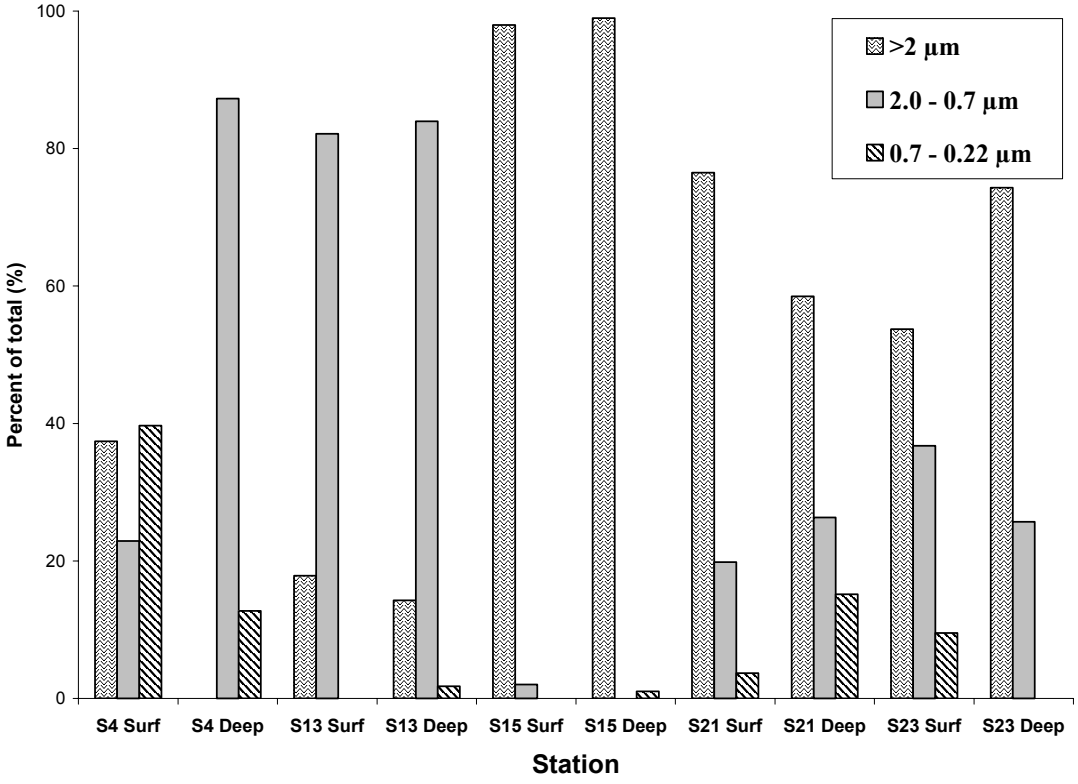

Figure 25. Percent of phytoplankton belonging to the different size classes at the Mayagüez Bay stations during the February 2002 cruise.

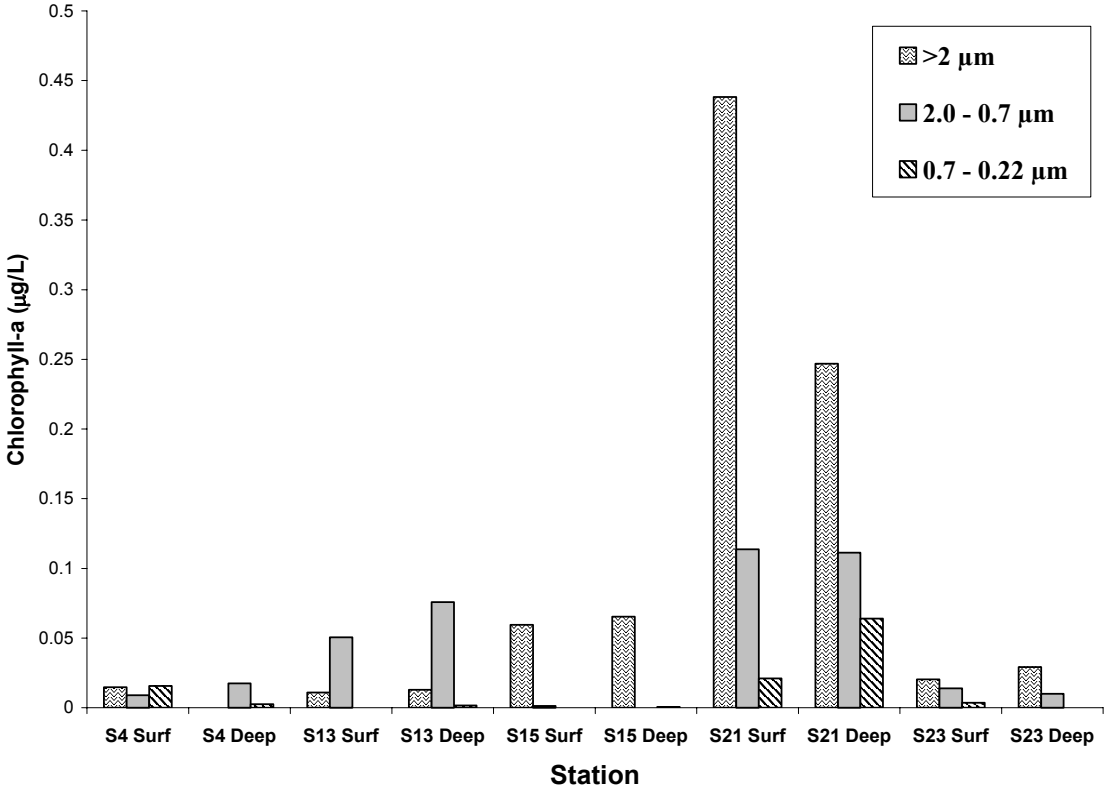

Figure 26. Chlorophyll-a concentration accounted for by the different size classes of phytoplankton at the Mayagüez Bay stations during the February 2002 cruise.

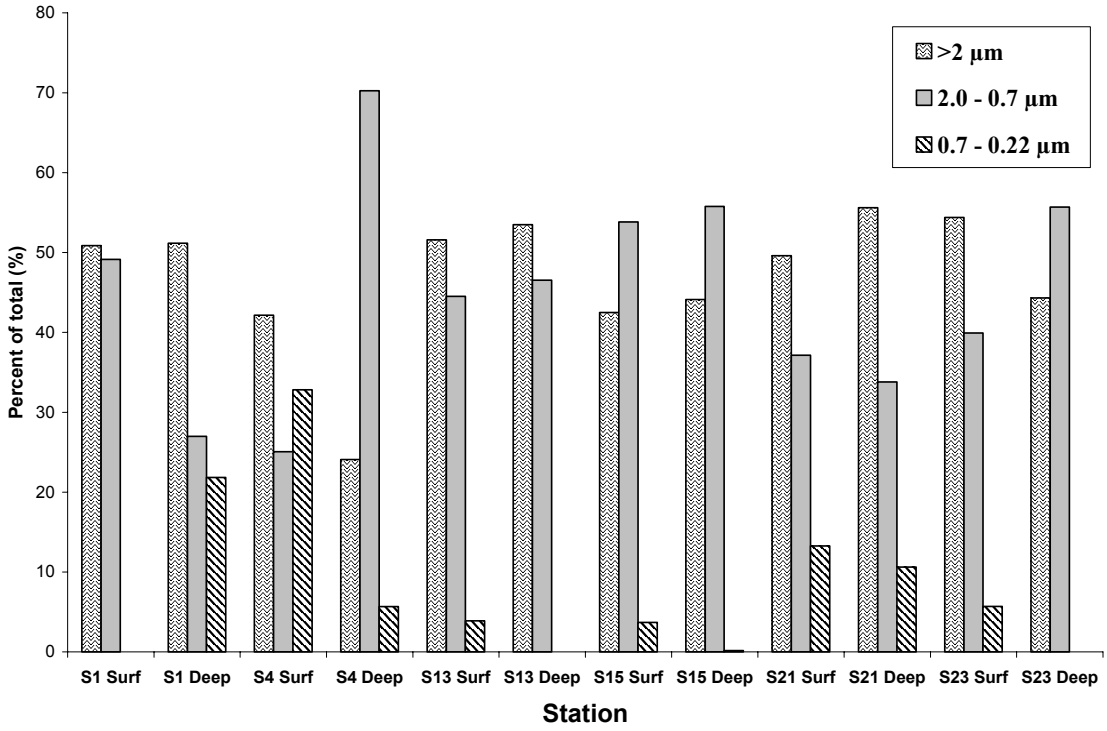

Figure 27. Percent of phytoplankton belonging to the different size classes at the Mayagüez Bay stations during the August 2002 cruise.

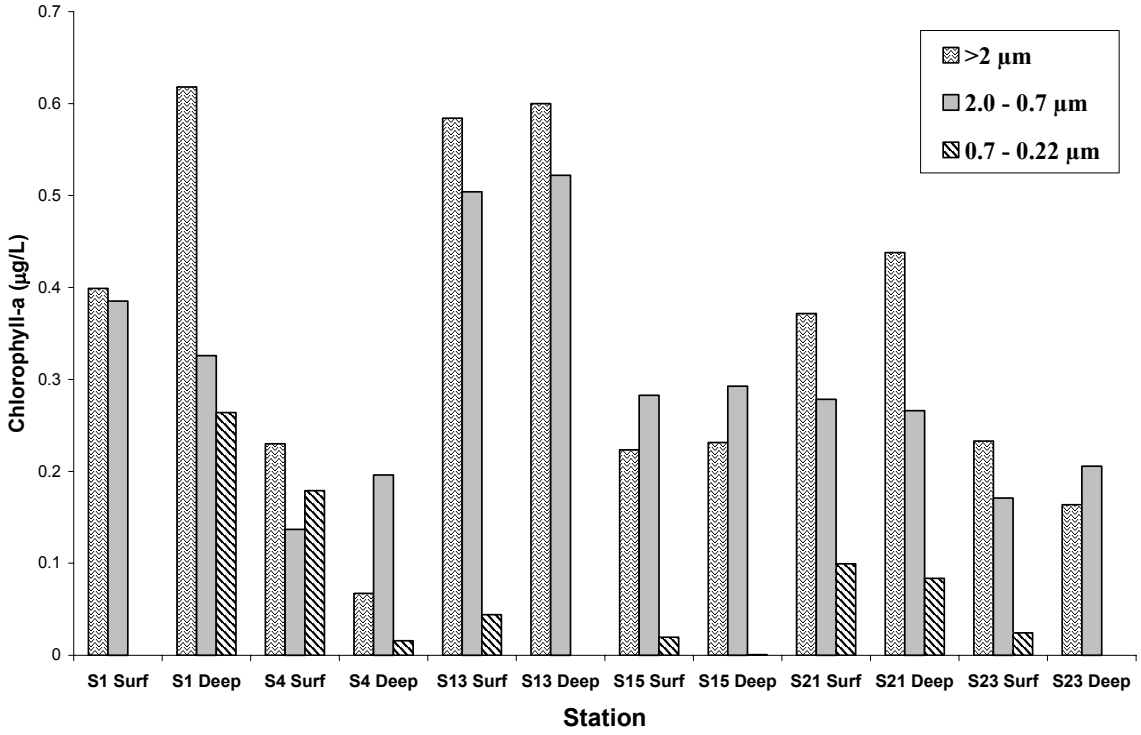

Figure 28. Chlorophyll-a concentration accounted for by the different size classes of phytoplankton at the Mayagüez Bay stations during the August 2002 cruise.

Finally, chlorophyll-a values were correlated to the percent loss of picoplankton, for oceanic and coastal waters (Fig. 29). The correlations were, r=-0.50 for oceanic waters, and r=-0.34 for coastal waters. Negative correlations imply that as chlorophyll-a values increased, the picoplankton loss decreased, suggesting that high chlorophyll-a regions are dominated by larger phytoplankton, and low chlorophyll-a regions are dominated by small phytoplankton. Of course this is a much too simplistic relationship, and as the correlation coefficient suggest, only 50% and 34% of the variation in the variables can be explained by the other, so other forces must be affecting the population dynamics of phytoplankton.

The higher correlation between picoplankton loss and chlorophyll-a value in oceanic waters might be due the fact that nutrient levels in CaTS are low throughout most of the year (Corredor and Morell, 2001). Under low nutrient concentrations picoplankton are at an advantage over the larger phytoplankton, and dominate the phytoplankton population. Low chlorophyll-a values are associated with high picoplankton concentrations, this would explain the negative correlation between chlorophyll-a and picoplankton loss. It has been suggested that the Orinoco River plume transports substantial amounts of terrestrial derived humic material which could ultimately be transformed to the readily available form of ammonium that may constitute a nutrient source to the phytoplankton (Corredor and Morell, 2001). This suggests that the periodic intrusions of continental origin might be a significant force driving the dynamic changes in the population size and size frequency distribution of the phytoplankton at CaTS.

In coastal waters, river runoff and/or urban/industrial discharge provides large amounts of nutrients for the phytoplankton. Under no nutrient limitation the bigger

phytoplankton would be in a competitive advantage over the smaller picoplankton. Hence, the correlation between chlorophyll-a and picoplankton loss would diminish.

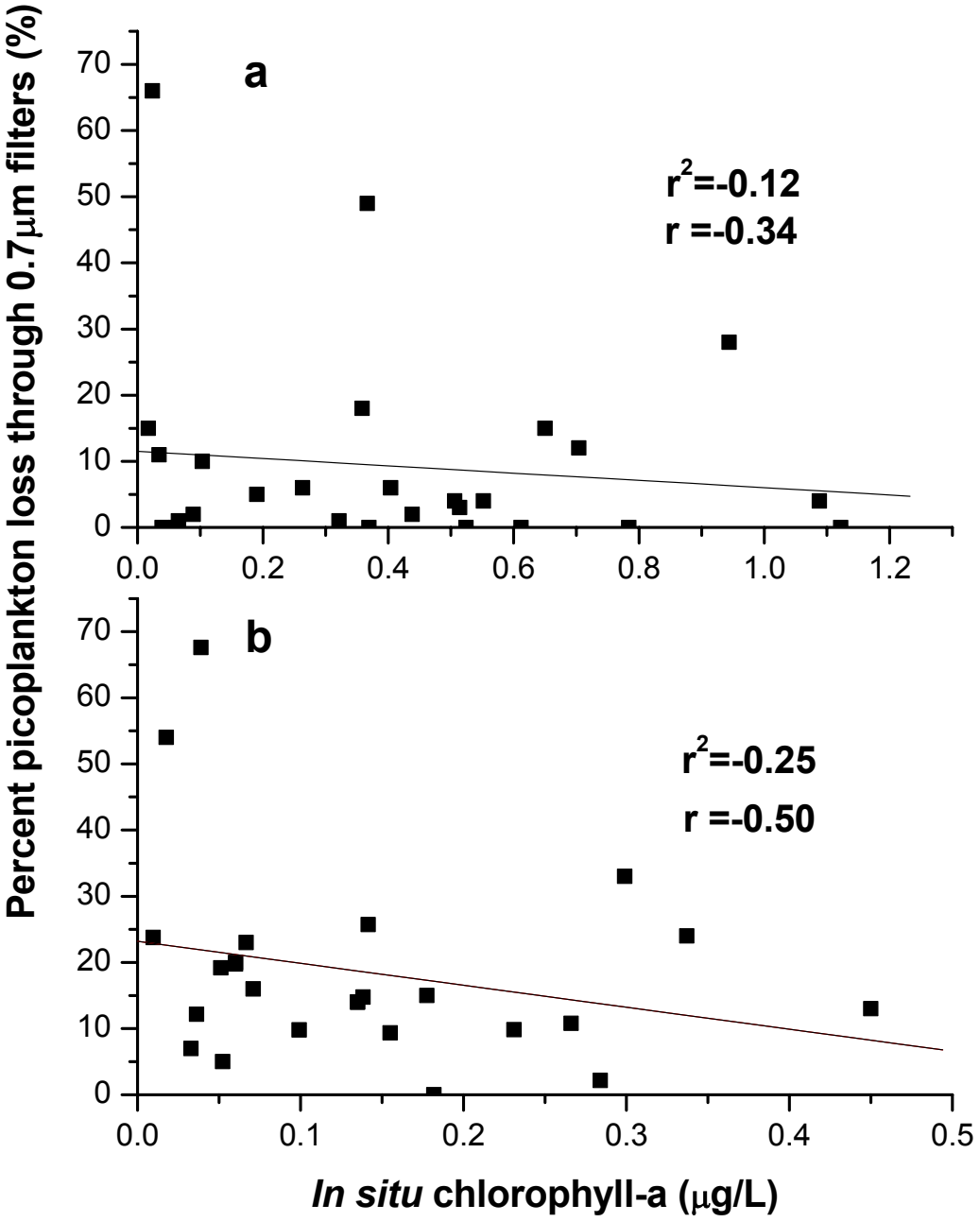

Figure 29. Correlations between *in situ* chlorophyll-a values versus percent picoplankton loss through traditional 0.7 μm GF/F filters: (a) coastal waters, and (b) oceanic waters.

An explanation for the temporal shifts in size frequency distribution seen at CaTS is; that the Eastern Caribbean is under massive freshwater inputs from both direct precipitation and continental runoff (Corredor and Morell, 2001). Zonal trade winds maintained by high-pressure systems in the North Atlantic undergo latitudinal excursions with seasonal displacement of the inter-tropical convergence zone (ICTZ) along a gradient from the Amazon River basin across the Orinoco River basin and into the Central Caribbean. These phenomena result in alternations of dry and rainy periods over the Caribbean and the northern portion of South America. During the dry period, normally centered on the month of April in northern South America, strong easterly winds enhance surface flow through the Caribbean and induce upwelling along the southern Caribbean (Morrison and Smith 1990) and erosion of the pycnocline in the central and northern portion of the basin (Margalef, 1965; Corredor, 1979). Conversely, during the low wind period when the northern portion of the ITCZ is centered over the Caribbean and northern South America there is a strong pycnocline. Satellite remote sensing of chlorophyll-a depicts the seasonality of riverine influence. In the spring, high chlorophyll-a associated with the Amazon river plume can be seen far out in the Atlantic. At this time, high surface chlorophyll-a in the east-central Caribbean is maintained by upwelling processes not related to riverine flow. The NE Caribbean is deeply influenced by the oceanic waters of the Atlantic Ocean at this time. During the fall, flow from the Orinoco River spreads throughout the Eastern Caribbean. This seasonal dynamics in CaTS can help explain in part the shifting size-distribution structure seen in our data over time, as the arrival of nutrient rich waters shifts the size structure of the community towards larger phytoplankton.

The observed dynamics of chlorophyll-a and suspended particulate matter in Mayagüez Bay is related to the dry and rainy season (Gilbes et al., 1996). During the dry season (February and August 2002) low rainfall equals low river run-off (low turbidity) and decrease nutrient concentration, this leads to phytoplankton adaptations, which could include a population shift towards smaller phytoplankton. This community shift towards smaller phytoplankton would be based on the concept that small size is associated to small diffusion boundary layers and large surface area per unit volume (Raven, 1986). This confers small phytoplankton cells an advantage in nutrient poor waters by leading to a greater capacity to acquire nutrients and the efficiency in their use for growth and maintenance (Raven, 1998). During the wet season (October 2001) high rainfall equals high river run-off (increase turbidity) which translates to increase nutrient concentrations, phytoplankton adaptations and increased concentrations of chlorophyll-a. Under no nutrient limitation the bigger phytoplankton would be in a competitive advantage over the smaller picoplankton.

From the above mentioned, we can reach the following conclusions: First, in Case 1 waters, the picoplankton contributes, on average, 74% of the total chlorophyll-a concentration in surface, and 70% in the DCM. For Case 2 waters, the picoplankton accounts 40% of the total chlorophyll-a concentration in surface and 34% for deep samples. Secondly, using traditional 0.7 μm GF/F filters compared to 0.22 μm Millipore membrane filters, there is an average 20% loss of picoplankton in the oceanic stations of the Eastern Caribbean, and an average 9% loss in coastal stations of Mayagüez Bay. Finally, temporal and spatial variability was observed in the contribution of the

picoplankton to the phytoplankton community, and in the amount of picoplankton lost through 0.7 μm filters.

The Contribution of Picoplankton to Remote Sensing Measurements of Ocean Color.

Introduction

The use of remote sensors has allowed us to estimate the concentration of phytoplankton chlorophyll-a based on ocean color measurements. However, these estimates still involve uncertainties due to several factors such as atmospheric conditions, variability in the water constituents, and sensor characteristics. Still, with the recent improvements in ocean color applications, the estimated accuracy level for remote sensed chlorophyll-a concentration is 40-80% (Liu et al., 2003). In order to reduce this margin of error, we need to improve the current ocean color algorithms by collecting more and better field data.

Several bio-optical models and algorithms use the inherent optical properties, those whose magnitude depends only on the substances that compose the medium, and not on the geometric structure of the light field. These properties are the absorption coefficient (a), the scattering coefficient (b) and the beam attenuation coefficient (c). The absorption coefficient is defined as the flow of incident light that is absorbed, divided by the width of the medium. The components that absorb light in the water column are: water itself, particles (detritus and phytoplankton), dissolved organic matter and inanimate particulate matter. The scattering coefficient is equivalent to the flow of incident light that is dispersed, divided by the width of the medium. The beam attenuation coefficient is the sum of the scattering and the absorption coefficients ($c = a + b$). The inherent optical properties can affect the color of the ocean surface, the heat transfer, the penetration of ultraviolet light and photosynthetic available radiation (PAR)

in the water column and the visibility of the water. Retrieval of inherent optical properties is the critical first step in satellite determination of oceanic constituents and their concentrations (Kirk, 1994).

Ocean color, and in particular, the chlorophyll-a concentration in the upper layers of the ocean has been measured by the Coastal Zone Color Scanner (CZCS) carried on the Nimbus-7 satellite launched in 1978 and by the Sea-viewing Wide Field-of-view Sensor (SeaWiFS) carried on Orbview-2, launched in 1997, and most recently by the Moderate-Resolution Imaging Spectroradiometer (MODIS) carried on the Terra and Aqua satellites. The latter instruments measures upwelling radiance in different wavelength bands. Most of the upwelling radiance seen by the satellite comes from the atmosphere and only about 10% comes from the sea surface. Since both air molecules and aerosols scatter light very accurate techniques have been developed to remove the influence of the atmosphere. The total radiance L_t received by an instrument in space is:

$$L_t(\lambda_i) = t(l_i)\, L_W(l_i) + L_r(l_i) + L_a(l_i) \qquad (1)$$

where λ_i is the wavelength of the radiation in the band measured by the instrument, L_W is the radiance leaving the sea surface, L_r is radiance scattered by molecules, called the Rayleigh radiance, L_a is radiance scattered from aerosols, and t is the transmittance of the atmosphere. L_r can be calculated from theory and L_a can be calculated from the amount of red light received at the instrument because very little red light is reflected from the water. Therefore L_W can be calculated from the radiance measured at the spacecraft.

Since the launch of the SeaWiFS, global ocean color data are readily available to the scientific community. This sensor has a 2801 km swath width and a nadir resolution of 1.1 km^2 per pixel. It has six spectral bands (412, 443, 490, 510, 555, 670 nm) in the

visible region and two in the near infrared (NIR), which are used for atmospheric correction. Most recently, the launch of MODIS on board the Terra (EOS AM-1) and Aqua (EOS PM) satellites has provided yet another tool for the large scale study of the ocean. MODIS has a 2330 km swath width with a nadir resolution of 1.0 km^2 per pixel at bands 8-36. It has 36 spectral bands, being bands 8-36 primarily used for ocean color, phytoplankton, and biogeochemistry. Bands 9 (443 nm), 12 (551 nm), and 13 (667 nm) being analogous to the SeaWiFS bands utilized in the bio-optical algorithms. Still with all the latest improvements in the development of algorithms and more sensitive sensors, in order to get good estimates, it is necessary to assume that the parameters of the model are consistent with the studied waters. There have been very few studies in the Eastern Caribbean to determine the optical properties of these waters and no studies on the contribution of the picoplankton to these properties.

Eastern Caribbean waters are diverse and can be classified according to their bio-optical characteristics. A classification which has been found useful in the context of remote sensing of the oceans is that of "Case 1" and "Case 2" waters, put forward by Morel and Prieur (1977) and further refined by Gordon and Morel (1983). Case 1 waters are those for which phytoplankton and their derived products (organic detritus and dissolved yellow substance, arising by zooplankton grazing, or natural decay of algal cells) play a dominant role in determining the optical properties of the ocean. Case 2 waters are those for which an important or dominant contribution to the optical properties comes from resuspended sediments from continental shelf, or from particles and/or dissolved organic matter in river runoff or urban/industrial discharge. In Case 2 waters, phytoplankton and their derivative products may or may not also be present in significant

amount. We studied Case I waters in CaTS, Mona, Minipex, and Caratlan II stations, and Case 2 waters in Mayagüez Bay.

The aim of this work was to use remote sensing data to measure the spatial and temporal variations in phytoplankton and picoplankton composition, and how this is affected by the intrusions of Orinoco and Amazon river waters into the Caribbean Sea (Müller-Karger et al., 1989) and at local scales by the influence of small rivers in Mayagüez Bay (Gilbes et al., 1996).

The objectives of this study were to:

- Compare *in situ* chlorophyll-a values with those estimated using different algorithms with a field spectroradiometer, and from SeaWIFS imagery for the Caribbean Time Series Station (CaTS).
- Determine the associated optical properties of the picoplankton found in the selected Case 1 and Case 2 waters.
- Evaluate the contribution of the picoplankton to the optical properties of the studied waters.

Materials and Methods

Bio-Optical Measurements

Particulate absorption samples were collected on 0.7 μm GF/F filters, which were placed on a drop of distilled water and the absorption of the total particulate $a_p(\lambda)$ (relative to a blank filter saturated with distilled water) was measured with a Li-Cor integrating sphere attached to a GER 1500 portable spectroradiometer using the method developed by Mitchell and Kiefer (1984). Methanol- extractable pigments were removed by slowly passing hot methanol through the filter pad (Roesler et al., 1989). The absorption spectrum of this pad was measured to determine the detritus absorption coefficient, $a_d(\lambda)$. Optical density measurements were divided by the geometrical path length (volume filtered divided by clearance area of the filter) and multiplied by a factor of 2.3 (conversion factor for transforming decimal logarithms to natural logarithms) to obtain the absorption coefficient. The value of the absorption coefficient at 750 nm was subtracted from the values at all other wavelengths, as a rudimentary correction for errors arising from scattering by the phytoplankton cells. The measurements were corrected for path-length amplification, β factor, using the method of Bricaud and Stramski (1990). The difference between the particulate and detritus spectra, before and after the methanol extraction, is considered the *in vivo* phytoplankton absorption, $a_{ph}(\lambda)$. Pigment specific absorption coefficient of phytoplankton, $a_{ph*}(\lambda)$ was calculated by dividing absorption by the chlorophyll-a concentration obtained fluorometrically.

Bio-optical algorithms:

Chlorophyll-a concentration was calculated using the following algorithms with the normalized water leaving radiance (nL_w) and remote sensing reflectance (Rrs) being calculated by data obtained from a portable spectroradiometer (GER 1500).

Water radiance, $L_0(\lambda)$, sky radiance, $L_s(\lambda)$, and the above surface downwelling irradiance, $E_d(0+,\lambda)$ were measured using a GER 1500 portable spectroradiometer. $L_0(\lambda)$ was measured aiming the GER 45º to the vertical into the water surface, maintaining an azimuth of 90º from the solar plane to minimize sun glint. $L_s(\lambda)$, was measured pointing the GER 45º to the vertical to the sky, maintaining an azimuth of 90º from the solar plane. $E_d(0+,\lambda)$ was measured pointing directly upward using a cosine collector attached to the GER. The remote sensing reflectance, $R_{rs}(\lambda)$, was calculated using the following equation:

$$R_{rs}(\lambda) = L_0(\lambda) - f\,(L_s(\lambda))/E_d(0+,\lambda) \qquad (2)$$

where *f* is the Fresnel's number, the percent of sky radiance reflected back to the atmosphere. Fresnel's number has a value of 0.028 at a 45º angle.

The algorithms used for estimating chlorophyll-a concentration were the following:

(1) CZCS Algorithm (Gordon et al., 1983)

Case 1 waters, pigments < 1.5 mg m^{-3}

$$\text{Pigments} = 1.13(nL_w\,443 / nL_w550)^{-1.71} \qquad (3)$$

where $nL_w(\lambda) = R_{rs}(\lambda) * F_o(\lambda)$, and F_o = is the extraterrestrial irradiance, and it varies with wavelength.

(2) SeaWiFS Algorithms (O'Reilly et al., 1998)

OC-2_{v4}

Chl-a (µg/l) $=10^{[a_0 + a_1 R + a_2 R^2 + a_3 R^3 \}+ a_4}$ (4)

where $R= \log_{10} (R_{rs} 490/R_{rs}555)$

$a_0 = 0.319$
$a_1 = -2.336$
$a_2 = 0.879$
$a_3 = -0.135$
$a_4 = -0.071$

OC-4_{v4}

Chl-a (µg/l) $=10^{[a_0 + a_1 R + a_2 R^2 + a_3 R^3 + a_4 R^4]}$ (5)

where $R= \log_{10} (R_{rs} 443 > R_{rs} 490 > R_{rs} 510/R_{rs}555)$

$a_0 = 0.366$
$a_1 = -3.067$
$a_2 = 1.930$
$a_3 = 0.649$
$a_4 = -1.532$

(3) MODIS Algorithm (Clark et al., 1999)

log total chlorophyll-a = $-1.594 (\log (R_{rs} 442/R_{rs} 547))^3 + 1.122 (\log (R_{rs} 442/R_{rs} 547))^2 - 1.396 (\log (R_{rs} 442/R_{rs} 547)) - 0.0922$ (6)

Satellite Imagery

SeaWiFS Level 1 images were obtained, for the different dates (from October 1997 to August 2002) in which CaTS was sampled, from the satellite receiving stations at the University of Puerto Rico-Mayagüez and the University of South Florida. Some SeaWiFS images from the date of the sample were unusable because of large cloud coverage, in which case the SeaWiFS image closest to the sampling date was used. Images were then be processed from Level 1 to Level 0 then to Level 1, Level 2, and

finally to Level 2 mapped (Level 3) using the NASA SeaDAS 4.1 program (Fig. 30). The pixel that represented the exact location of CaTS was located on the image, and was used as the center pixel for generating a 3 x 3 grid. The values for the nine pixels were averaged, and the standard deviation and confidence intervals were calculated. Chlorophyll-a values obtained from SeaWIFS imagery, using the OC-2_{V4} and OC-4_{V4} algorithms, were compared to values obtained *in situ* and from different algorithms calculated with data obtained from a GER 1500 spectroradiometer.

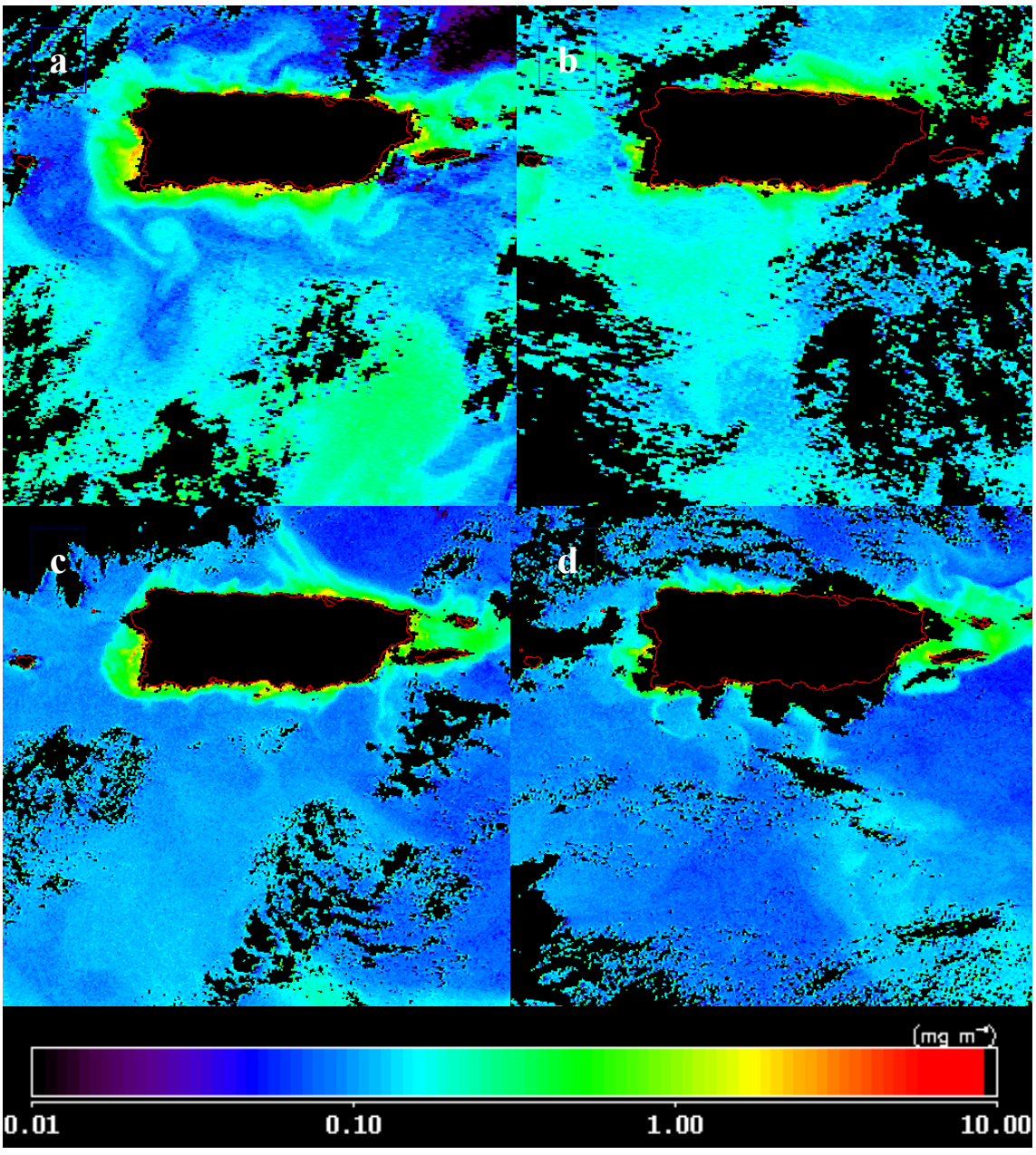

Figure 30. Sample images of Puerto Rico and CaTS station obtained from SeaWiFS. a) October, 21, 1997. b) December, 11, 1998. c) March, 17, 1999. d) March, 1, 2000.

Statistical analysis

Correlation coefficients, *r*, and coefficients of determination, r^2, were calculated through MicroCal Origin 6.0. Correlations were calculated for the different algorithms from GER 1500 data or SeaWiFS imagery, versus the *in situ* chlorophyll-a. Correlations in which the amount of picoplankton loss through the use of 0.7 μm filters was taken into consideration where then calculated. As already described, in the oceanic waters of the Eastern Caribbean there is an approximate 20% loss of picoplankton through traditional 0.7 μm filters. We decided to add 20% of the chlorophyll-a value (which represented the picoplankton loss) to those chlorophyll-a values <0.20 μg/L. Those values, referred from know on as "*in situ* + pico", were then correlated to the satellite and algorithm values.

Tests were performed to determine: a) if a significant correlation between the values existed and b) if two correlation coefficients were significantly different from one another, following the procedure in Sokal and Rohlf, 1995.

Results and discussion

Satellite versus *in situ* chlorophyll-a

The correlation between satellite and calculated algorithm was higher for OC-4_{v4} than the correlation for the OC-2_{v4} algorithm, r^2=0.696 and r^2=0.549 respectively (Fig.31). The correlation between satellite data, obtained through the OC-4_{v4} algorithm, and *in situ* data was low, r^2=0.456, while slightly higher, r^2=0.615, when *in situ* data was compared to the chlorophyll-a concentration obtained with the OC-4_{v4} algorithm using GER data (Fig. 32). Extending this further, we compared the *in situ* chlorophyll-a concentration with the corresponding chlorophyll-a value retrieved with the SeaWiFS OC-4_{v4} algorithm (Fig. 33), and found that when the *in situ* chlorophyll-a concentration falls bellow 0.20 μg/L, SeaWiFS overestimated the chlorophyll-a value in 78% (24 of 31) of the samples. Conversely when the concentration *in situ* chlorophyll-a were above 0.20 μg/L, SeaWiFS underestimated the value in 100% of the samples (5 of 5). These results are consistent with those of Clementson et al. (2001) and Barlow et al. (2001), who working in the Southern Ocean and in the southern Benguela ecosystem, respectively, noticed that SeaWiFS overestimated chlorophyll-a for concentrations <0.2 μg/L and underestimated chlorophyll-a for concentrations >0.2 μg/L.

Correlations between Gordon algorithm calculated with GER data and *in situ* chlorophyll-a values were slightly higher, r^2=0.634, than the correlation with the *in situ* chlorophyll-a + pico, r^2=0.624 (Fig. 37). The correlation value for OC-4_{v4} calculated with GER data versus *in situ* chlorophyll-a and *in situ* chlorophyll-a + pico, was r^2=0.615 and r^2=0.674, respectively (Fig. 34). The correlation of MODIS versus *in situ*

chlorophyll-a and *in situ* chlorophyll-a + pico, was r^2=0.671 and r^2=0.701 respectively (Fig. 35). Complete comparisons are given in Figs 31-37.

Adding the estimated picoplankton loss to the in situ chlorophyll-a value increased the correlations between all algorithms, except for the Gordon 1 algorithm (Table 1). The increases in the correlation values were not statistically significant in any of the comparisons (Table 1).

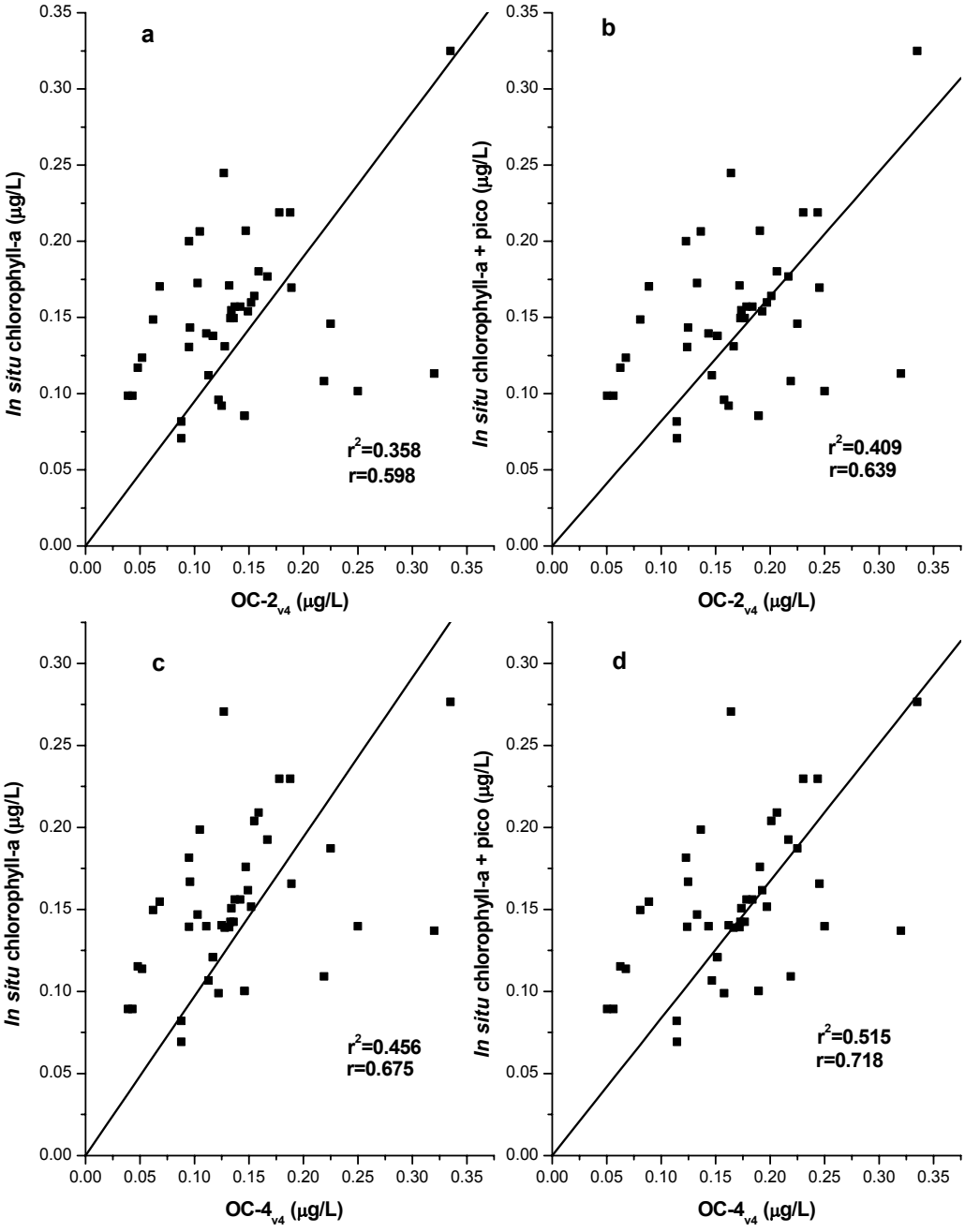

Figure 31. Comparisons between chlorophyll-a concentrations obtained with: (a) SeaWiFS OC-2_{v4} algorithm from imagery and *in situ*, (b) SeaWiFS OC-2_{v4} algorithm from imagery and *in situ* + pico, (c) SeaWiFS OC-4_{v4} algorithm from imagery and *in situ*, and (d) SeaWiFS OC-4_{v4} algorithm from imagery and *in situ* + pico. n=42.

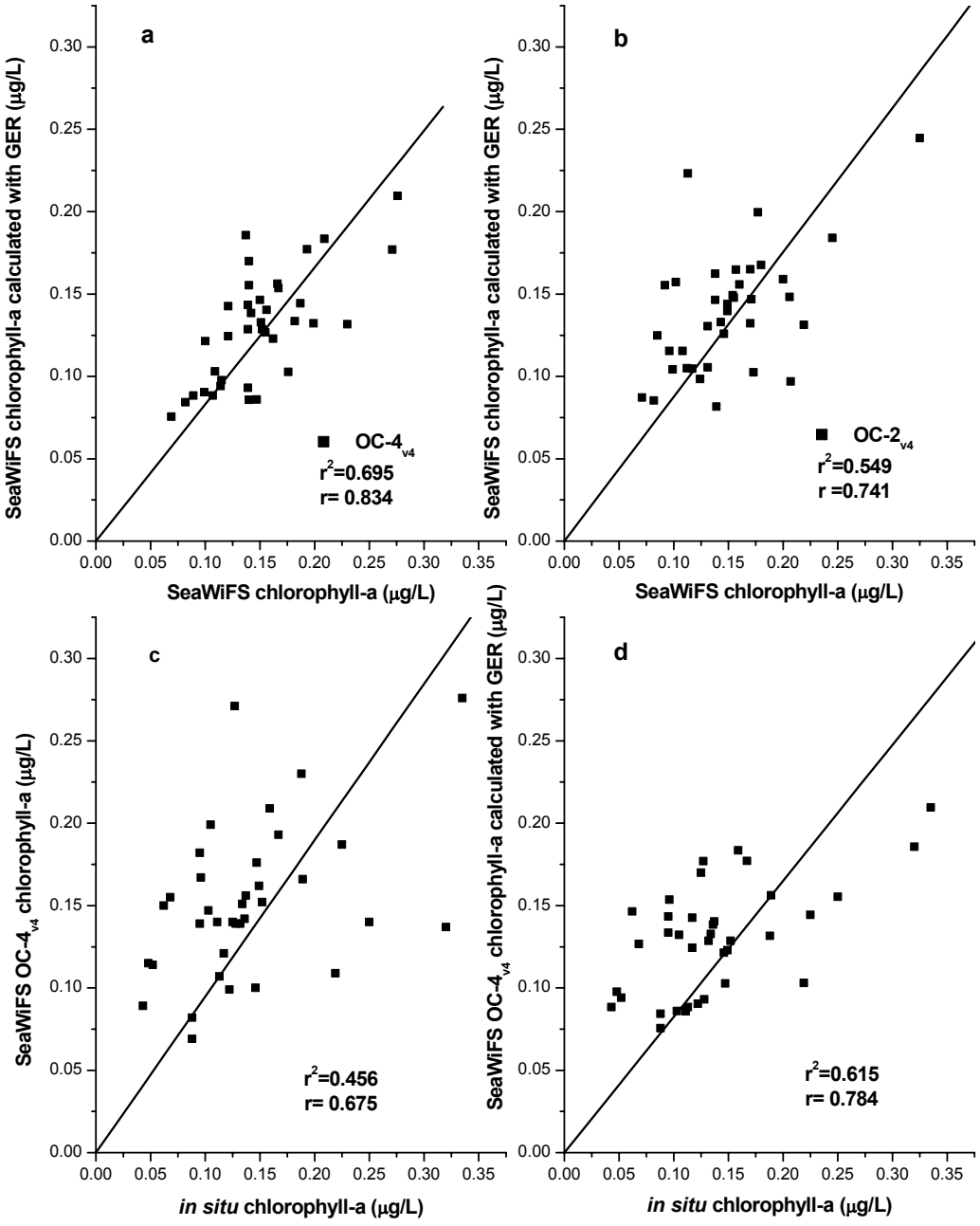

Figure 32. Comparisons between chlorophyll-a concentrations obtained with: (a) SeaWiFS OC-4_{v4} algorithm from imagery and calculated from GER data, (b) SeaWiFS OC-2_{v4} algorithm from imagery and calculated from GER data, (c) SeaWiFS OC-4_{v4} algorithm from imagery and *in situ*, and (d) OC-4_{v4} algorithm calculated from GER data and *in situ*. n=42.

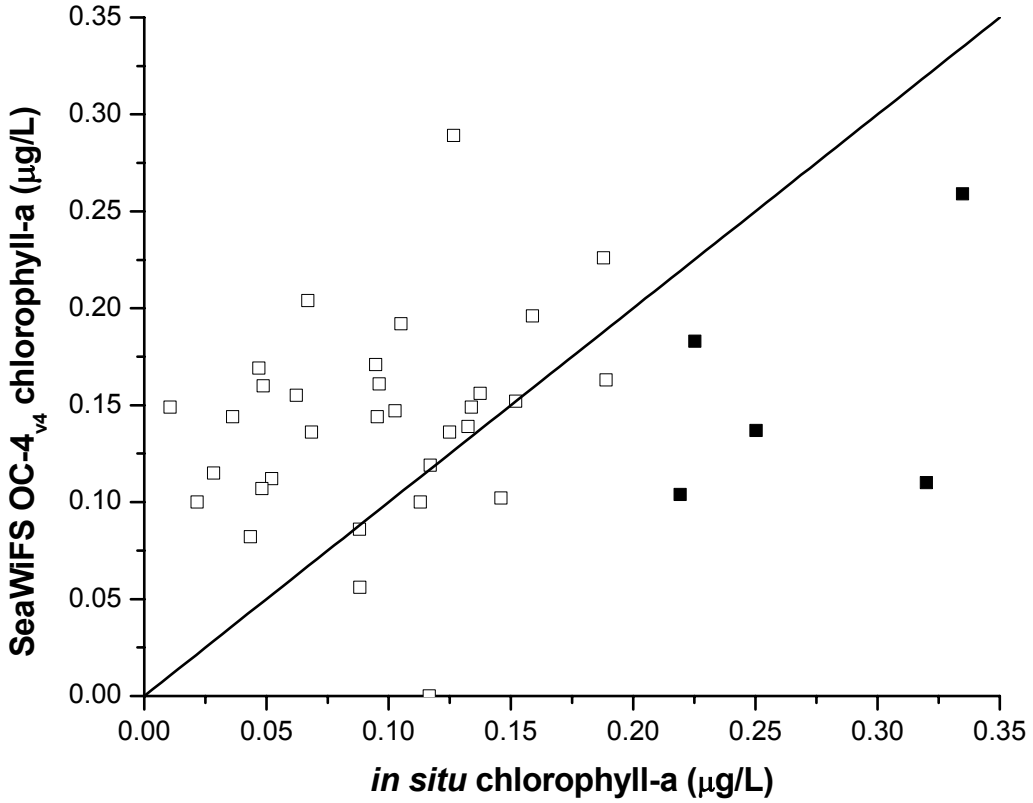

Figure 33. Comparison of *in situ* chlorophyll-a concentration with the corresponding chlorophyll-a value retrieved using the SeaWiFS OC-4_{v4} algorithm, where the *in situ* chlorophyll-a concentration was >0.20 μg/L (open circles) and <0.20 μg/L (solid circles).

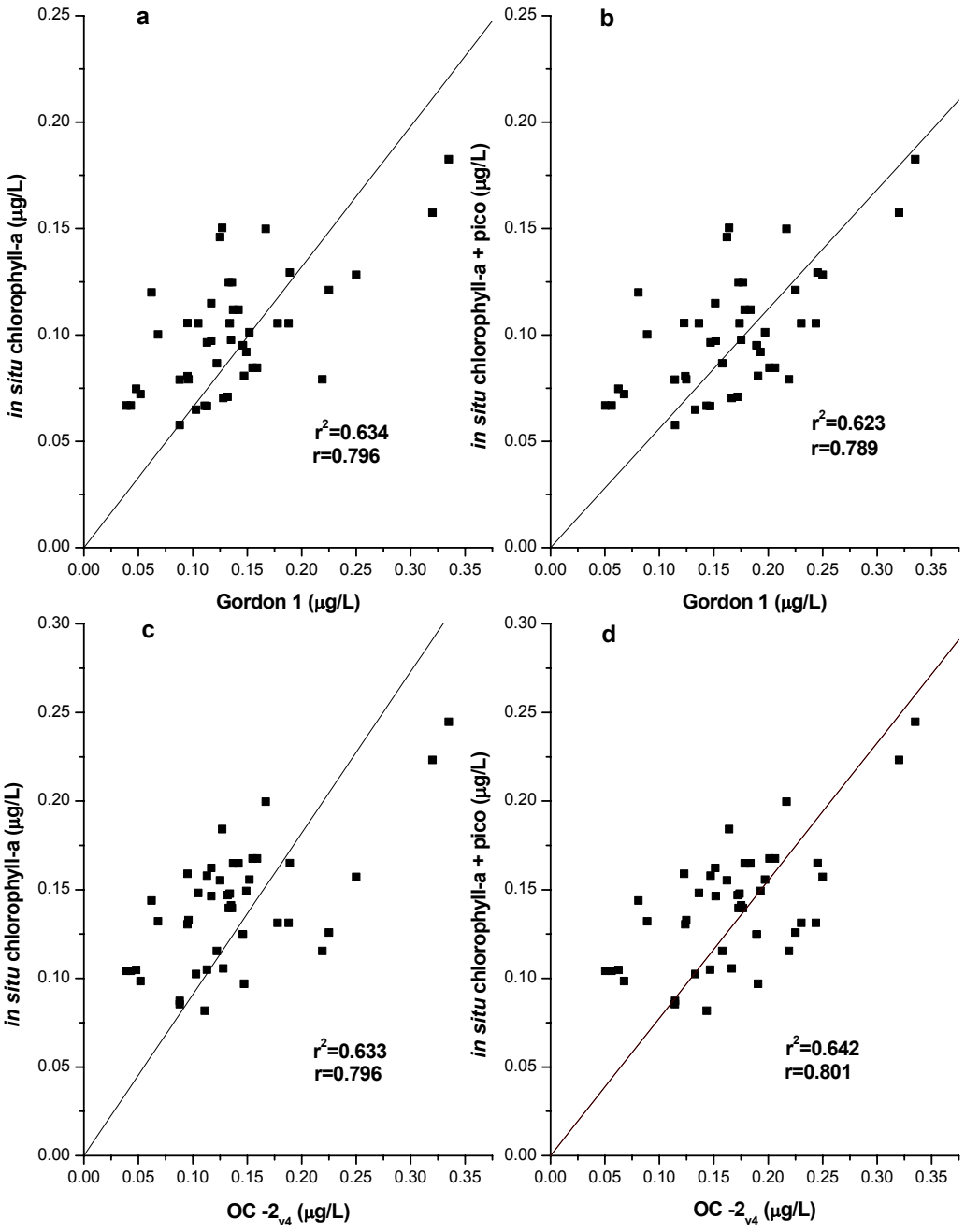

Figure 34. Comparisons between chlorophyll-a concentrations obtained with: (a) Gordon 1 algorithm calculated from GER and data *in situ*, (b) Gordon 1 algorithm calculated from GER and data *in situ* + pico, (c) SeaWiFS OC-2_{v4} algorithm calculated from GER data and *in situ*, and (d) SeaWiFS OC-2_{v4} algorithm calculated from GER data and *in situ* + pico. n=42.

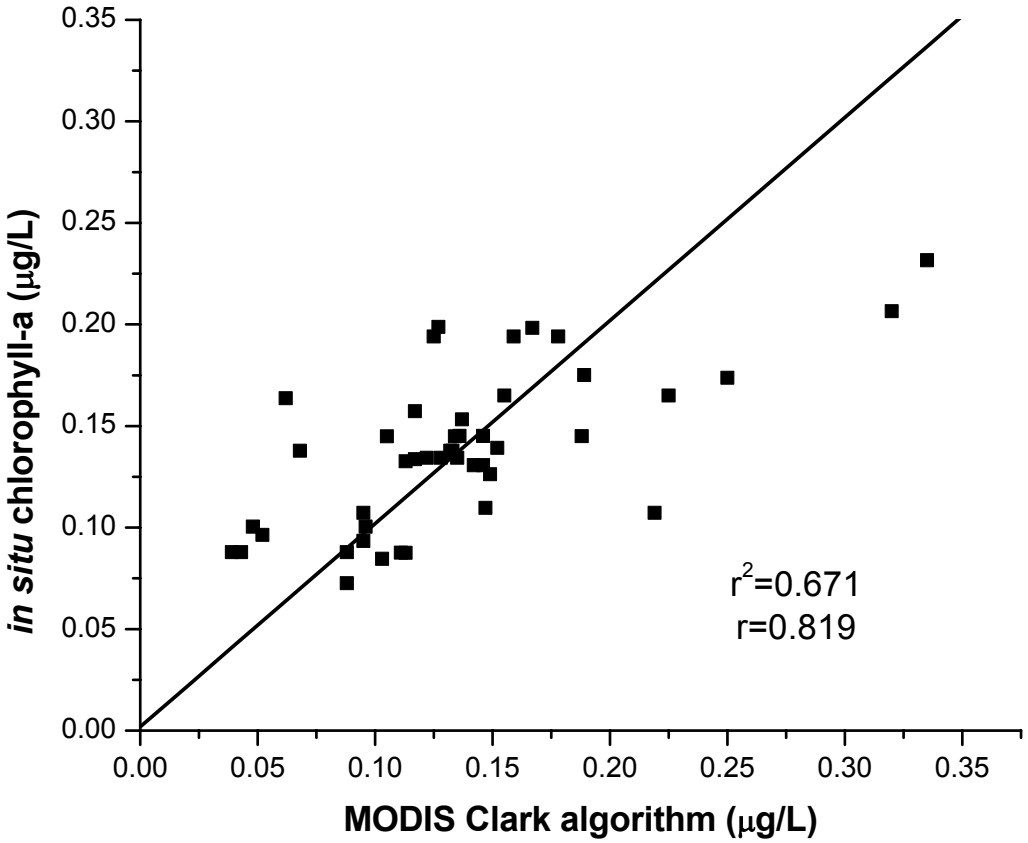

Figure 35. Comparison of *in situ* chlorophyll-a concentration with the corresponding chlorophyll-a concentration retrieved using the MODIS algorithm.

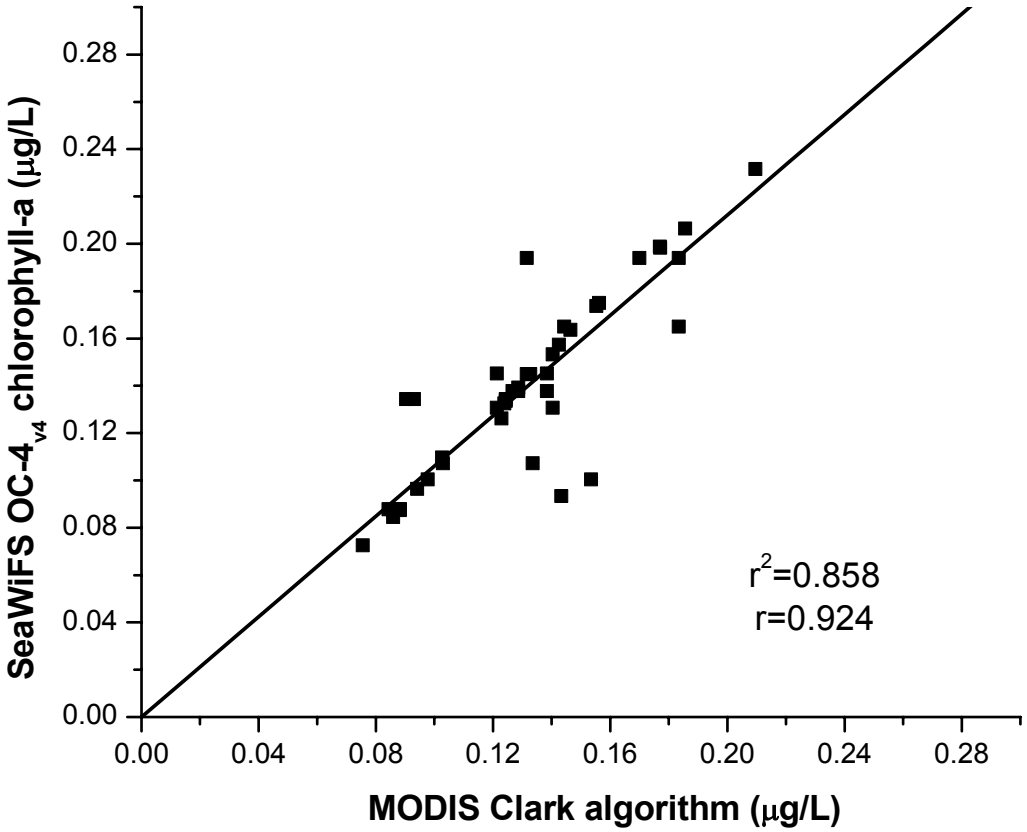

Figure 36. Comparison of chlorophyll-a concentration obtained from SeaWiFS OC-4_{v4} algorithm and the corresponding value retrieved using the MODIS algorithm.

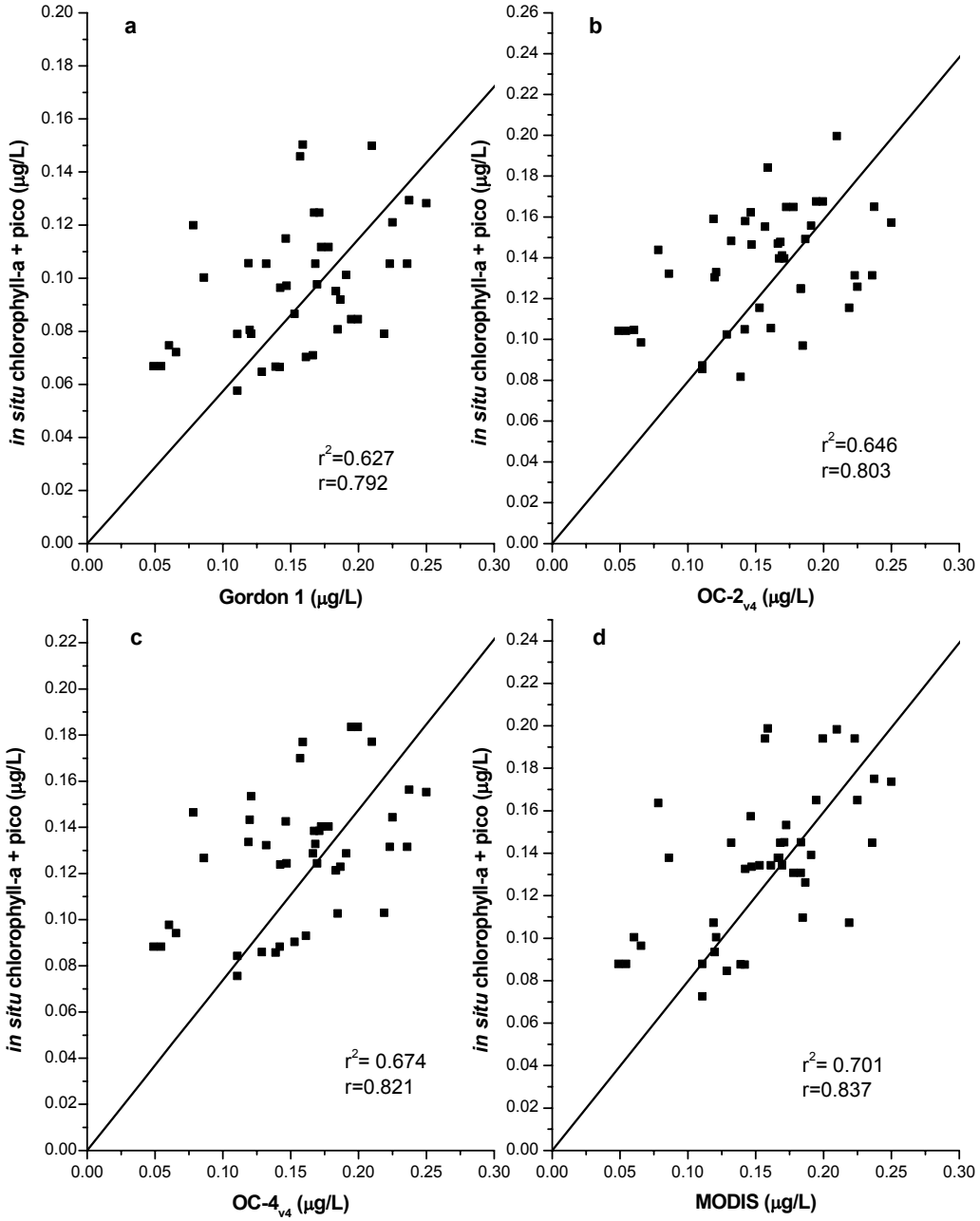

Figure 37. Comparisons between chlorophyll-a concentrations obtained with: (a) Gordon 1 algorithm calculated from GER and data *in situ* + pico, (b) SeaWiFS OC-2_{v4} algorithm calculated from GER and data *in situ* pico, (c) SeaWiFS OC-4_{v4} algorithm calculated from GER data and *in situ* + pico, and (d) MODIS algorithm calculated from GER data and *in situ* + pico.

Table 1. Correlation coefficients between chlorophyll-a values obtained with the different algorithms, compared with the *in situ* or *in situ* + pico value.

	in situ	*in situ* + pico	P
Gordon GER	0.634	0.624	NS
OC-2_{v4} Satellite	0.358	0.409	NS
OC-2_{v4} GER	0.633	0.642	NS
OC-4_{v4} Satellite	0.456	0.515	NS
OC-4_{v4} GER	0.615	0.674	NS
MODIS GER	0.671	0.701	NS

Correlation values between the different absorption coefficients at different wavelengths, and chlorophyll-a values obtained by different methods are shown in Table 2. The highest correlation for a_p was obtained between a_p at 670 nm versus *in situ* chlorophyll-a. The correlation values for a_p 443 and ap 670 were very similar for all the comparisons, being a_p 555 always the lowest correlation. The highest correlation for a_d was obtained between a_d at 670 nm versus *in situ* chlorophyll-a + pico. Again, the correlation values for ad 443 and a_d 670 were very similar for all the comparisons, being a_d 555 always the lowest correlation.

Explanations for the discrepancies between *in situ* and satellite-derived chlorophyll-a data are: (1) atmospheric conditions, since the atmosphere contributes up to 80% of the optical signal that is detected by the satellite sensor (Barlow et al., 2001), (2) gradients in phytoplankton species composition (Chavez, 1995), the different phytoplankton groups utilize light in different ways, this depends on such factors as light adaptation, accessory pigment composition, pigment packaging and size of the phytoplankton, and (3) the underestimation of phytoplankton resulting from the use of 0.7 μm filters as had been mentioned in a previous part of this work, there is a 20% loss of picoplankton with the use of 0.7 μm GF/F filters compared to 0.2 μm membrane filters in Case 1 waters of the Eastern Caribbean Sea.

Table 2. Comparisons of the different correlations between *in situ* chlorophyll-a, *in situ* chlorophyll-a + pico, SeaWiFS OC-4_{v4}, and MODIS, versus the different absorption coefficients at the three wavelengths associated with SeaWiFS.

Absorption coefficients	*in situ* chlorophyll-a	*in situ* chlorophyll-a + pico	SeaWiFS OC-4_{v4}	MODIS
ap 443	0.664	0.672	0.569	0.591
ap 555	0.583	0.631	0.490	0.478
ap 670	0.707	0.678	0.565	0.605
a_d 443	0.497	0.557	0.420	0.450
a_d 555	0.509	0.586	0.419	0.442
a_d 670	0.533	0.620	0.460	0.485
a_{ph} 443	0.605	0.583	0.522	0.565
a_{ph} 555	0.495	0.474	0.393	0.392
a_{ph} 670	0.6789	0.630	0.516	0.597
a_{ph*} 443	-0.189	-0.180	-0.365	-0.286
a_{ph*} 555	-0.118	-0.100	-0.313	-0.235
a_{ph*} 670	-0.160	-0.150	-0.342	-0.262

Seasonal Variability of chlorophyll-a at CaTS

There is an apparent seasonal cycle at CaTS with peaks in May-July and October-January (Figs. 38 and 39). Satellite derived chlorophyll-a was also consistent with this pattern (Figs. 38 and 39), and shows the seasonality of riverine influence. In the spring, high chlorophyll-a is associated with the Amazon River plume can be seen far out in the Atlantic. At this time, high surface chlorophyll-a in the east-central Caribbean is maintained by upwelling processes not related to riverine flow. The NE Caribbean is deeply influenced by the oceanic waters of the Atlantic Ocean at this time. During the fall, flow from the Orinoco River spreads throughout the Eastern Caribbean increasing the nutrient concentration, and hence increasing the chlorophyll-a concentration in the region.

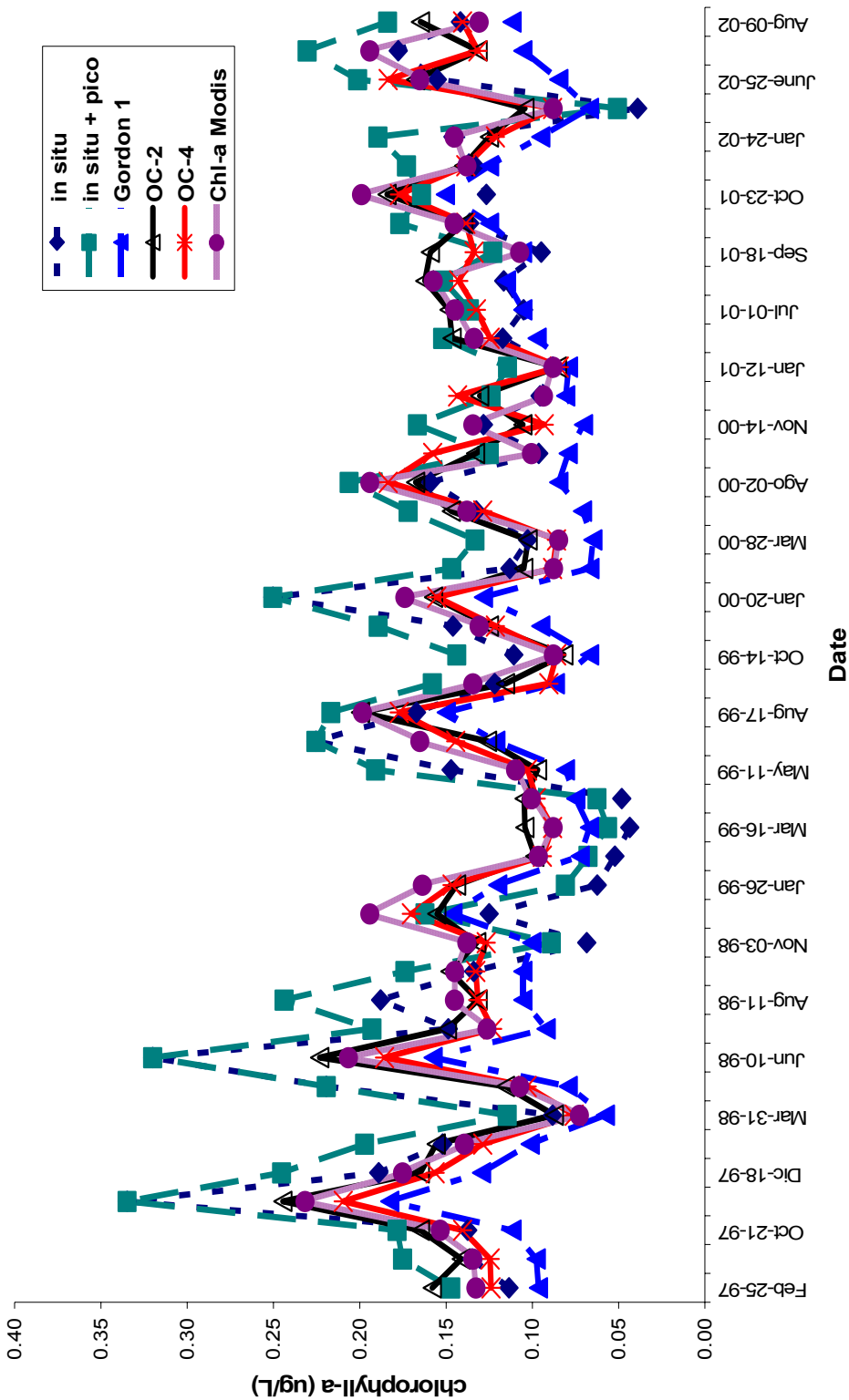

Figure 38. Comparison of *in situ* chlorophyll-a and *in situ* chlorophyll-a + pico concentration with the corresponding chlorophyll-a concentration calculated using the Gordon, SeaWiFS; OC-2_{v4}, OC-4_{v4}, and MODIS algorithms with GER data.

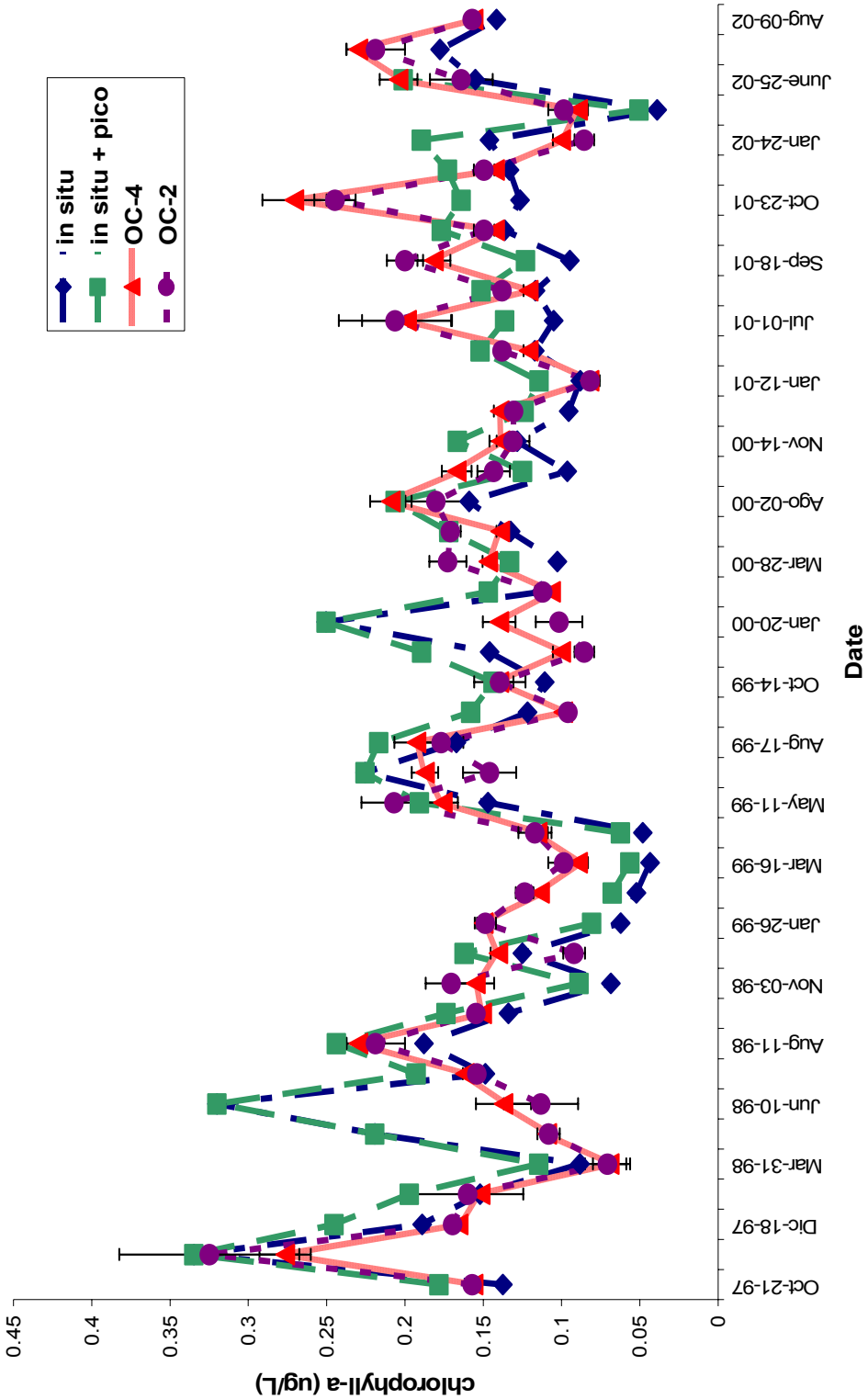

Figure 39. Comparison of *in situ* chlorophyll-a and *in situ* chlorophyll-a + pico concentration with the corresponding chlorophyll-a value retrieved from SeaWiFS imagery with the OC-2_{v4}, OC-4_{v4}, algorithms.

Absorption properties of particulate matter

Absorption of particles and phytoplankton at CaTS surf and DCM stations showed peaks at 425-475 nm and 660-680 nm (Figs. 40-41), the absorption spectra of particles and phytoplankton for the picoplankton component showed the same peaks for the surf and DCM samples (Figs. 42-43). Average absorption spectra of particles and phytoplankton for CaTS surf and DCM exhibited these to peaks for phytoplankton and picoplankton as well (Fig. 44). Average values for a_p, a_d, a_{ph}, and a_{ph*} at 443, 550 and 670 nm are given in Table 3. The average a_p value was highest for DCM at 443 nm (0.044 m^{-1}), while the picoplankton accounted for 60-70% of the absorption at both depths and at all three wavelengths. The average a_d value was highest for DCM at 443 nm (0.008 m^{-1}). For a_{ph} the highest average value was also found in the DCM at 443 nm (0.031 m^{-1}), while the picoplankton accounted for 67-73% in the surface, and from 61-77% at the DCM, over the different wavelengths. Finally for a_{ph*} the highest average was found in DCM at 443 nm. Since a_{ph*} is a measure of absorption per chlorophyll-a unit, we can't ascertain the contribution of picoplankton in this respect. Picoplankton values were equal to total phytoplankton for the surface station, but lower in the DCM. Similar results were obtained for the Minipex, Caratlan II and Mona cruises (Figs. 45-49). In the Mona cruise it is interesting to notice the differences in the absorption spectra of a_p, a_d, a_{ph}, and a_{ph*} for the 9:00 am and 3:00 pm samples, these differences can be attributed, at least in part, to diel patterns of growth and division by the phytoplankton and picoplankton (Jacquet, 2001; Claustre, 2002).

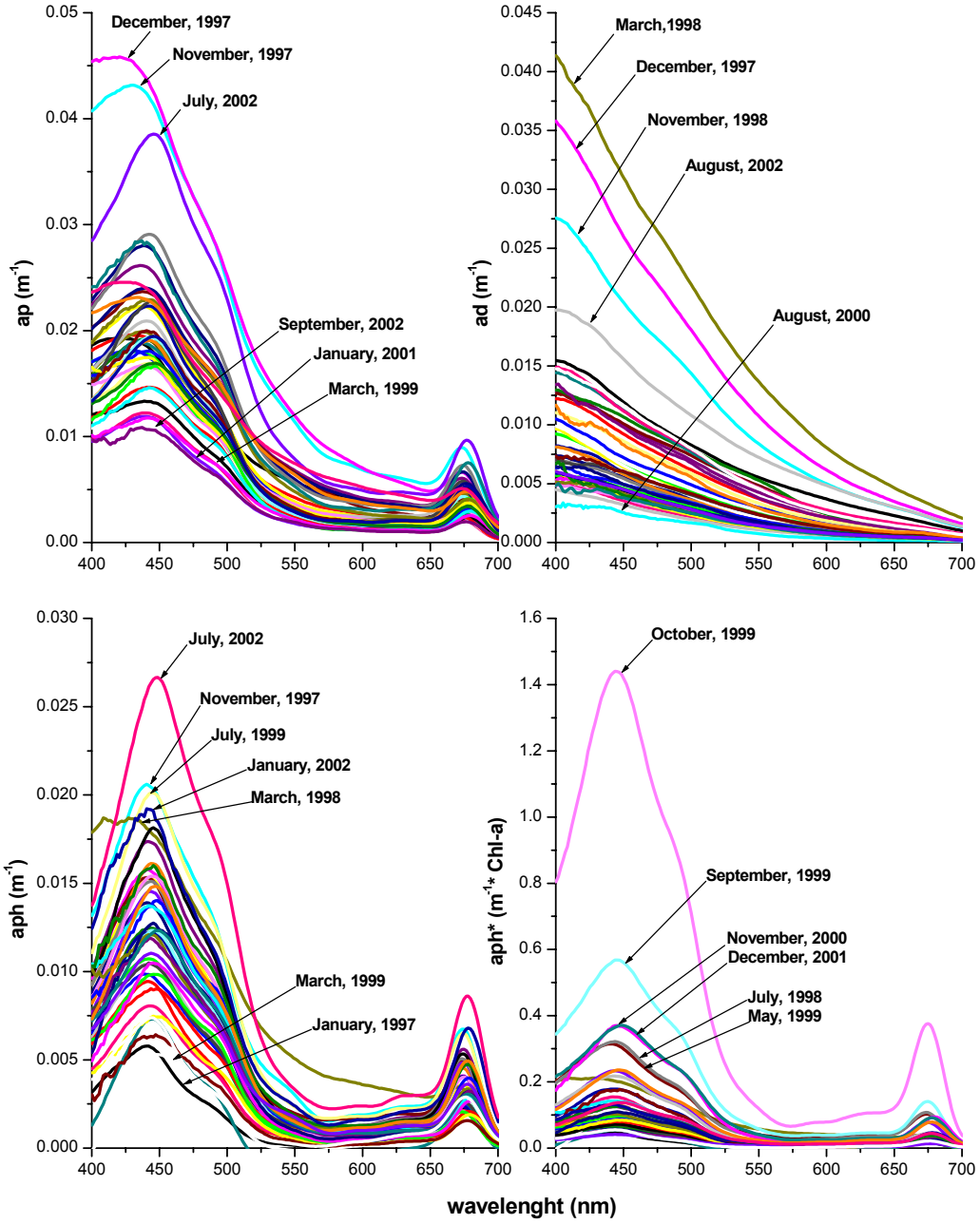

Figure 40. Absorption spectra of a_p, a_d, a_{ph}, and a_{ph^*} for the surface stations of CaTS from February 1997 to August 2002.

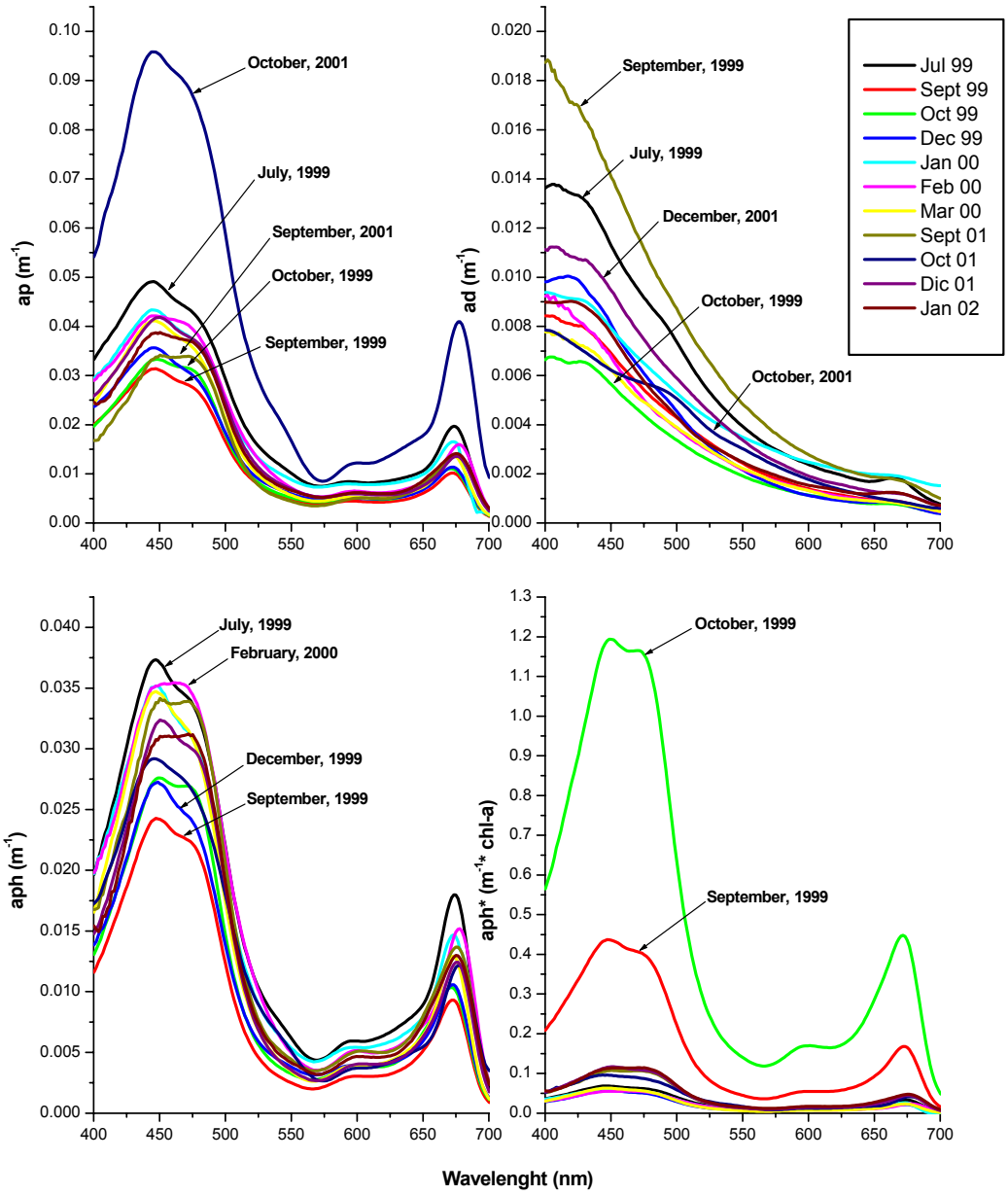

Figure 41. Absorption spectra of a_p, a_d, a_{ph}, and a_{ph*} for DCM of CaTS from July 1999 to January 2002. The legend applies to all graphs.

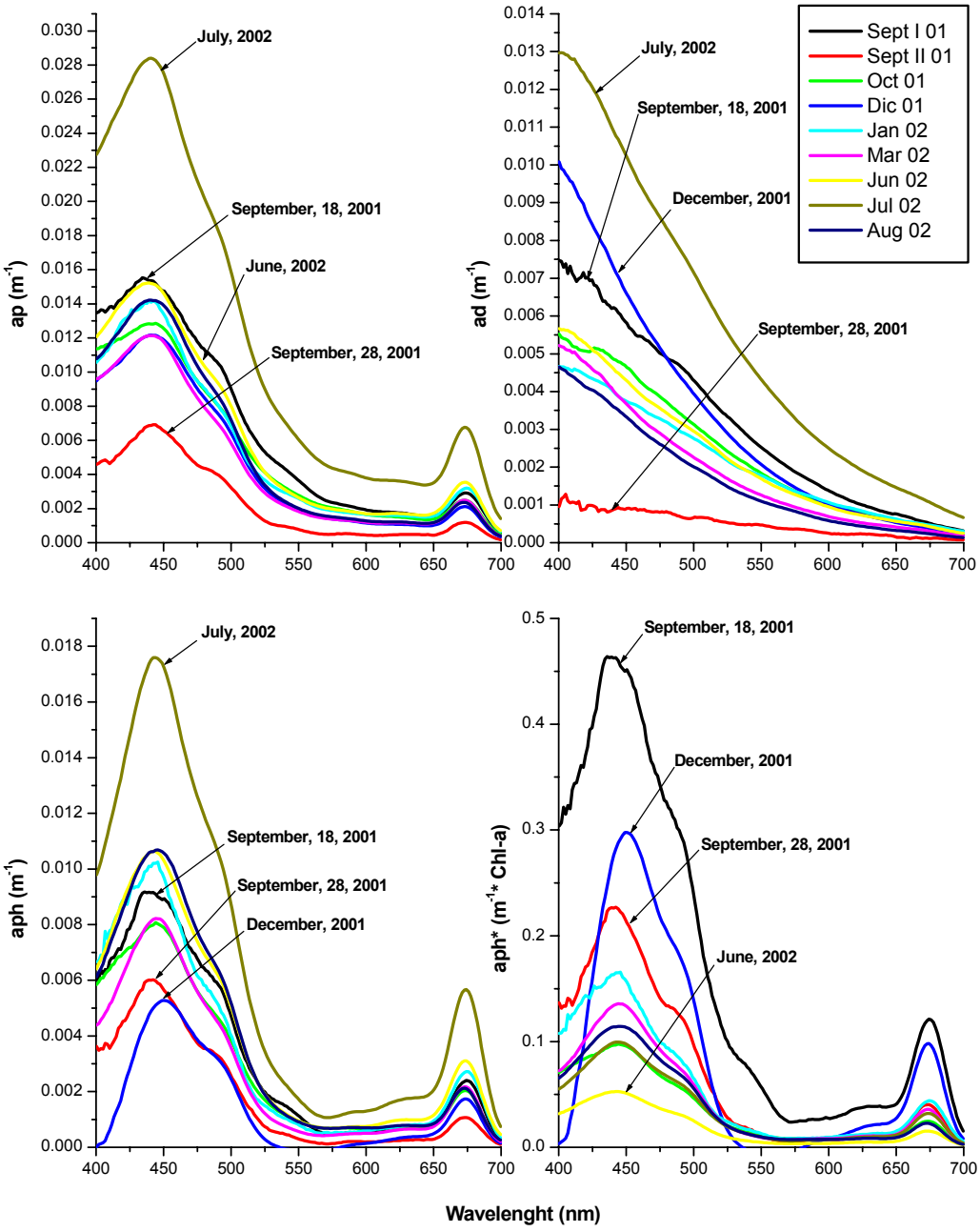

Figure 42. Picoplankton absorption spectra of a_p, a_d, a_{ph}, and a_{ph*} for the surface stations of CaTS from September 2001 to August 2002. The legend applies to all graphs.

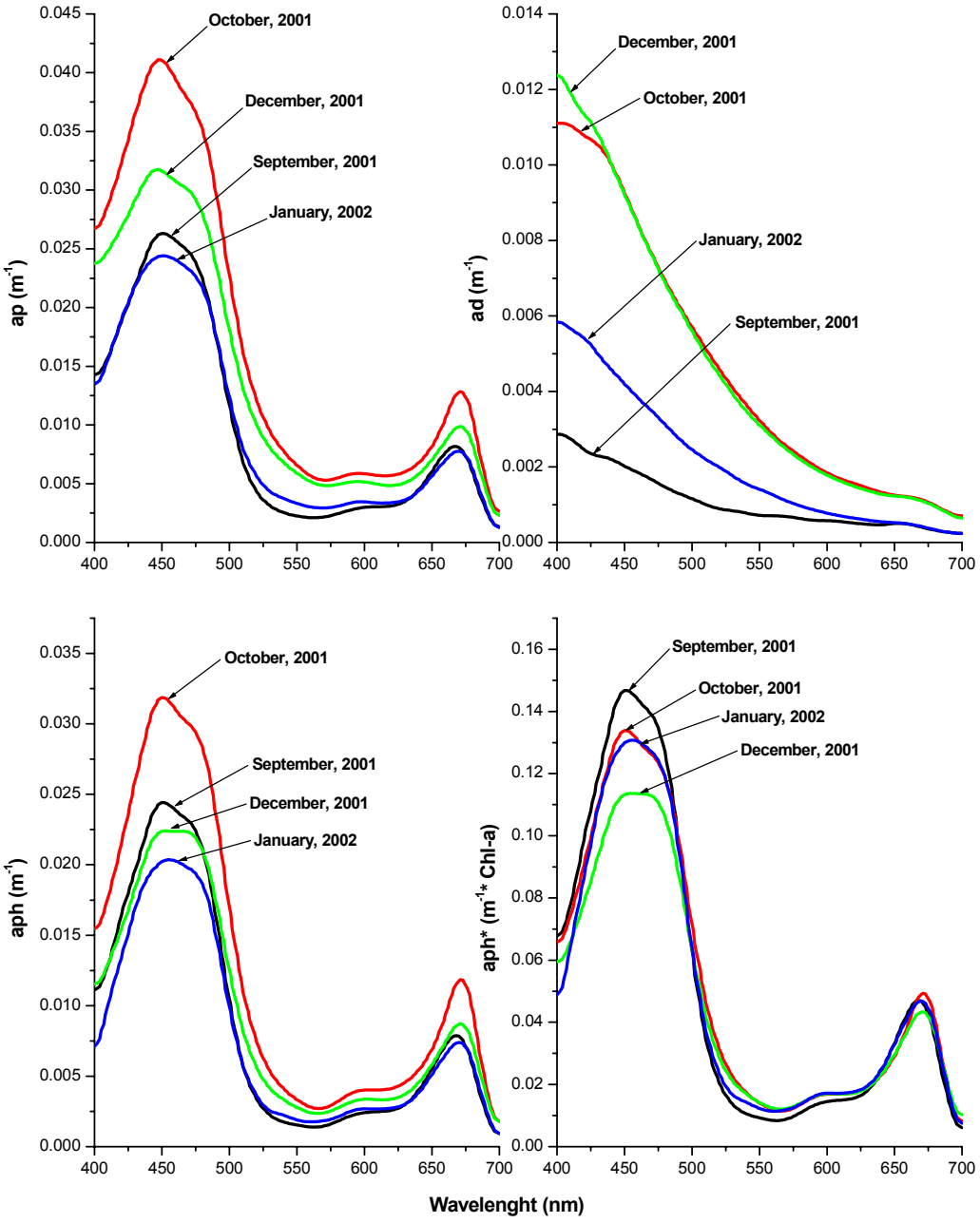

Figure 43. Picoplankton absorption spectra of a_p, a_d, a_{ph}, and a_{ph*} for the DCM stations of CaTS from September 2001 to January 2002.

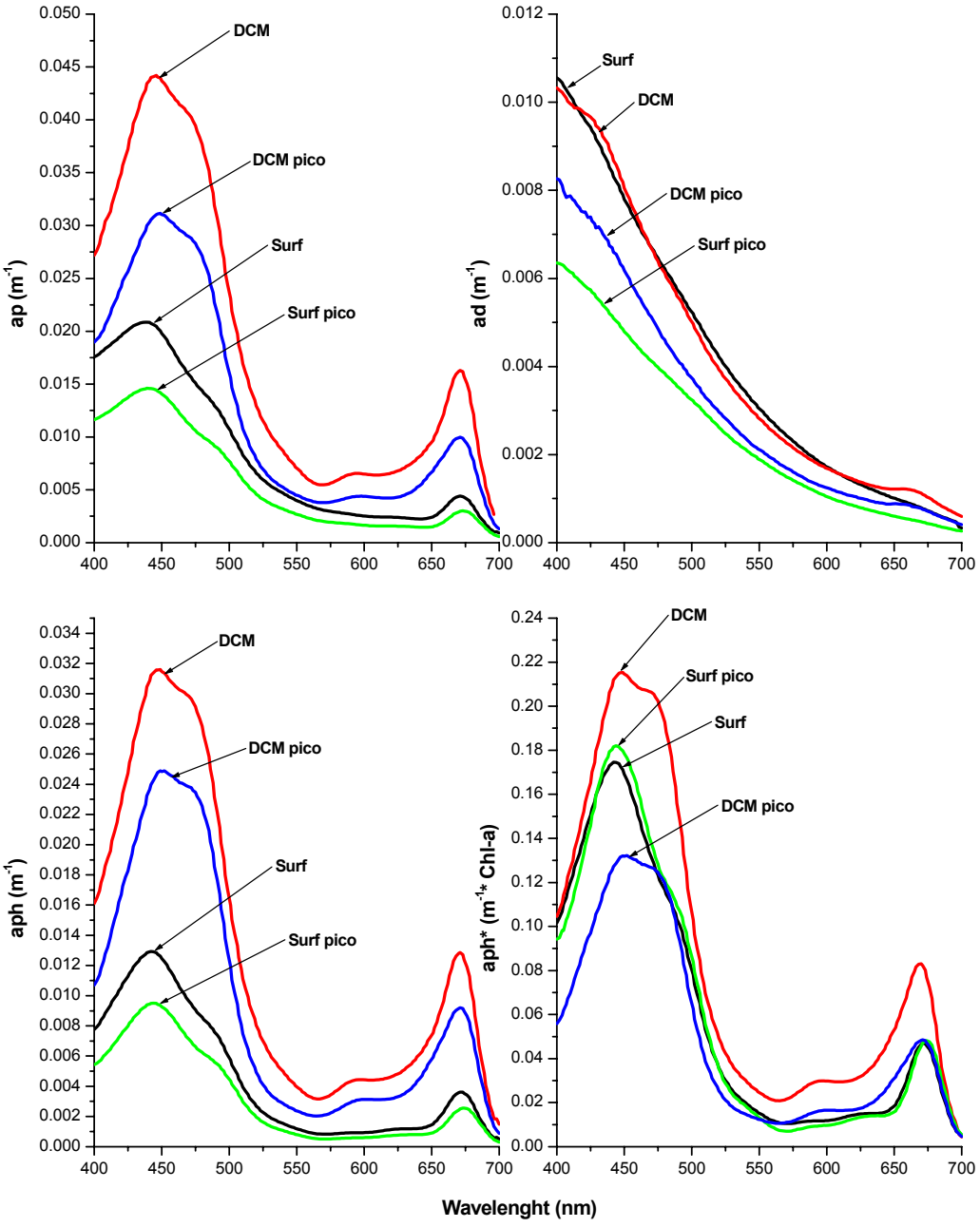

Figure 44. Average absorption spectra of a_p, a_d, a_{ph}, and a_{ph*} for CaTS station.

Table 3. Average absorption coefficients for CaTS at three different wavelengths. Values in parenthesis represent the percent of picoplankton absorption compared to the total absorption value.

Station/wavelength (nm)	**443**	**555**	**670**
a_p (m^{-1})			
CaTS surf	0.0206	0.0037	0.0044
CaTS surf pico	0.0145 (70%)	0.0025 (67%)	0.0029 (66%)
CaTS DCM	0.0441	0.0065	0.0162
CaTS DCM pico	0.0308 (70%)	0.0042 (65%)	0.0099 (61%)
a_d (m^{-1})			
CaTS surf	0.0082	0.0027	0.0008
CaTS surf pico	0.0050 (61%)	0.0017 (66%)	0.0005 (59%)
CaTS DCM	0.0086	0.0026	0.0011
CaTS DCM pico	0.0066 (76%)	0.0020 (75%)	0.0008 (69%)
a_{ph} (m^{-1})			
CaTS surf	0.0129	0.0012	0.0036
CaTS surf pico	0.0095 (73%)	0.0008 (67%)	0.0024 (68%)
CaTS DCM	0.0354	0.0039	0.0148
CaTS DCM pico	0.0235 (66%)	0.0023 (60%)	0.0091 (62%)
a_{ph*} (m^{-1} * chlorophyll-a)			
CaTS surf	0.1746	0.0142	0.0470
CaTS surf pico	0.1816 (104%)	0.0119 (83%)	0.0470 (100%)
CaTS DCM	0.2119	0.0236	0.0822
CaTS DCM pico	0.1271 (60%)	0.0118 (50%)	0.0484 (59%)

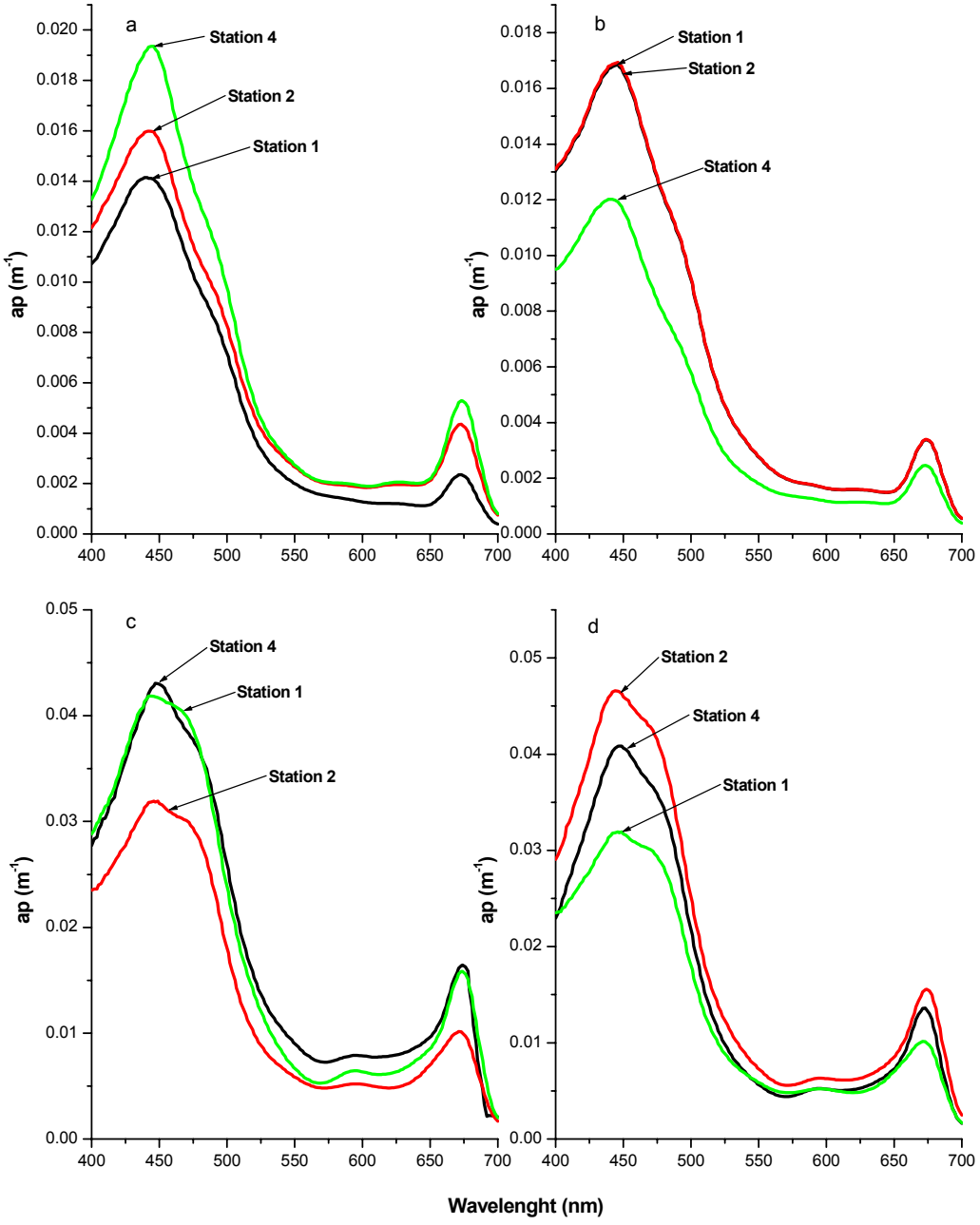

Figure 45. Absorption spectra of a_p for: (a) surface total phytoplankton (b) surface picoplankton (c) DCM total phytoplankton and (d) DCM picoplankton, for the Caratlan II cruise.

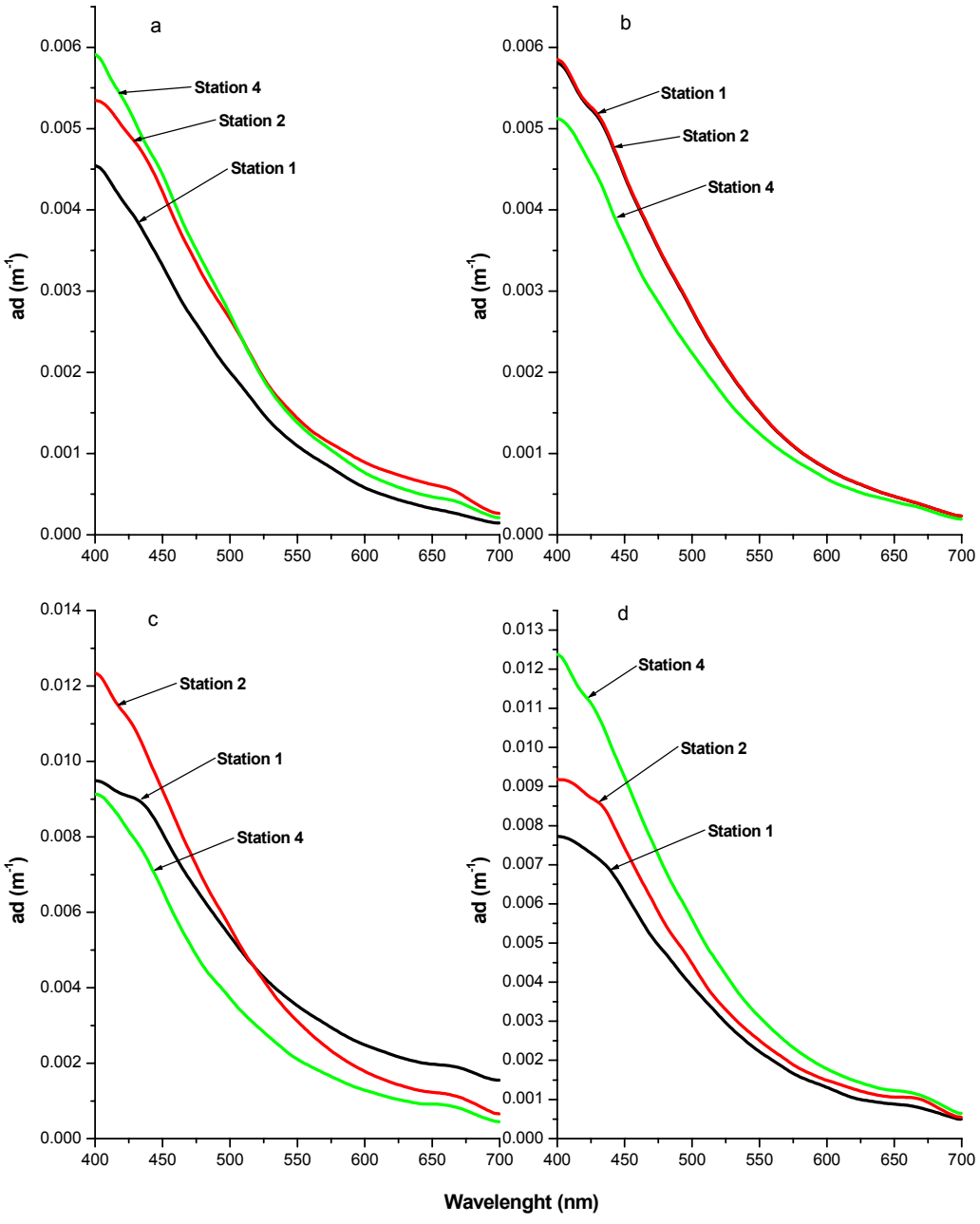

Figure 46. Absorption spectra of a_d for: (a) surface total phytoplankton (b) surface picoplankton (c) DCM total phytoplankton and (d) DCM picoplankton, for the Caratlan II cruise.

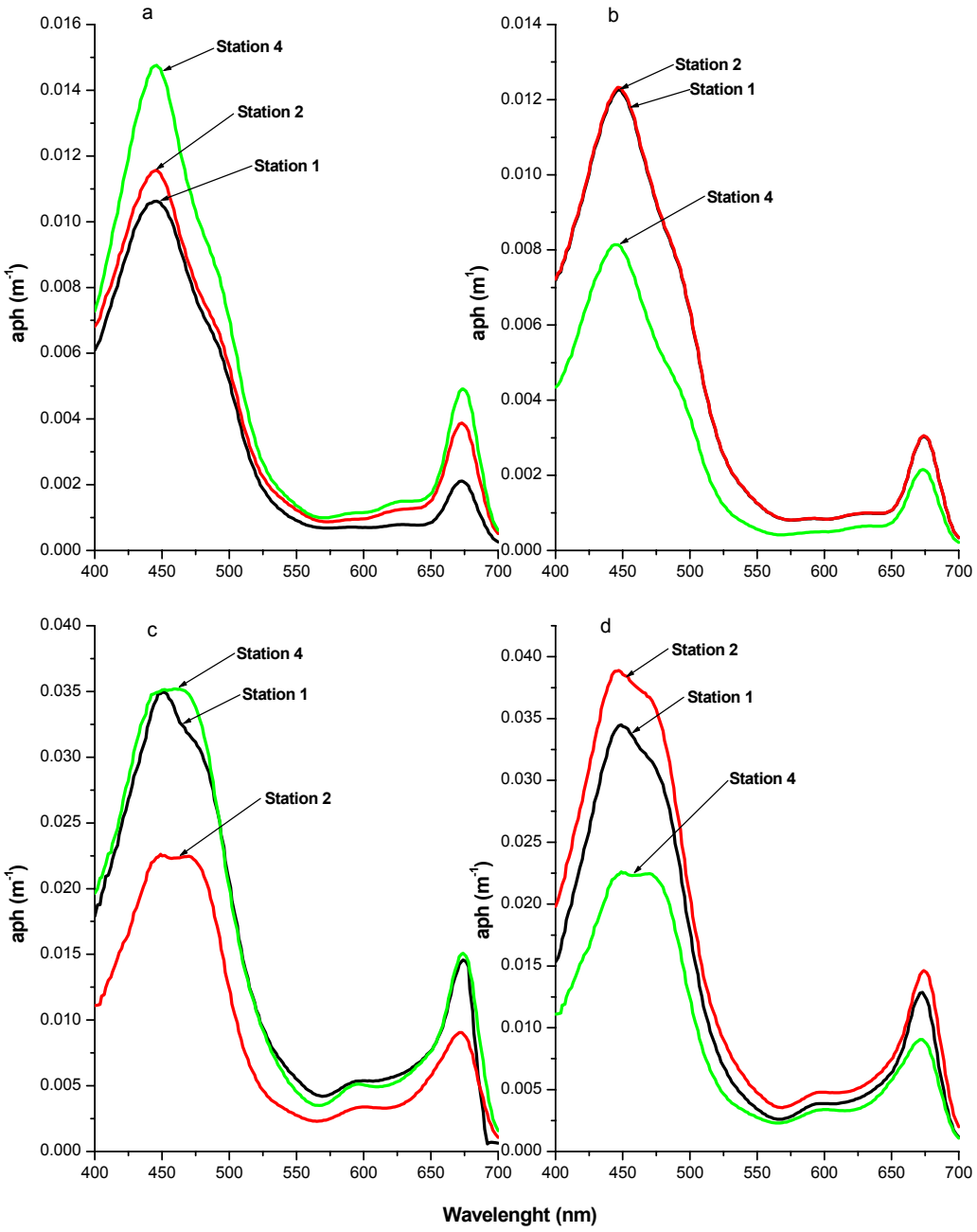

Figure 47. Absorption spectra of a_{ph} for: (a) surface total phytoplankton (b) surface picoplankton (c) DCM total phytoplankton and (d) DCM picoplankton, for the Caratlan II cruise.

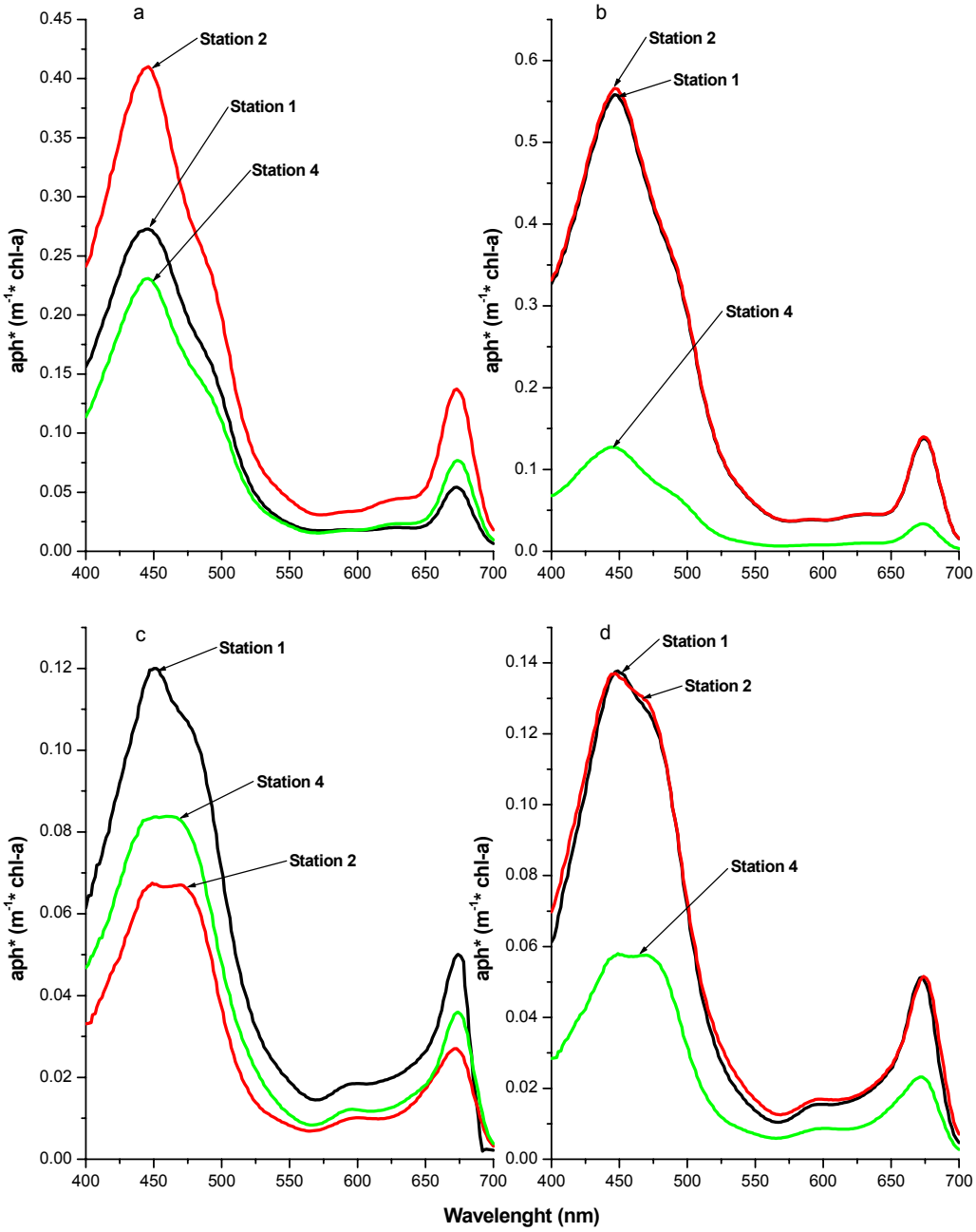

Figure 48. Absorption spectra of a_{ph*} for: (a) surface total phytoplankton (b) surface picoplankton (c) DCM total phytoplankton and (d) DCM picoplankton, for the Caratlan II cruise.

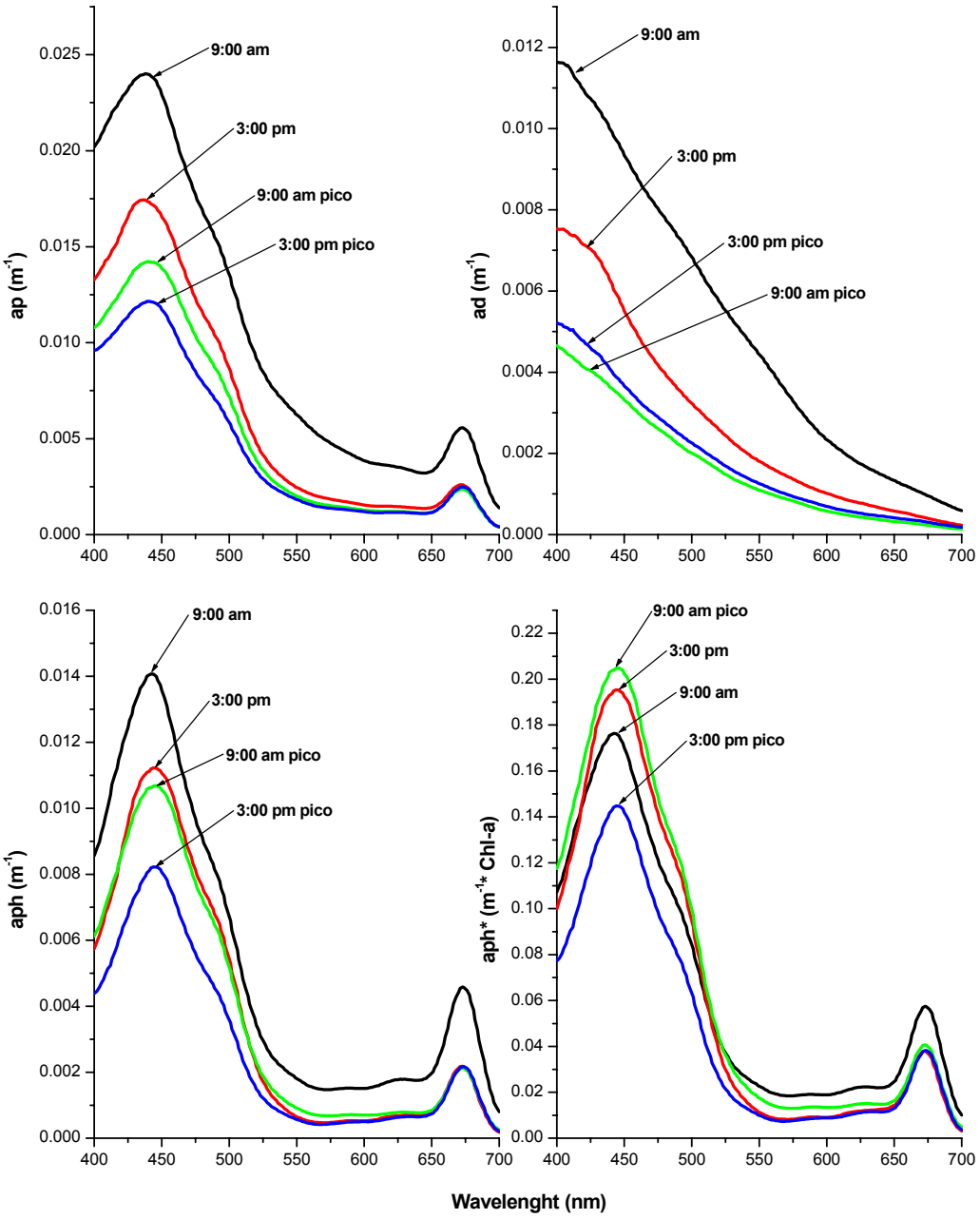

Figure 49. Absorption spectra of a_p, a_d, a_{ph}, and a_{ph^*} for the surface stations of Mona for total phytoplankton and picoplankton.

In Mayagüez Bay the absorption spectra for a_{ph} and a_{ph*} shows much more variability in terms of absorption peaks than the oceanic stations due to the presence of different accessory pigments (Figs. 50-51). Average absorption spectra for the two cruises in Mayagüez Bay are shown in Figures 52-53. Tables 4 and 5 summarize the average absorption coefficients for Mayagüez Bay, at 443, 555, and 670 nm wavelengths. For the October 2001 cruise, picoplankton accounted for 30-58% of the a_p value in the surface and for 35-49% in the deep samples, while for the August 2002 it accounted for 33-52% for surface and 37-48% for the deep samples. For the a_{ph} value, in October 2001 the picoplankton was responsible for 53-68% in the surface and for 45-90% in the deep samples, while for the August 2002 cruise it accounted for 70-83% in surface and 58-63% in the deep samples.

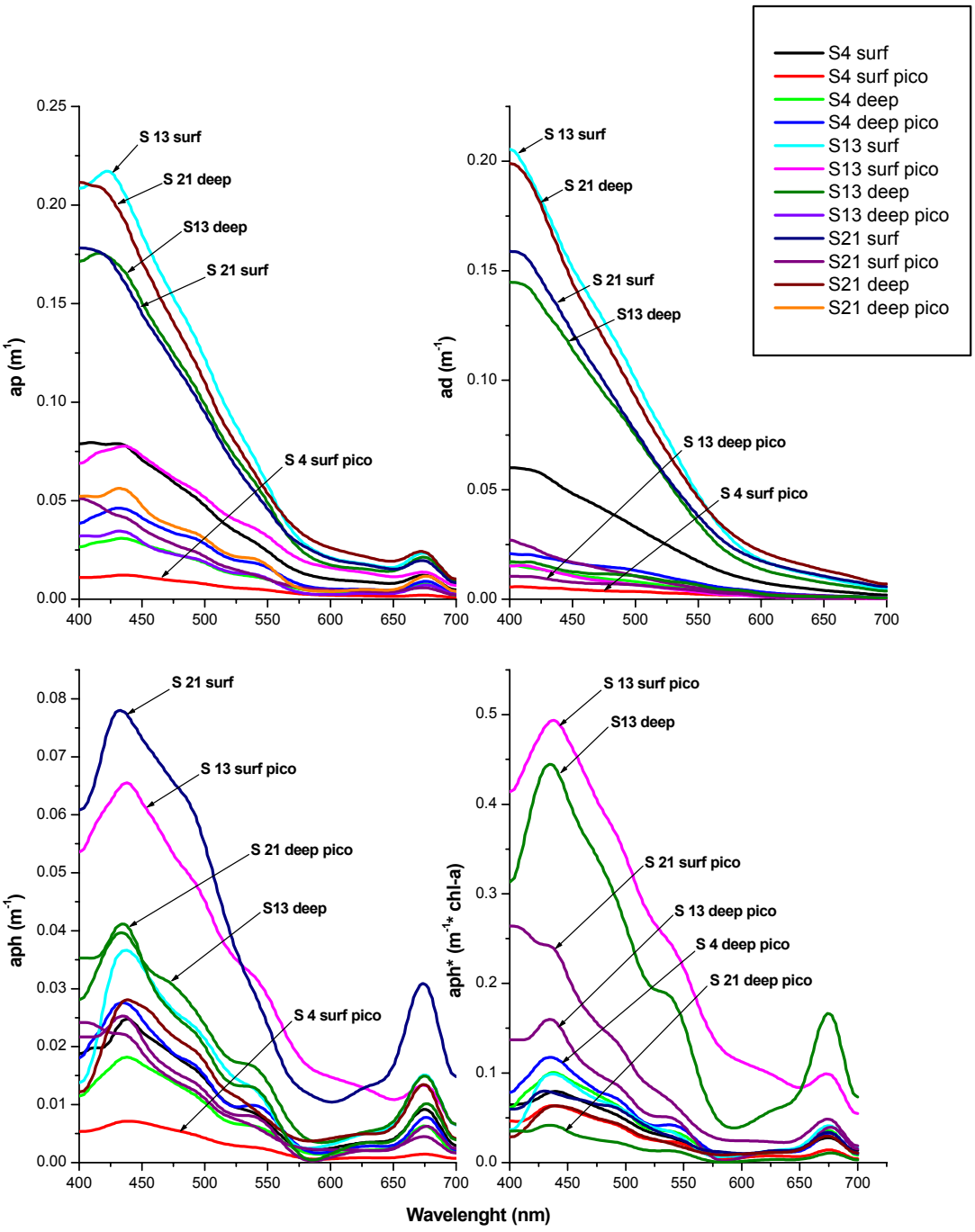

Figure 50. Absorption spectra of a_p, a_d, a_{ph}, and a_{ph^*} for the Mayagüez Bay stations on October 2001 for phytoplankton and picoplankton. The legend applies to all graphs.

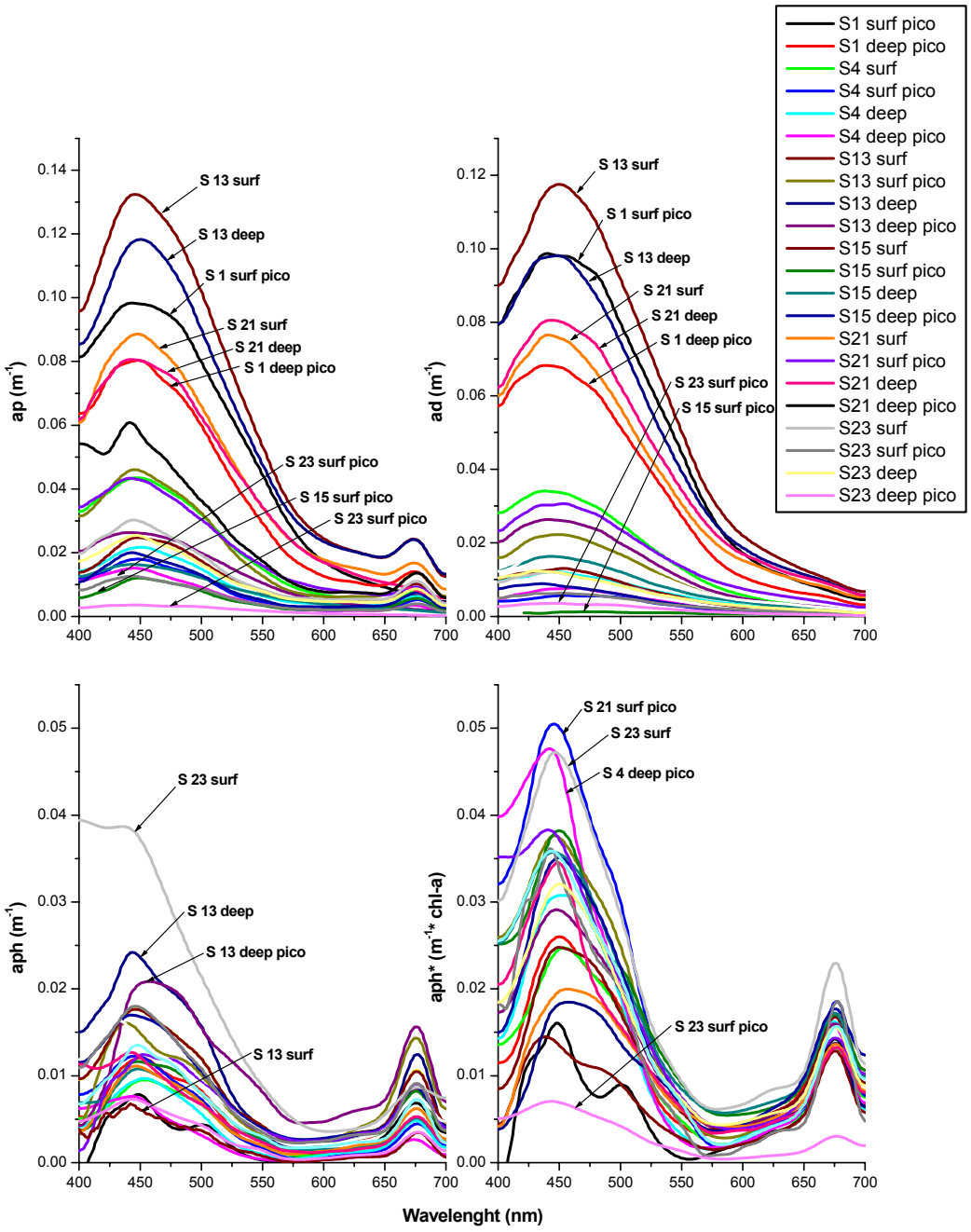

Figure 51. Absorption spectra of a_p, a_d, a_{ph}, and a_{ph^*} for the Mayagüez Bay stations on August 2002 for phytoplankton and picoplankton. The legend applies to all graphs.

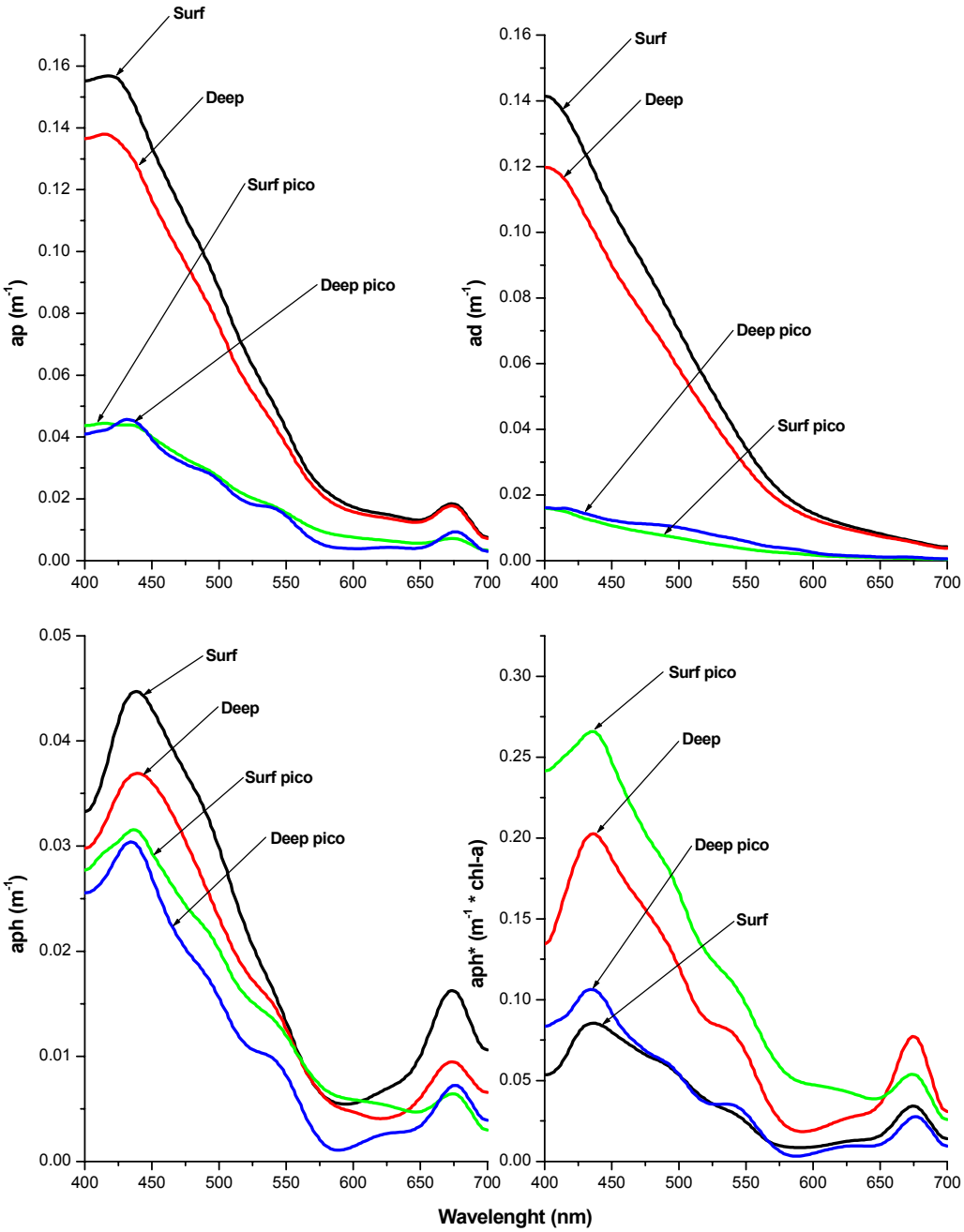

Figure 52. Average absorption spectra of a_p, a_d, a_{ph}, and $a_{ph*}$for Mayagüez Bay, October 2001 cruise.

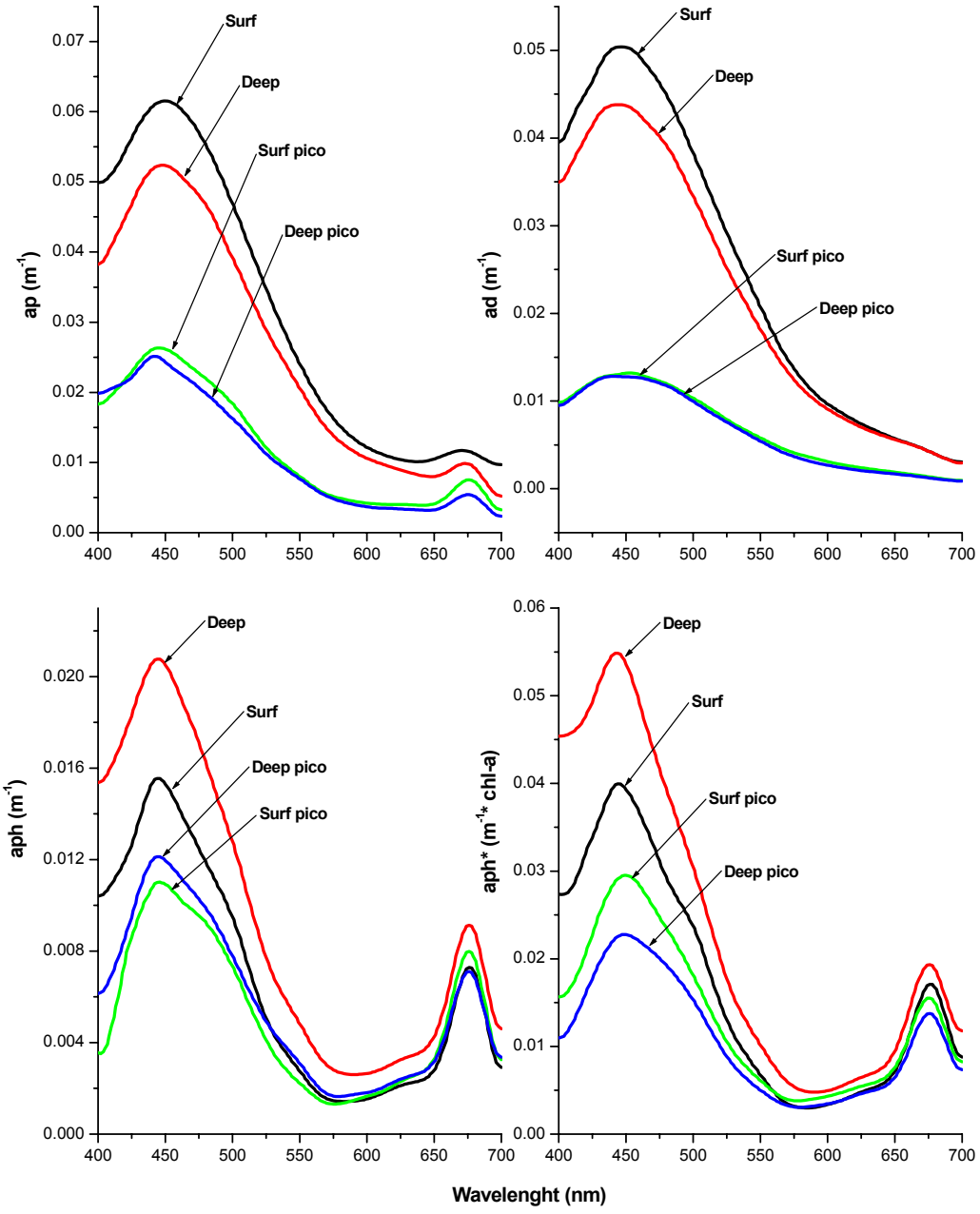

Figure 53. Average absorption spectra of a_p, a_d, a_{ph}, and a_{ph*} for Mayagüez Bay, August 2002 cruise.

Table 4. Average absorption coefficients for Mayagüez Bay, October 2001 cruise at three different wavelengths. Values in parenthesis represent the percent of picoplankton absorption compared to the total absorption value.

Station/wavelength (nm)	**443**	**555**	**670**
a_p (m^{-1})			
Surf	0.1403	0.0374	0.0181
Surf pico	0.0421 (30%)	0.0140 (37%)	0.0104 (58%)
Deep	0.1226	0.0333	0.0071
Deep pico	0.0426 (35%)	0.0122 (37%)	0.0035 (49%)
a_d (m^{-1})			
Surf	0.1021	0.0209	0.0064
Surf pico	0.0113 (11%)	0.0033 (16%)	0.0040 (63%)
Deep	0.0646	0.0257	0.0058
Deep pico	0.0128 (19%)	0.0053 (21%)	0.0011 (20%)
a_{ph} (m^{-1})			
Surf	0.0450	0.0162	0.0117
Surf pico	0.0308 (68%)	0.0108 (66%)	0.0063 (53%)
Deep	0.0576	0.0075	0.0160
Deep pico	0.0296 (51%)	0.0069 (90%)	0.0072 (45%)
a_{ph^*} (m^{-1} * chlorophyll-a)			
Surf	0.0835	0.0200	0.0327
Surf pico	0.0788 (94%)	0.0172 (87%)	0.0327 (100%)
Deep	0.1965	0.0565	0.0733
Deep pico	0.1006 (51%)	0.0238 (42%)	0.0248 (34%)

Table 5. Average absorption coefficients for Mayagüez Bay, August 2002 cruise at three different wavelengths. Values in parenthesis represent the percent of picoplankton absorption compared to the total absorption value.

Station/wavelength (nm)	**443**	**555**	**670**
a_p (m^{-1})			
Surf	0.0638	0.0215	0.0135
Surf pico	0.0263 (41%)	0.0071 (33%)	0.0070 (52%)
Deep	0.0522	0.0188	0.0107
Deep pico	0.0250 (48%)	0.0069 (37%)	0.0051 (48%)
a_d (m^{-1})			
Surf	0.0504	0.0189	0.0046
Surf pico	0.0160 (32%)	0.0054 (28%)	0.0015 (32%)
Deep	0.0338	0.0147	0.0046
Deep pico	0.0128 (38%)	0.0043 (29%)	0.0014 (29%)
a_{ph} (m^{-1})			
Surf	0.0136	0.0023	0.0093
Surf pico	0.0110 (81%)	0.0019 (83%)	0.0065 (70%)
Deep	0.0208	0.0042	0.0062
Deep pico	0.0121 (58%)	0.0026 (63%)	0.0039 (63%)
a_{ph^*} (m^{-1} * chlorophyll-a)			
Surf	0.0399	0.0056	0.0156
Surf pico	0.0291 (73%)	0.0053 (95%)	0.0147 (94%)
Deep	0.0549	0.0088	0.0183
Deep pico	0.0225 (41%)	0.0044 (49%)	0.0129 (70%)

The shape and magnitude of the absorption spectra for phytoplankton are reflections of the pigment composition and concentration, respectively. Each algal group has its own pigment signature, and the combination of the pigments that compose this signature determines the shape of the absorption spectra (Lohrenz et al., 2003).

The shoulders found at 470 to 480 nm and 650 nm are characteristic of samples taken in deeper layers of blue subtropical waters (Bricaud and Stramski, 1990; Hoepffner and Sathyendranath, 1992; Lazzara et al., 1996; and Allali et al., 1997). These shoulders are caused by a marked increase in the concentration of divinyl chlorophyll-b within and below the DCM (Bouman et al., 2000). While the variability in the shape of the absorption spectra was most pronounced between 450-550 nm, this is the region where the accessory chlorophylls and caratenoids have their maximum absorptions. Hence the changes in the composition of accessory pigments should affect this region more than anywhere else.

Although the magnitude of a_{ph} is strongly influenced by the relative concentration of accessory pigments, pigment packaging can also be an important contributor to variation in the chlorophyll-specific absorption coefficient of marine phytoplankton. Pigment packaging is a function of two properties of the cell: its size and its intracellular pigment concentration (Platt and Jasby, 1976). An increase in cell size or intracellular pigment concentration will result in a corresponding decrease in the absorption efficiency of phytoplankton pigments (Platt and Jasby, 1976; Sathyendranath et al., 1987). This decrease in the *in vivo* specific absorption of aggregated pigments, compared with that of the same quantity of pigment evenly dispersed in solution, is referred to as the packaging or flattening effect (Kirk, 1994).

Comparative studies of the optical properties of phytoplankton conducted in different regions of the open ocean have shown that the highest values of a_{ph} are found in highly stratified, picoplankton dominated surface waters (Bricaud and Stramski, 1990; Hoepffner and Sathyendranath, 1992; Sosik and Mitchell, 1995; Lazzara et al., 1996; Allali et al., 1997; and Stuart et al., 1998). Smaller cells have lower pigment packaging than larger cells of the same intracellular pigment concentration, leading to a higher absorptive efficiency per unit pigment (Platt and Jassby, 1976). In general there are two main sources of variation in the magnitude and shape of a_{ph}, changes in pigment composition and changes in pigment packaging (Sathyendranath et al., 1987; Bricaud et al., 1988; Mitchell and Kiefer, 1988).

In view of the essential role of a_{ph} for the estimation of light penetration and primary production in the ocean it is important to separate any systematic trends in a_{ph} from random variations, and to determine if they are associated with changes in geographical location and/or season.

The results of the studies carried out by Marshall and Cohn (1983) and Matta and Marshall (1984) have demonstrated that year-to-year variations can be important, but that if this long-term variation is removed, seasonal and geographical patterns of distribution can also be detected. Thus year-to-year variation, as well as short term variations, like those produced by the intrusions of water from the Orinoco River (Corredor and Morel, 2001) may affect the regional distribution of phytoplankton.

In principle the absorption of light by phytoplankton pigments follows Beer's Law, i.e. absorption increases linearly with pigment concentration. However, when dealing with *in vivo* absorption by phytoplankton cells, this linear relationship is affected

by the pigment composition and the flattening effect (Sathyendranath et al., 1987). Since the total phytoplankton absorption at a given wavelength is the sum of the contributions from each of the pigments to absorption in that wavelength, changes in the pigment composition will certainly affect the relationship between absorption and chlorophyll-a concentration. The flattening effect refers to the relative flattening of the absorption spectrum of particles in suspension relative to the same material in solution. It depends on the particle size and shape and on the concentration of the absorbing material within the cells. It is known that the specific absorption coefficients decrease with cell size and intracellular pigment concentration (Bricaud et al., 1981). Natural environments with low chlorophyll-a concentrations are often associated with a predominance of small phytoplankton cells, and high chlorophyll-a concentrations with large cells (Yentsch and Phinney, 1989). As a consequence, the relationship between absorption and pigments is often non-linear.

The chlorophyll-specific absorption coefficient of phytoplankton, a_{ph*}, is a fundamental input parameter in models of underwater light attenuation, and hence it is important to know its magnitude and natural variation. The shape of the absorption spectrum is often used to approximate the photosynthetic action spectrum of phytoplankton in spectral models of primary production.

Several environmental variables are known to affect the physiological status of phytoplankton cells. Therefore, one might expect that vertical gradients in such physical-chemical properties as nutrient concentration, light and temperature that are found in tropical waters would have an impact upon the vertical structure of the physiological parameters of phytoplankton. In many cases one environmental variable co-varies with

several others, frustating attempts to determine the cause of variation in the physiological parameters (Sosik, 1996).

Another possible explanation for this temporal (daily to seasonal) and spatial variability in the absorption spectra, are the changes in light availability and utilization (Siegel et al., 1995). Light is an essential factor for phytoplankton, and has a complex pattern of variability both in time and space. The effects of spatial heterogeneity in light supply on competition of phytoplankton have been investigated by Britton and Timm (1993) and Huisman and Weissing (1994). The vertical gradient in light availability in a well-mixed water column is not sufficient for more than one species to occur at equilibrium (Huisman and Weissing, 1994). Britton and Timm (1993) demonstrated, however, that a spatial gradient in light distribution with depth coupled with diffusion of algal cells through the water column may allow coexistence of many species of phytoplankton as well as their vertical segregation. Huisman et al. (1999a, 1999b) showed that incomplete mixing may lead to coexistence of competing species, although the coexistence region is small.

Nonequilibrium conditions prevail in nature. Environmental factors and resources, as well as population densities fluctuate in both time and space. Hutchinson (1961) suggested that nonequilibrium environmental conditions may explain the coexistence of many species of phytoplankton in a seemingly homogeneous environment, the so-called paradox of the plankton.

Often in natural systems, resources other than light limit phytoplankton growth: phosphorous in many temperate lakes, nitrogen and iron in marine systems, and carbon in highly productive lakes (Litchman and Klausmeier, 2001). Experimental studies have

shown that light fluctuations of nonlimiting levels can mediate competition for nutrients and either reverse competitive outcome reached under constant light or lead to coexistence (Brzezinski and Nelson, 1988).

From the mentioned above, we can conclude that the picoplankton are the dominant component of the picoplankton community in oceanic waters, and contribute from 60-70% to the a_p, and 61-77% to a_{ph}. While in Mayagüez Bay, which is dominated by larger sized phytoplankton, the picoplankton contributes 30-58% to the a_p, and 45-90% to the a_{ph}. Temporal and spatial variability was observed in the picoplankton contribution to the different absorption coefficients.

Restriction Fragment Length Polymorphism in Picoplankton Populations.

Introduction

Even with all the recent interest in the picoplankton its' taxonomic composition is poorly known. New molecular phylogenetic techniques have helped in the identification of small eukaryotic phytoplankton. Nucleic acid probing has become a common approach for assessing the diversity of microorganisms (Amann et al., 1995). In pelagic marine environments, the focus has been on prokaryotic plankton, including eubacteria, bacteria, and archae (Pace, 1997). Recent findings have been dramatic; many novel groups of bacterioplankton and archae have been described by variations in the small-subunit (SSU) rRNA gene (rDNA) sequences, with most having thus far evaded culture in the laboratory. Oligonucleotide probes based on SSU rRNA sequence signatures are being designed for widespread application to ecological problems, including the distribution of bacterial species in their natural habitats.

Parts of the ribosomal RNA sequences were highly conserved during evolution and the differences in rRNA sequences correlate well with evolutionary relations. The application of rRNA probes for detection of bacterioplankton groups and archae species was recently established (Simon et al., 1995; Knauber et al., 1996). A large number of rRNA gene sequences have already been analyzed and their sequences available through the Internet (GenBank at http://www.ncbi.nlm.nih.gov/Web/Search/index.html)(Schmidt et al., 1991).

Approaches that have been used to obtain rRNA gene sequences include direct sequencing of extracted 5S rRNA gene (Stahl et al., 1984; Stahl et al., 1985), analysis of

clonal DNA (cDNA) libraries containing the 16S rRNA (Ward et al., 1990; Weller and Ward, 1989), and analysis of cloned 16S rRNA genes obtained by amplification using the polymerase chain reaction (PCR) (Giovannoni et al., 1990). Recently, the 18S rRNA gene has been used to infer the abundance and diversity of eukaryotic plankton (Moon van der Staay et al., 2000; Moon van der Staay et al., 2001; Díez et al., 2001a,b). Molecular studies using RNA have the disadvantage of the liability of the RNA itself. RNA is less stable than DNA, and is also more susceptible to environmental changes such as pH and ionic strength of the medium. Therefore, in this study we used DNA fingerprinting techniques to identify the different groups of phytoplankton in the environmental sample as reflected by their restriction fragment length polymorphism pattern seen in an agarose electrophoresis gel.

The objective of this work was to:

- Identify the different taxonomic groups that compose the picoplankton by DNA fingerprinting using different restriction enzymes on the genomic DNA (gDNA).

Materials and Methods

Sample collection and nucleic acid isolation

Plankton samples were collected on different dates at CaTS from surface and DCM (Table 6). The water was pre-filtered onto 90 mm, 2.0 μm glass microfibre filters (Whatman Multigrade GMF 150) and transported in polyethelene 1L bottles to the laboratory, where the plankton sample was collected by centrifugation. Samples were centrifuged on a Beckman Coulter J2-HS refrigerated centrifuge at RCF= 15,300 x g for 15 minutes at 4-6°C. Genomic DNA was isolated by hypotonic cell lyses (0.4 M NaCl/10 mM Tris Hcl pH 8.0/2.0 mM EDTA) enriched by proteinase K (1 mg/ml), RNAse, and Sodium Dodecyl Sulfate (SDS 1% w/v), proteins and polysaccharides were removed by phenol-chloroform extraction and nucleic acids were collected by alcohol precipitation DNA yield was quantified by a Shimadzu spectrophotometer. DNA extracts were stored at -70°C until further analysis.

Genomic DNA samples were cut using three restriction enzymes, *Hind III*, *Eco RI*, and *Bam HI*. Each digestion was set up independently from one another. Tables 7 and 8 summarize the DNA isolation and restriction endonuclease digestion protocol. Electrophoretic analysis was through 0.7% agarose/1.0 x TAE pH 8.0, in a mini gel submarine horizontal apparatus (BioRad Laboratories), at 25° C and a run time of 45 minutes at 50V, constant voltage. The *Hind III* digest of lambda DNA was run as a molecular weight marker. Gels were stained with 0.5 mg/L ethidium bromide and documented under UV illumination by the KODAK Image Station 2000R. Visual analysis of electrophoretic patterns was carried out, and different electrophoretic patterns were assigned to different isolates.

Table 6. Description of samples collected

Sample	Station	Date collected	Volume filtered (L)
JLB01	CaTS Surf	Sept-01	5.0
JLB02	CaTS Surf	Oct-01	5.0
JLB03	CaTS Surf	Dic-01	5.0
JLB04	CaTS Surf	Jan-01	5.0
JLB05	CaTS Surf	Mar-01	5.0
JLB06	CaTS Surf	Jun-01	5.0
JLB07	CaTS Surf	Jul-01	5.0
JLB08	CaTS Surf	Aug-01	5.0
JLB09	CaTS DCM	Sept-01	4.0
JLB10	CaTS DCM	Oct-01	4.0
JLB11	CaTS DCM	Dic-01	4.0
JLB12	CaTS DCM	Jan-01	4.0

Table 7. DNA isolation data.

Sample	Total Volume (μL)	OD 260	μg/μl	μg total
JLB01	100	0.240	12.0	1200
JLB02	100	0.270	13.5	1350
JLB03	100	0.226	11.3	1130
JLB04	100	0.221	11.1	1105
JLB05	100	0.256	12.8	1280
JLB06	100	0.263	13.2	1315
JLB07	100	0.200	10.0	1000
JLB08	100	0.414	20.7	2070
JLB09	100	0.362	18.1	1810
JLB10	100	0.363	18.2	1815
JLB11	100	0.364	18.2	1820
JLB12	100	0.424	21.2	2119

Table 8. Restriction endonuclease digestion protocol.

					enzimes				
Sample	DNA Conc. (μg/μL)	volume used (μL)	μg digested	μg DNA: enzyme ratio	μL	units	Buffer	water	total volume (μL)
JLB01	12.0	2.0	24.0	5:3	2.0	20.0	1.0	5.0	10.0
JLB02	13.5	2.0	27.0	5:3	2.0	20.0	1.0	5.0	10.0
JLB03	11.3	2.0	22.6	5:3	2.0	20.0	1.0	5.0	10.0
JLB04	11.1	2.0	22.1	5:3	2.0	20.0	1.0	5.0	10.0
JLB05	12.8	2.0	25.6	5:3	2.0	20.0	1.0	5.0	10.0
JLB06	13.2	2.0	26.3	5:3	2.0	20.0	1.0	5.0	10.0
JLB07	10.0	2.0	20.0	5:3	2.0	20.0	1.0	5.0	10.0
JLB08	20.7	2.0	41.4	5:3	3.0	20.0	1.0	4.0	10.0
JLB09	18.1	2.0	36.2	5:3	2.0	20.0	1.0	5.0	10.0
JLB10	18.2	2.0	36.3	5:3	2.0	20.0	1.0	5.0	10.0
JLB11	18.2	2.0	36.4	5:3	2.0	20.0	1.0	5.0	10.0
JLB12	21.2	2.0	42.4	5:3	3.0	20.0	1.0	4.0	10.0

Results and Discussion

Electrophoretic patterns of RFLP for surface and DCM stations of CaTS are summarized in tables 9 and 10, while representations of the gels are presented in Figures 54-59. RFLP pattern obtained with *Bam HI* in surface station reveals different patterns that suggest the presence of different picoplankton groups in a temporal scale. At least two main patterns are identified, one of them is predominant from August to December (JLB08, JLB01, JLB02, JLB03), and a different pattern is observed during June and July (JLB06, and JLB07). The first pattern shows an upshift in one band that could be explained by partial digestion of DNA available and/or variation due to a shift of the population structure of the picoplankton. Surface samples digested with *Hind III* also get a basic pattern that is predominant from September to June. Variation in the pattern is observed during July and August. This variation could be explained by the arrival of the Orinoco plume to the Caribbean waters. The *Eco RI* digestion pattern on surface waters shows a myriad pattern of bands among the samples. This suggests that the recognition sequence of this endonuclease is abundant in the picoplankton population, making the identification of a particular pattern difficult. The RFLP patterns suggest that temporal variations in the genetic composition of the picoplankton population are occurring at CaTS. As was suggested in the previous chapters this variability can be attributed to the seasonal dynamics of the Eastern Caribbean.

Analysis of the DCM samples digested with *Bam HI* also shows temporal variations in which a particular group is present during September, then is seems to be reduce at October but it reappears on December and January. RFLP patterns also reveal that variation during December and January is present. Similar results are observed when

Hind III and *Eco RI* enzymes were used to produce the RFLP's patterns in DCM samples. These RFLP patterns not only corroborate the temporal variability in the surf and DCM stations, which had been observed in the size-fraction distribution and in the bio-optical characteristics of the waters sampled, but also suggests that even within the picoplankton population changes in terms of its composition are occurring.

When surface RFLP's patterns are compared to DCM RFLP's patterns, they show a great variability among them. This suggests that there is temporal and spatial variation in the picoplankton population.

Table 9. Number of bands found in the RFLP electrophoretic pattern for the different restriction enzymes for CaTS surface stations.

	Number of bands		
Sample	*Bam HI*	*Eco RI*	*Hind III*
JLB 01	12	6	7
JLB 02	12	14	7
JLB 03	13	11	7
JLB 04	13	14	7
JLB 05	13	12	7
JLB 06	11	15	7
JLB 07	12	13	12
JLB 08	12	11	10

Table 10. Number of bands found in the RFLP electrophoretic pattern for the different restriction enzymes for CaTS DCM stations.

	Number of bands		
Sample	*Bam HI*	*Eco RI*	*Hind III*
JLB09	11	12	8
JLB10	13	14	8
JLB11	12	12	9
JLB12	12	10	5

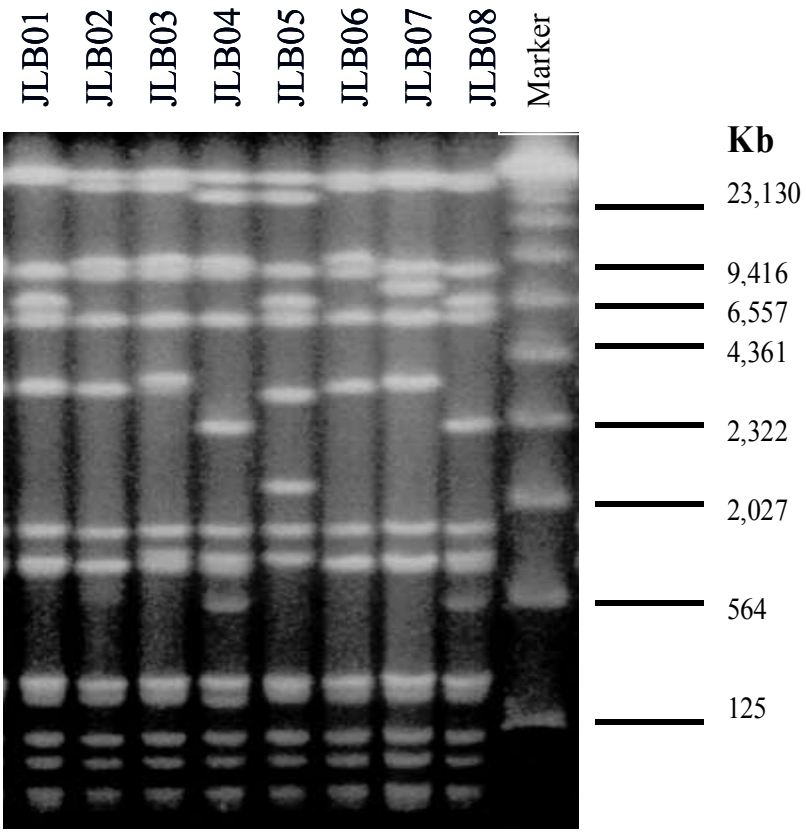

Figure 54. Electrophoretic pattern obtained with *Bam HI* for surface samples of CaTS.

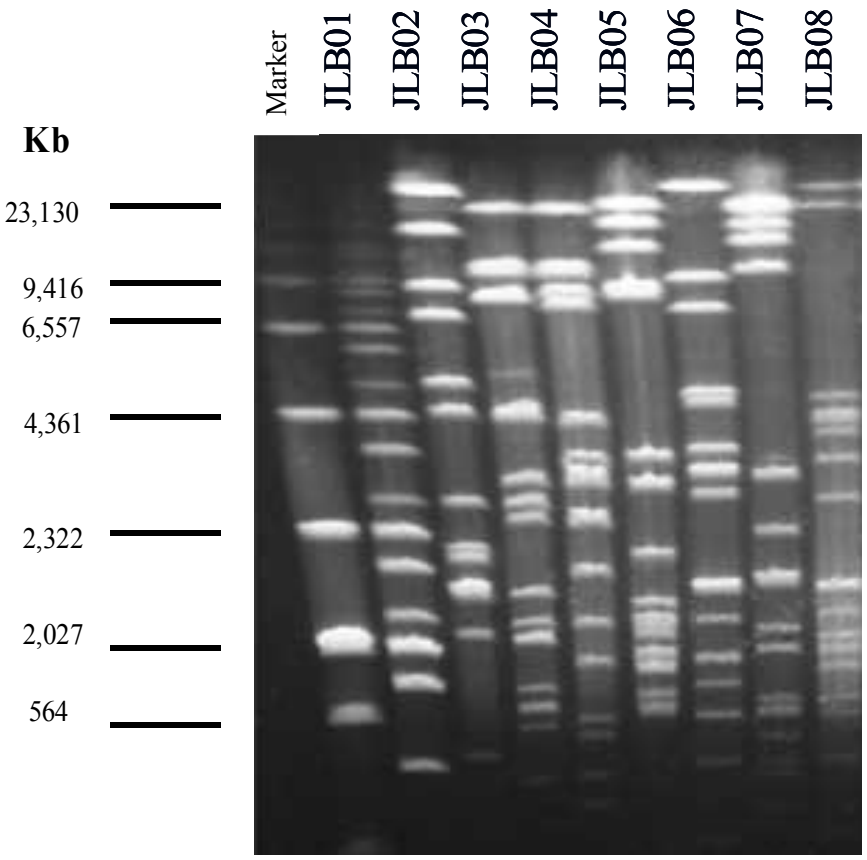

Figure 55. Electrophoretic pattern obtained with *Eco RI* for surface samples of CaTS.

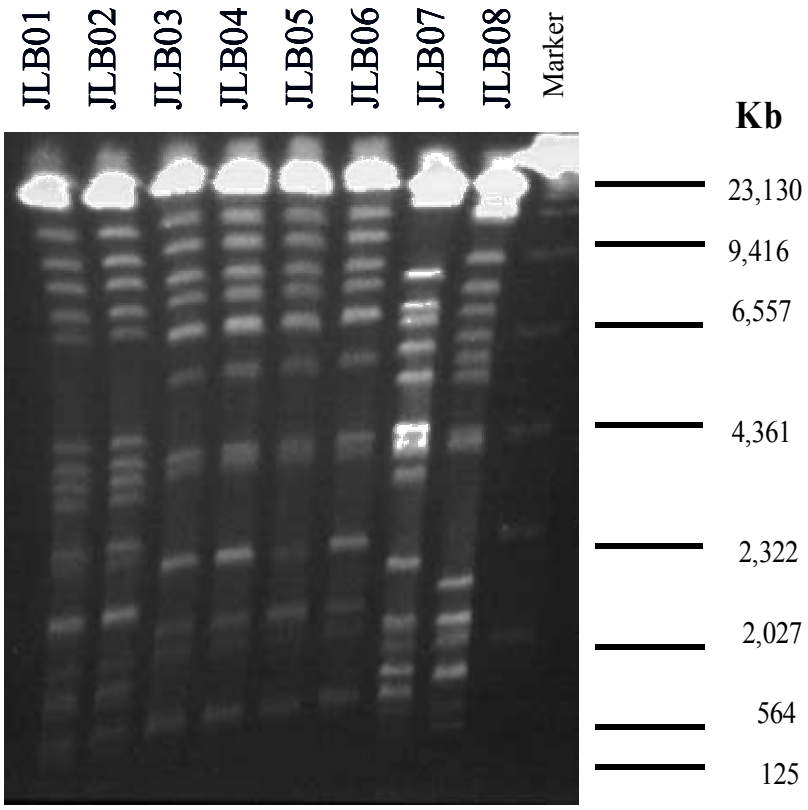

Figure 56. Electrophoretic pattern obtained with *Hind II*\ for surface samples of CaTS.

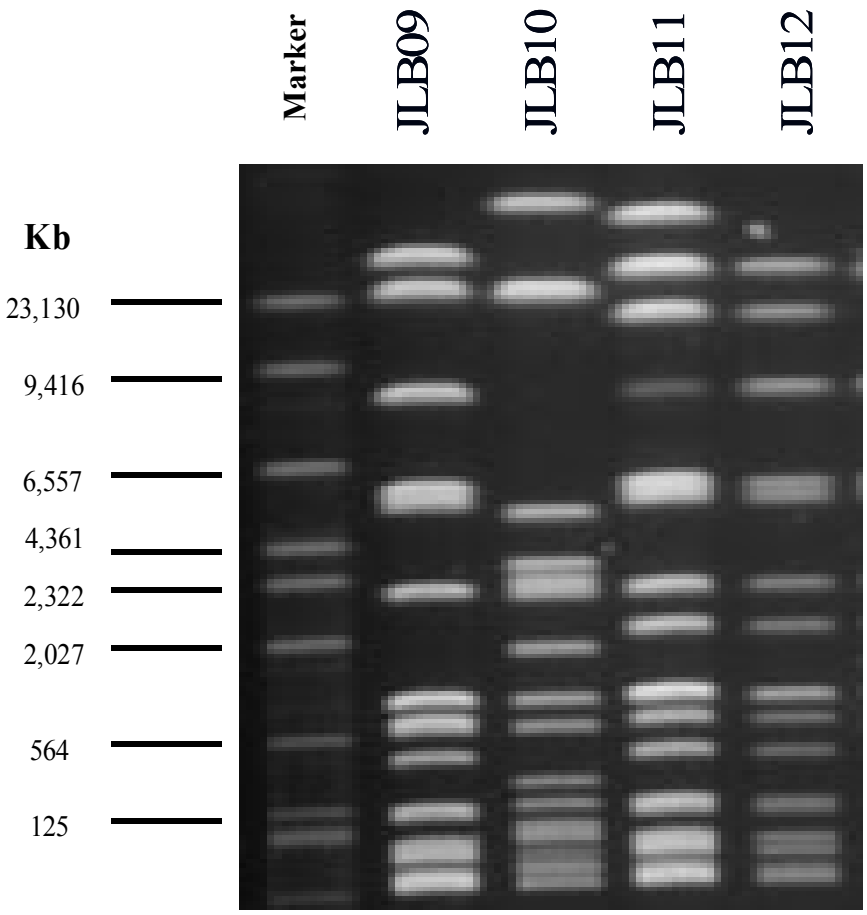

Figure 57. Electrophoretic pattern obtained with *Bam HI* for DCM samples of CaTS.

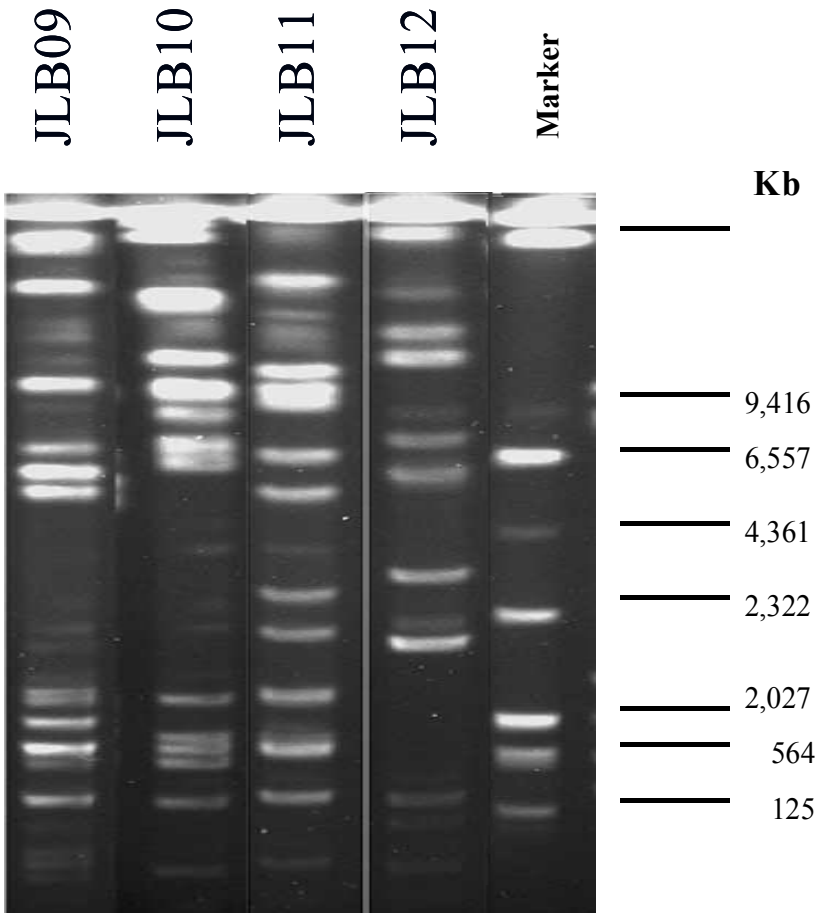

Figure 58. Electrophoretic pattern obtained with *Eco RI* for DCM samples of CaTS.

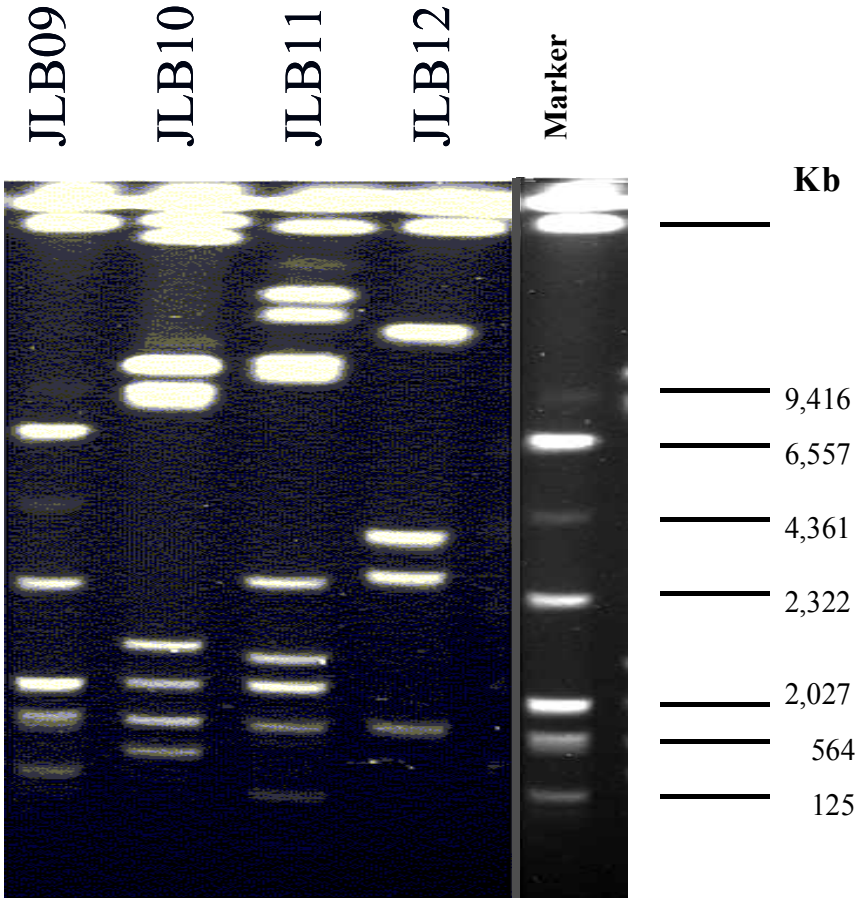

Figure 59. Electrophoretic pattern obtained with *Hind III* for DCM samples of CaTS.

Conclusion

From this study it can be concluded that picoplankton is an important component of the phytoplankton community structure in the warm oligotrophic waters of the Eastern Caribbean, and that future studies must take into consideration not only the importance of picoplankton to the community structure of phytoplankton, but also the bias sample obtained with 0.7 μm filters. For remote sensing purposes, picoplankton has been sometimes overlooked, and yet, it is a very important component in oceanic and coastal waters. If we hope to improve satellite estimates of phytoplankton biomass, future algorithms must take into account this component of the population of phytoplankton. The data also suggests that the population dynamics of phytoplankton in Case 1 and 2 waters of the Eastern Caribbean Sea is very complex, varying at the temporal, spatial and size-structure level. Furthermore, since satellites are taking snapshots in time and averaging it out over a 1 km^2, small temporal and spatial variations in phytoplankton populations are a potential source of error for remote sensing measurements of ocean color.

Our data from CaTS and Mayagüez Bay showed temporal variation in size frequency distribution. Mona data suggested short-time variability, while Caratlan II and Mayagüez Bay data suggest spatial variability at small spatial scales. Further evidence for the temporal and spatial variation in the picoplankton composition was observed with the RFLP electrophoretic patterns observed for CaTS.

While the importance of small plankton has been documented in the literature for more than a decade (Stockner and Antia, 1986), and numerous comparative studies of the retention properties of glass fiber and membrane filters have demonstrated that glass fiber

filters inadequately retain <1 μm diameter cells, routine sampling and treatment of the group has yet to be universally adopted. Until this occurs, our understanding of aquatic ecosystem dynamics remains fragmented and incomplete. As has been shown, picoplankton is an important component of the ecosystem dynamics of not only the oligotrophic waters of the Eastern Caribbean, but of seasonal importance in the coastal waters of Mayagüez Bay.

The dominance of picoplankton in terms of biomass was a recurrent feature of all the oceanic stations sampled during the study. It seems that the importance of picoplankton in the Eastern Caribbean and even in more productive coastal waters like Mayagüez Bay cannot be overlooked. These results emphasize the importance of picoplankton variability when temporal and spatial scales are considered, and suggests that this group of photoautotrophs, rather than simply representing a "background noise", constitutes an active and changing component of the microbial community in the open ocean and even in productive waters.

The main findings of our work can be summarized as following:

- In Case 1 waters, the picoplankton contributes, on average, 74% of the total chlorophyll-a concentration in surface, and 70% in the DCM. For Case 2 waters, the picoplankton accounts 40% of the total chlorophyll-a concentration in surface and 34% for deep samples.
- There is an average 20% loss of picoplankton in the oceanic stations of the Eastern Caribbean, and an average 9% loss in the coastal stations of Mayagüez Bay when using 0.7 μm GF/F filters compared to 0.22 μm Millipore membrane

filters,. Temporal and spatial variability was observed in the amount of loss of picoplankton through the 0.7 μm filters.

- Picoplankton are the dominant component of the phytoplankton population in oceanic waters, and contribute 60-70% to the a_p, and 61-77% to a_{ph}, while Mayagüez Bay, which is dominated by larger sized phytoplankton, the picoplankton contributes 30-58% to the a_p, and 45-90% to the a_{ph}. Temporal and spatial variability was observed in the size distribution of the phytoplankton and in the contribution of the picoplankton to the different absorption coefficients in the waters sampled.
- RFLP electrophoresis patterns corroborated the spatial and temporal variability in phytoplankton, and suggest variability within the picoplankton component of the phytoplankton population.

Literature Cited

Agawin, N.S., C.M. Duarte, and S. Agustí. 1998. Growth and abundance of *Synechococcus sp*. in a Mediterranean Bay: Seasonality and relationship with temperature. Marine Ecological Progress Series. 170:45-53.

Agawin, N.S., C.M. Duarte, and S. Agustí. 2000. Nutrient and temperature control of the contribution of picoplankton to phytoplankton biomass and reproduction. Limnology and Oceanography. 45:591-600.

Allali, K., A. Bricaud, and H. Claustre. 1997. Spatial variations in the chlorophyll-specific absorption coefficients of phytoplankton and photosynthetically active pigments in the equatorial Pacific. Journal of Geophysical Research. 102:12413-12423.

Amann, R., W. Ludwig, and K.H. Schleifer. 1995. Phylogenetic identification and *in situ* detection of individual microbial cells without cultivation. Microbiology Review. 59:143-169.

Armstrong, R.A. 1994. Grazing limitation and nutrient limitation in marine ecosystems: steady-state solutions of an ecosystem model with multiple food-chains. Limnology and Oceanography. 39:597-608.

Azam, F., T. Fenchel, J.G. Field, J.S. Gray, L.A. Meyer-Reil, and F. Thingstad. 1983. The ecological role of water-column microbes in the sea. Marine Ecological Progress Series. 10:257-263.

Barlow, R.G., J.Aiken, H.E. Sessions, S. Lavender, and J. Mantel. 2001. Phytoplankton pigment, absorption and ocean colour characteristics in the southern Benguela ecosystems. South African Journal of Science. 97:230-239.

Bouman, H, T. Platt, G. Kraay, S. Sathyendranath, and B. Irwin. 2000. Bio-optical properties of the subtropical North Atlantic. I Vertical Variability. Marine Ecological Progress Series. 200:3-18.

Bricaud, A., A. Morel, and L. Prieur. 1981. Absorption by dissolved organic matter of the sea (yellow substance) in UV and visible domains. Limnology and Oceanography. 26:43-53.

Bricaud, A., A.L. Bedhomme, and A. Morel. 1988. Optical properties of diverse phytoplanktonic species: Environmental results and theoretical interpretation. Journal of Plankton Research. 10:851-873.

Bricaud, A. and D. Stramski. 1990. Spectral absorption coefficients of living phytoplankton and nonalgal biogenous matter: A comparison between the Peru upwelling area and the Sargasso Sea. Limnology and Oceanography. 35:562-582.

Britton, N.F., and U. Timm. 1993. Effects of competition and shading in planktonic communities. Journal of Mathematical Biology. 31:655-673.

Brown, S.L., M.R. Landry, R.T. Barber, L. Campbell, D.L. Garrison, and M.M. Gowing. 1999. Picophytoplankton dynamics and production in the Arabian Sea during the 1995 Southwest Monsoon. Deep-Sea Research II. 46:1745-1768.

Brzezinski, M.A., and D.M. Nelson. 1988. Interactions between pulsed nutrient supplies and a photocycle affect phytoplankton competition for limiting nutrients in long-term culture. Journal of Phycology. 24:346-356.

Campbell, L., H. Liu, H.A. Nolla, and D. Vaulot. 1997. Annual variability of phytoplankton and bacteria in the subtropical North Pacific Ocean at station ALOHA during the 1991-1994 ENSO event. Deep Sea Research. 44:167-192.

Carrick, H.J. and C.L. Schelske. 1997. Have we overlooked the importance of small phytoplankton in productive waters? Limnology and Oceanography. 42:1613-1621.

Charpy, L. and J. Blanchot. 1999. Picophytoplankton biomass, community structure and productivity in the Great Astrolabe Lagoon, Fiji. Coral Reefs. 18:255-262.

Chavez, F.P. 1995. A comparison of ship and satellite chlorophyll from California and Peru. Journal of Geophysical Research. 100:24855-24862.

Chen, Y.L.L. 2000. Comparisons of primary productivity and phytoplankton size structure in the marginal regions of southern East China Sea. Continental Shelf Research. 20:437-458.

Chisholm, S.W. 1988. A novel free-living prochlorophyte abundant in the oceanic euphotic zone. Nature. 334:340-343.

Chisholm, S.W. 1992. Phytoplankton size, in: P.G. Falkowsky and A.D. Woodhead (eds.). Primary production and biogeochemical cycles in the sea, pp. 323-350. Plenum Press, New York.

Clark, D. K., H. R. Gordon, K. J. Voss, Y. Ge, W. Broenkow, and C.Trees. 1997. Validation of atmospheric correction over the oceans. Journal of Geophysical Research-Atmospheres. 102:17209-17217.

Claustre, H., A. Bricaud, M. Babin, F. Bruyant, L. Guillou, F. Le Gall, D. Marie, and F. Partensky. 2002. Diel variations in *Prochlorococcus* optical properties. Limnology and Oceanography. 47:1637-1647.

Clementson, L., J.S. Parslow, A.R. Turnbull, D.C. McKenzie, and C.E. Rathbone. 2001. Optical properties of waters in the Australasian sector of the Southern Ocean. Journal of Geophysical Research. 106:31611-31625.

Corredor, J.E. 1979. Phytoplankton response to low-level nutrient enrichment through upwelling in the Colombian Caribbean basin. Deep Sea Research. 26:731-741.

Corredor, J.E. and J.M. Morell. 2001. Seasonal variation of physical and biogeochemical features in eastern Caribbean Surface Water. Journal of Geophysical Research. 106:4517-4525.

Dickson, M.L. and P.A. Wheeler. 1993. Chorophyll-a concentrations in the North Pacific: Does a latitudinal gradient exist? Limnology and Oceanography. 38:1813-1818.

Díez, B., C. Pedrós-Alió, T. Marsh, and R. Massano. 2001a. Application of denaturing gradient gel electrophoresis (DGGE) to study the diversity of marine picoeukaryotic assemblages and comparison of DGGE with other molecular techniques. Applied and Environmental Microbiology. 67:2942-2951.

Díez, B., C. Pedrós-Alió, and R. Massano. 2001b. Study of genetic diversity of eukaryotic picoplankton in different oceanic regions by small-subunit rRNA gene cloning and sequencing. Applied and Environmental Microbiology. 67:2932-2941.

Fouilland E., C. Courties, and C. Descolas-Gros. 2000. Size-fractionated phytoplankton carboxilase activities in the Indian sector of the Southern Ocean. Journal of Plankton Research. 22:1185-1201.

Gasol, J. and X.A. Morán. 1999. Effects of filtration on bacterial activity and picoplankton community structure as assessed by flow cytometry. Aquatic Microbial Ecology. 16:251-264.

Gieskes, W.W. and G.W. Kraay. 1986. Floristic and physiological differences between the shallow and the deep nanoplankton community in the euphotic zone in the open tropical Atlantic revealed by HPLC analysis of pigments. Marine Biology. 91:567-576.

Gilabert, J. 2001. Short-term variability of the planktonic size structure in a Mediterranean coastal lagoon. Journal of Plankton Research. 23:219-226.

Gilbes, F., J.M. Lopez, and P. Yoshioka. 1996. Spatial and temporal variations of phytoplankton chlorophyll-a and suspended particulate matter in Mayagüez Bay, Puerto Rico. Journal of Plankton Research. 18:29-43.

Giovannoni, S.J., E.F. DeLong, T.M Schmidt, and N.R. Pace. 1990. Tangential flow filtration and preliminary phylogenetic analysis of marine picoplankton. Applied and Environmental Microbiology. 56:2572-2575.

Glibert, P.M., C.A. Miller, C. Garside, M.R. Roman, and G.B. McManus. 1992. NH_4^+ regeneration and grazing: interdependent processes in size-fractionated $^{15}NH_4^+$ experiments. Marine Ecological Progress Series. 82:65-74.

Gordon, H.R. and A. Morel. 1983. Remote assessment of ocean colour for interpretation of satellite visible imagery, In: R.T. Barber (ed.). A Review, Lecture Notes on Coastal and Estuarine Studies, vol. 4, pp. 68-114. Springer-Verlag, New York.

Gordon, H.R., D.K. Clark, J.W. Brown, O.B. Brown, R.H. Evans, and W.W. Broenkow. 1983. Phytoplankton Pigment Concentrations in the Middle Atlantic Bight: Comparison of Ship Determinations and Coastal Zone Color Scanner Measurements. Applied Optics. 22:20-36.

Hein, M., M.F. Pederson, and K. Sand-Jensen. 1995. Size-dependent nitrogen uptake in micro- and macroalgae. Marine Ecological Progress Series. 118:247-253.

Hirose, M., Y. Nishibe, M. Ueki, and S. Nakano. 2003. Seasonal changes in the abundance of autotrophic picoplankton and some environmental factors in hyper eutrophic Furuike Pond. Aquatic Ecology. 37:37-43.

Hoepffner, N. and S. Sathyendranath. 1993. Determination of the major groups of phytoplankton pigments from the absorption spectra of total particulate matter. Journal of Geophysical Research. 98:22789-22803.

Huisman, J. and F.J. Weissing. 1994. Light-limited growth and competition for light in well-mixed aquatic environments: an elementary model. Ecology. 75:507-520.

Huisman, J., P. van Oostveen, and F.J. Weissing. 1999a. Critical depth and critical turbulence: two different mechanisms for the development of phytoplankton blooms. Limnology and Oceanography. 44:1781-1787.

Huisman, J., P. van Oostveen, and F.J. Weissing. 1999b. Species dynamics in phytoplankton blooms: incomplete mixing and competition for light. American Naturalist. 154:46-48.

Hutchinson, G.E. 1961. The paradox of the plankton. American Naturalist. 95:135-147.

Jacquet, S., F. Partensky, J.F. Lennon, and D. Vaulot. 2001. Diel patterns of growth and division in marine picoplankton in culture. Journal of Phycology. 37:357-369.

Johnson, P.W. and J.M. Sieburth. 1979. Chroococcoid cyanobacteria in the sea: a ubiquitous and diverse phototrophic biomass. Limnology and Oceanography. 24:928-935.

Johnson, P.W. and J.M. Sieburth. 1982. *In situ* morphology and occurrence of eukaryotic phototrophs of estuarine and oceanic waters. Journal of Phycology. 18:318-327.

Joint, I.R. and A.G. Pomroy. 1986. Photosynthetic characteristics of nanoplankton and picoplankton from surface mixed layer. Marine Biology. 92:465-474.

Kirk, J. 1994. Light and Photosynthesis in aquatic ecosystems. Cambridge University Press, Cambridge. 509 pp.

Knauber, D.C., E.S. Berry, and M.W. Fawley. 1996. Ribosomal RNA-based oligonucleotide probes to identify marine green ultraphytoplankton. Journal of Eukaryotic Microbiology. 48:89-94.

Lazzara, L., A. Bricaud, and H., Claustre. 1996. Spectral absorption and fluorescence excitation properties of phytoplanktonic populations at a mesotrophic and an oligotrophic site in the tropical North Atlantic EUMELI program). Deep-Sea Research. 43:1215-1240.

Lee, S., Y.C. Kang, and J.A. Fuhrman. 1995. Imperfect retention of natural bacterioplankton cells by glass fiber filters. Marine Ecological Progress Series. 119:285-290.

Lenz, J. 1992. Microbial loop, microbial food web and classical food chain: Their significance in pelagic marine ecosystems. Archives Hydrobiology - Advances in Limnology. 37:265-279.

Li, W.K.W. 1998. Annual average abundance of heterotrophic bacteria and *Synechococcus* in surface ocean waters. Limnology and Oceanography. 43:1746-1753.

Li, W.K.W., D.V. Subba, W.G. Harrison, J.C. Smith, J.J. Cullen, B. Irwin, and T. Platt. 1983. Autotrophic picoplankton in the tropical ocean. Science. 219:292-295.

Liu, Y., M.A. Islam, and J. Gao. 2003. Quantification of shallow water quality parameters by means of remote sensing. Progress in Physical Geography. 27:24-43.

Litchman, E. and C. Klausmeier. 2001. Competition of Phytoplankton under fluctuating light. American Naturalist. 157:170-187.

Lohrenz, S.E., A.D. Weidemann, and M. Tuel. 2003. Phytoplankton spectral absorption as influenced by community size structure and pigment composition. Journal of Plankton Research. 25:35-61.

Magazzú, G. and F. Decembrini. 1995. Primary production, biomass and abundance of phototrophic picoplankton in the Mediterranean Sea: A review. Aquatic Microbiol Ecology. 9:97-104.

Marañón, E., P.M. Holligan, R. Barciela, N. González, B. Mouriño, M.J. Pazó, and M. Varela. 2001. Patterns of phytoplankton size structure and productivity in contrasting open-ocean environments. Marine Ecological Progress Series. 216:43-56.

Margalef, R. 1965. Composición y distribución del fitoplancton. Sociedad de Ciencias Naturales La Salle. 25:141-205.

Marshall, H.G. and M.S. Cohn. 1983. Distribution and composition of phytoplankton in northeastern coastal waters of the United States. Estuarine Coastal Shelf Science. 17:119-131.

Matta, J.F. and H.G. Marshall. 1984. A multivariate analysis of phytoplankton assemblages in the western North Atlantic. Journal of Plankton Research. 6:663-675.

McClain, C.R., M.L. Cleave, G.C. Feldman, W.W. Gregg, S.B. Hooker, and N. Kuring. 1998. Science quality SeaWiFS data for global biosphere research. Sea Technology. 39:10-16.

Mitchell, B.G. and D.A. Kiefer. 1984. Determination of absorption and fluorescence excitation spectra for phytoplankton. In: O. Holm-Hansen, L. Bolis, and R. Giles (eds.). Marine phytoplankton and productivity, pp. 157-169. Springer-Verlag, Berlin.

Moon-van der Staay, S.Y., R. De Wachter, and D. Vaulot. 2000. Oceanic 18S rDNA sequences from picoplankton reveal unsuspected eukaryotic diversity. Nature. 409:607-610.

Moon-van der Staay, S.Y., G.W.M. van der Staay, L. Guillou, D. Vaulot, H. Claustre, and L.K. Medlin. 2001. Abundance and diversity of prymnesiophytes in the picoplankton community from the equatorial Pacific Ocean inferred from 18S rDNA sequences. Limnology and Oceanography. 45:98-109.

Morel, A. and L. Prieur. 1977. Analysis of variations in ocean color. Limnology and Oceanography. 22:709-722.

Morrison, J.M. and O.P. Smith. 1990. Geostrophic transport variability along the Aves Ridge in the Eastern Caribbean Sea during 1985 and 1986. Journal of Geophysical Research. 95:699-710.

Müller-Karger, F.E., C.R. McClain, T.R. Fisher, W.E. Esaias, and R. Varela. 1989. Pigment distribution in the Caribbean Sea: Observations from space. Progressive Oceanography. 23:23-64.

O'Reilly, J.E., S. Maritorena, B.G. Mitchell, D.A. Siegel, K.L. Carder, S.A. Garver, M. Kahru, and C. McClain. 1998. Ocean color chlorophyll algorithms for SeaWiFS. Journal of Geophysical Research. 103:24937-24953.

Oviatt, C., P. Lane, F. French III, and P. Donaghay. 1989. Phytoplankton species and abundance in response to eutrophycation in coastal marine mesocosms. Journal of Plankton Research. 11:1223-1244.

Pace, N.R. 1997. A molecular view of microbial diversity and the biosphere. Science. 276:734-740.

Painting, S.J., C.L. Maloney, and M.I. Lucas. 1993. Simulation and field measurements of phytoplankton-bacteria-zooplankton interactions in the southern Benguela upwelling region. Marine Ecological Progress Series. 100:55-69.

Platt, T. and A.D. Jassby. 1976. The relationship between photosynthesis and light for natural assemblages of coastal marine phytoplankton. Journal of Phycology. 12:421-430.

Peña, M.A., M.R. Lewis, and W.G. Harrison. 1990. Primary productivity and size structure of phytoplankton biomass on a transect of the equator at 135 W in the Pacific Ocean. Deep Sea Research. 37:295-315.

Phinney, D.A. and C.S. Yentsch. 1985. A novel phytoplankton chlorophyll technique: toward automated analysis. Journal of Plankton Research. 7:633-642.

Pomeroy, L. 1974. The ocean’s food web, a changing paradigm. Bioscience. 24:499-504.

Raimbault, P., M. Rodier, and I. Taupier-Letage. 1988. Size fraction of phytoplankton in the Ligurian Sea and the Algerian Basin (Mediterranean Sea): Size distribution versus total concentration. Marine Microbial Food Webs. 3:1-7.

Raven, J.A. 1986. Physiological consequences of extremely small size for autotrophic organisms in the sea. In: T. Platt and W.K.W. Li (eds.). Photosynthetic picoplankton. Canadian Bulletin of Fisheries and Aquatic Sciences. 214:1-70.

Raven, J.A. 1998. The twelfth Tansley Lecture. Small is beautiful: The picophytoplankton. Functional Ecology. 12:503-513.

Robles-Rajero, E.G. and J.R. Lara-Lara. 1993. Phytoplankton biomass and primary productivity by size classes in the Gulf of Tehuantepec, México. Journal of Plankton Research. 15:1341-1358.

Rodríguez, J., J.M. Blanco, F. Jiménez-Gómez, F. Echevarría, J. Gil, V. Rodríguez, J. Ruiz, B. Bautista, and F. Guerrero. 1998. Patterns in the size structure of the phytoplankton community in the deep fluorescence maximun of the Alborean Sea (southwestern Mediterranean). Deep-Sea Research. 45:1577-1593.

Roesler, C.S., M.J. Perry, and K.L. Carder. 1989. Modeling in situ phytoplankton absorption from total absorption spectra. Limnology and Oceanography. 34: 1512-25.

Rosado, M.A. 2000. Variability of Bio-Optical Properties in Mayagüez Bay. Masters of Marine Sciences Thesis. University of Puerto Rico Mayagüez Campus. 61 pp.

Sakshaug, E., A. Bricaud, Y. Dandonneau, P.W. Falkowski, D.A. Kiefer, L. Legendre, A. Morel, J. Parslow, and M. Takahashi. 1997. Parameters of photosynthesis: definitions, theory and interpretation of results. Journal of Plankton Research. 19:1637-1670.

Sathyendranath, S., L. Lazzara, and L. Prieur. 1987. Variations in the spectral values of specific absorption of phytoplankton. Limnology and Oceanography. 32:403-415.

Schmidt, T.M., E.F. DeLong, and N.R. Pace. 1991. Analysis of a marine picoplankton community by 16S rRNA gene cloning and sequencing. Journal of Bacteriology. 173:4371-4378.

Sieburth, J.M., V. Smetaceck, and J. Lenz. 1978. Pelagic ecosystem structure: Heterotrophic compartments of the plankton and their relationship to plankton size fractions. Limnology and Oceanography. 23:1256-1263.

Siegel, D.A., A.F. Michaels, J.C. Sorensen, M.C. O'Brien, and M.A. Hammer. 1995. Seasonal variability of light availability and utilization in the Sargasso Sea. Journal of Geophysical Research. 100:8695-8713.

Simon, N., N. Le Bot, D. Marie, F. Partensky, and D. Vaulot. 1995. Fluorescent in situ hybridization with rRNA-targeted probes for identifying small phytoplankton by flow cytometry. Applied Environmental Microbiology. 61:2506-2513.

Sokal, R.R. and F.J. Rohlf. 1995. Biometry. The principles and practice of statistics in biological research. 3rd edition. W.H. Freeman and Co., New York, NY. 887pp.

Sosik, H.M. 1996. Bio-optical modeling of primary production: consequences of variability in quantum yield and specific absorption. Marine Ecological Progress Series. 143:225-238.

Sosik, H.M. and B.G. Mitchell. 1995. Light absorption by phytoplankton, photosynthetic pigments and detritus in the California Current System. Marine Ecological Progress Series. 143:225-238.

Stahl, D.A., D.J. Lane, G.J. Olsen, and N.R. Pace. 1984. Analysis of hydrothermal vent-associated symbionts by ribosomal RNA sequences. Science. 224:409-411.

Stahl, D.A., D.J. Lane, G.J. Olsen, and N.R. Pace. 1985. Characterization of a Yellowstone hot spring microbial community by 5S rRNA sequences. Applied and Environmental Microbiology. 45:1379-1384.

Stockner, J.G. and P. Antia. 1986. Algal picoplankton from marine and freshwater ecosystems: a multidisciplinary perspective. Canadian Journal of Fisheries and Aquatic Sciences. 43:2472-2503.

Stuart, V., S. Sathyendranath, T. Platt, H. Maass, and B.D. Irwin. 1998. Pigments and species composition of a natural phytoplankton populations: effect on the absorption spectra. Journal of Plankton Research. 20:187-217.

Tagushi, S. and E.A. Laws. 1988. On the microparticles which pass through glass-fiber filter type GF/F in coastal and open waters. Journal of Plankton Research. 10:999-1008.

Venrick, E.L., S.L. Cummings, and C.A. Kemper. 1987. Picoplankton and the resulting bias in chlorophyll retained by traditional glass-fiber filters. Deep Sea Research. 34:1951-1956.

Walsh, J.J. 1976. Herbivory as a factor in patterns of nutrient utilization in the sea. Limnology and Oceanography. 21:1-13.

Ward, D.M., R. Weller, and M.M. Bateson. 1990. 16S rRNA sequences reveal numerous uncultured microorganisms in a natural community. Nature. 345:63-65.

Weller, R. and D.M. Ward. 1989. Selective recovery of 16S rRNA sequences from natural microbial communities in the form of cDNA. Applied and Environmental Microbiology. 55:1818-1822.

Yentsch, C. and D. Menzel. 1963. A method for the determination of phytoplankton chlorophyll and phaeophytin by fluorescence. Deep Sea Research. 10:221-231.

Yentsch, C. and D.A. Phinney. 1989. A bridge between ocean optics and microbial ecology. Limnology and Oceanography. 34:1694-1705.

Yongsik, S., R.L. Wetzel, and I.C. Anderson. 2000. Seasonal variations of size-fractionated phytoplankton along the salinity gradient in the York River estuary, Virginia (USA). Journal of Plankton Research. 22:1945-1960.